WT-1472

AEC Category: PHYSICS
Military Category: 32

OPERATION

PLUMBBOB

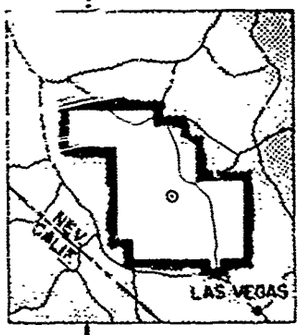

NEVADA TEST SITE
MAY-OCTOBER 1957

Project 34.1

EFFECTS OF A PRECURSOR SHOCK WAVE ON BLAST LOADING OF A STRUCTURE

Issuance Date: August 1961

CIVIL EFFECTS TEST GROUP

Report to the Test Director

EFFECTS OF A PRECURSOR SHOCK WAVE ON BLAST LOADING OF A STRUCTURE

By

J. R. Banister

and

L. J Vortman

Approved by: L. J. VORTMAN
Director
Program 34

Approved by: R. L. CORSBIE
Director
Civil Effects Test Group

Sandia Corporation
Albuquerque, New Mexico
October 1960

ABSTRACT

A 6- by 6- by 20-ft structure located at a distance of 2000 ft from Ground Zero (GZ) was subjected to a precursor wave from the Priscilla shot, a 37-kt balloon shot detonated at an altitude of 700 ft. The wave struck a 6- by 20-ft face of the structure with a peak incident overpressure of between 24 and 26 psi. Free-field measurements of overpressure, dynamic pressure, and force were made at the same radial distance about 25 ft from the end of the structure.

Local asymmetries in the blast wave gave different incident conditions for points separated on a fixed radius by only 35 ft. Dust concentrations and dust momentum flux were higher close to the ground than at the 10-ft-high gauge station located near the structure and contributed significantly to the blast loading on the front of the structure. This dust was accelerated through a high-velocity flow that feeds downward to the lower layers. The unusual oscillation seen in records of overpressures on the structures in earlier tests was again observed. A relation between the incident overpressure and the ratio of the impulse on the structure to the incident impulse is suggested.

Similar measurements were made on a $9\frac{2}{3}$- by 11- by 17-ft structure located at a distance of 1150 ft from GZ, where the peak overpressure was 87 psi.

ACKNOWLEDGMENTS

The authors wish to express their appreciation to the following individuals without whose conscientious efforts in the field these measurements could not have been made: H. E. Bell, R. W. Bradshaw, R. R. French, W. K. McCoy, J. H. Morrison, C. R. Pickens, O. E. Smith, and J. W. Wistor.

Appreciation is also expressed to L. N. Schofield and R. J. Beyatte for their assistance in reducing the data.

CONTENTS

ILLUSTRATIONS

CHAPTER 1 INTRODUCTION

ILLUSTRATIONS (Continued)

ILLUSTRATIONS (Continued)

TABLES

CHAPTER 1 INTRODUCTION

CHAPTER 2 TEST RESULTS

CHAPTER 3 DISCUSSION

Chapter 1

INTRODUCTION

1.1 OBJECTIVE

The purpose of Project 34.1 was to measure the characteristics of a nonideal shock wave and to describe the blast-loading effects of its impingement on a test structure. A 6- by 6- by 20-ft structure was subjected to a blast wave from the Priscilla shot at a range of 2000 ft from Ground Zero (GZ); a 6- by 20-ft surface faced the shot point. The overpressure, air dynamic pressure, dust momentum flux, and wind direction were measured in the incident wave. The experiment was supplemented by a similar, but more limited, loading study on a $9\frac{2}{3}$- by 11- by 17-ft structure at a range of 1150 ft. This structure had a $9\frac{2}{3}$- by 11-ft surface facing GZ.

1.2 BACKGROUND

An ideal shock wave is defined as one in which the overpressure rise observed from a fixed position is instantaneous and is followed by a gradual decay that can be analytically described by the equation

$$p = p_m \left(1 - \frac{t}{t^+}\right) e^{-c(t/t^+)}$$

where p = the overpressure at time t
p_m = the peak overpressure
t^+ = the duration of the positive phase of the blast wave
c = a constant describing the pressure decay rate

Over desert surfaces such as those at the Nevada Test Site (NTS), a nonideal shock wave known as the "precursor" is encountered for scaled heights of burst and yields such as in Priscilla shot.[1,2] This precursor overpressure vs. time history has a low-pressure step followed by a more or less gradual pressure rise rather than a sharp front. The gradual rise leads generally to a rounded peak that is followed by an irregular pattern of pressure vs. time. This wave form is difficult to reproduce with other than nuclear explosions, and wide differences in wave form are encountered at different stations (radial or azimuthal variation) on the same event. One of the unique characteristics of this type wave form is a degradation of peak overpressure and an enhancement of the dynamic pressure.

When a nuclear explosion produces a precursor over desert terrain, substantial amounts of dust are raised shortly after the blast wave arrives.[1,2] The mechanism of the dust-raising process and a revision of the Rankine-Hugoniot relations for the presence of dust have been considered by numerous authors.[2–4] After Operation Upshot-Knothole, it was suggested that suspended dust carried by the precursor blast wave might enhance dynamic pressure sufficiently to explain the high values of this parameter as well as the damage sustained by drag-sensitive targets.[2] This postulate was extensively examined during Operation Teapot.[5] In

particular, a study using specialized dynamic-pressure instruments demonstrated that about half the dynamic pressure observed over Frenchman Flat was attributable to dust.[6] The first of these instruments was the Greg gauge, which was used in the head-on sense to register the sum of side-on pressure, air dynamic pressure (uncorrected for Mach effects), and dust momentum flux. Dust momentum flux is defined as ϕ_d or $\rho_d \mu_d^2$, where ρ_d is the density of the suspended dust and μ_d is its velocity; it represents the head-on pressure exerted by dust on a target small compared to the dust-stopping distance in stagnant air. The other instrument was the Snob gauge, which senses the sum of overpressure and uncorrected air dynamic pressure by means of its head probe. Thus the difference between the head pressures measured by the Greg and Snob gauges is the dynamic pressure exerted by dust. The measurements from these specialized instruments, together with an air-density measurement, indicated that, although dust is a significant factor and accounts for half the dynamic pressure, abnormally high dynamic pressures are caused even more by high mass velocities.

Although considerable attention has been given to the precursor itself,[7] few quantitative measurements of its loading effects have been made. It has been obvious that the blast wave form was drastically effective against drag-sensitive targets. Shelton[7] has suggested that damage to such targets might be increased by maximizing the radial extent of the precursor. Merritt[8] has considered theoretically the effect of a slow rise time on the blast loading of structures based on the sound-pulse theories of Friedlander[9] and of Keller and Blank.[10] However, the sound-pulse theory is best applied to a treatment of the shock of an overpressure less than 10 psi. Ordinarily, by the time a shock has decayed to a peak overpressure of 10 psi or less, the shock wave is approaching the ideal form. In the first experiment to study the precursor loading of a cubicle,[11] the 6- by 12-ft face of a 6- by 6- by 12-ft-long structure was exposed to a precursor shock wave from Upshot-Knothole shot 10. The structure was destroyed by the shock wave, which had a peak over-pressure of about 50 psi. Valid pressure records were obtained only for the first 100 msec after shock arrival. The results during that period showed a pronounced oscillation of pressure on the front of the structure, less on the top, and the least on the back.

During Operation Teapot an attempt was made to measure the effect of a nonideal shock wave on the blast loading of a structure.[12] A 6- by 6- by 36-ft structure was subjected to a blast wave from the Turk shot at a range of 1850 ft from GZ in such a way that the nonideal wave front was incident upon the 6- by 36-ft face of the structure. The structure, since known as the "Galloping Domino," was demolished; however, pressure records were obtained on the structure for an average of 533 msec during which time the structure was being displaced. Calculation of the plane-motion response of the structure to the measured pressures indicated that, at the time of failure of the pressure record, the position of the structure was within a foot of the point at which the cables to the pressure gauges would have broken. The results of the calculation thus gave credence to the pressure measurements even though the structure was moving while pressures were being measured.

The measured peak incident overpressures at the structure were 13 to 14 psi. If the wave form had been ideal, the peak incident overpressure would have been 32 psi. Records of pressure measured on the structure showed an oscillation of about 18 to 30 cycles/sec, similar to that recorded by Project 3.1 of Operation Upshot-Knothole. The average overpressure measured by gauges located along the front center line of the structure displayed an unusually large pressure pulse between 200 and 300 msec after shock arrival, indicating a large dynamic-pressure surge.

The most significant results of the Operation Teapot experiment are summarized in Table 1.1

In addition to the ratios of measured impulse to predicted impulse, it is interesting also to consider ratios of measured impulse on the structure to measured impulse of the incident pressure wave. As will be pointed out later, the ratio of the impulse measured on the structure to the impulse of the incident wave varies from shot to shot. Thus the measured ratio of net translational impulse to incident impulse is actually a measure of the over-all dynamic-pressure effect. One might infer from the net translational ratios from tests at several pressure levels how the relative dynamic-pressure effect varies with increasing distance from GZ

to the point at which the precursor disappears and the wave shocks up into the ideal form, at which point the ratios must drop sharply to nearly unity.

In a second Teapot experiment[13] (shot 12), identical 3- by 3- by 6-ft structures were exposed on four controlled surfaces at the same radial distance from GZ to 20-psi shock waves. These four surfaces were a water surface, an asphalt surface, a loosened desert surface, and a compacted desert surface. The structures survived the blast, but no useful information was obtained for the water and asphalt lines. Higher peak pressures and net impulses were observed on structures located within the areas of loosened desert soil. Measured impulses are given in Table 1.2.

Static and dynamic pressures were obtained from gauges located on a radial blast line about 400 ft from the test structures.

1.3 INSTRUMENTATION

It was clear from the Teapot results that the understanding of loading phenomena could be improved by an examination of the free-field values of air and dust dynamic pressures at two elevations. The Project 34.1 experiment was designed accordingly. For a cross check, the Sandia SRI Pitot-static tube was used also as a dynamic-pressure indicator.

The head-on pressure registered by dust is a complex function of dust size and density, flow rate, and obstacle shape and size. A force plate was placed at the 3-ft elevation to serve as a target between the Greg gauge and the 34.1 structure. Since the direction of load as well as the magnitude is of interest, wind-direction gauges were mounted on the structure; these could also be used for pitch and yaw correction of the dynamic-pressure instruments.

1.3.1 Gauge Types

(a) *Pressure Gauges.* Wiancko variable-reluctance Bourdon type air-pressure gauges were used in this project.[14] Primarily for comparison purposes, two flush-diaphragm Ultradyne gauges were used for free-field measurements, and two Northam gauges were placed on the front face of the structure.

(b) *Greg and Snob Gauges.* The construction and theory of operation of the Greg and Snob gauges have been discussed in another report.[6] Both instruments were modified for this study. The Greg, as used during Operation Teapot, proved somewhat vulnerable to missiles. This weakness was lessened by using a protective piston, which was grease coupled to the pressure transducer; this improvement reduced the instrument response time somewhat but did not affect its sensitivity.

The Snob gauge was modified by making a 0.010-in. bleed orifice in the dust collecting chamber to reduce the possibility of dust clogging. The Snob was used in the head-on sense rather than as a dynamic-pressure gauge; however, the rear pressure transducer was still incorporated for side-on pressure measurement. Both instruments were equipped with Ultradyne flush-diaphragm pressure transducers.

(c) *Pitot-Static Tube.* This gauge had been used in previous operations.[2] In this study it was used only in the head-on sense; this was accomplished by sealing the side ports and placing the pressure transducer (Wiancko) in the rear position usually occupied by the side-on pressure-measuring transducer. This arrangement was employed to avoid the difficulties encountered in having the back of an uncovered transducer face the dust flow through the head port.

(d) *Force Plate.* Although an instrument of identical employment and name has been used in previous operations, the gauge used in Operation Plumbbob was essentially of new design. The old gauge had an 8-in.-diameter steel plate backed by an oil chamber. Pressure that was built up in this fluid chamber acted on a pressure transducer as an index of pressure against the plate. In the new gauge an 8-in. diaphragm is the pressure-sensing device. The diaphragm motion is indicated by a Shaevitz displacement gauge.

(e) *Wind-direction Gauge*. This instrument, a complete description of which is given in another report,[3] was used without modification.

1.3.2 Locations for Measurements of Incident Wave

Measurement of the incident wave was undertaken to provide free-field measurements of air and dust dynamic pressures in the vicinity of the Project 34.1 structure (see Figs. 1.1 and 1.2). For this purpose the Greg and Snob gauges were mounted at 3- and 10-ft elevations on the same instrument tower.

On a 3-ft tower, 6 ft north of the 10-ft-tower location, a force plate was mounted head-on at the same radial distance from GZ as the front of the 34.1 structure.

The only instruments used at the structure 1150 ft from GZ were a Pitot-static tube on a 3-ft tower for measuring free-field dynamic-pressure and a ground-baffle gauge for measuring overpressure (see Figs. 1.3 and 1.4). It was not feasible to use the dust instruments in their present stage of development.

Free-field measurements of overpressure were made by ground baffles at several locations fore and aft of the Project 34.1 structure (Fig. 1.2). Overpressures were also obtained at the 3- and 10-ft levels by the side-on transducers of the Snob gauges. Free-field gauges are listed in Table 1.3.

1.3.3 Locations for Measurements on Structure

Twenty-one air-pressure gauges were used on the 6- by 6- by 20-ft test structure in the locations shown in Fig. 1.5 (see also Fig. 1.6). Four such gauges were located on the forward footing of the structure (see Fig. 1.5).

Four force plates were located on the structure: two on the front and one each on the top and back. Two wind-direction gauges were mounted: one was used in the yaw sense on top of the cubicle and the other was used in the pitch sense on the structure side. Their locations are given in Fig. 1.7.

Seven Wiancko pressure gauges were located on the Project 30.4 vault[15] at a range of 1150 ft: two each on the front, top, and back and one on the forward footing (Fig. 1.8). Gauges on the structures are listed in Table 1.4

REFERENCES

1. C. J. Aronson et al., Free-air and Ground-level Pressure Measurements. Projects 1.3 and 1.5, Operation Tumbler Report, WT-513, Nov. 6, 1952. (Classified)
2. C. D. Broyles, Dynamic Pressure vs. Time and Supporting Air Blast Measurements, Project 1.10, Operation Upshot-Knothole Report, WT-714, February 1954. (Classified)
3. J. E. Whitney, The Behavior of Pressure in the Precursor Region, Report AFSWC-TN-55-3. (Classified)
4. F. B. Porzel, Height of Burst for Atomic Bombs, Report LA-1406, Los Alamos Scientific Laboratory, March 1952. (Classified)
5. H. K. Gilbert and E. B. Doll, Technical Summary of Military Effects, Programs 1-9, Operation Teapot Report, WT-1153, February 1960. (Classified)
6. J. R. Banister and F. H. Shelton, Special Measurements of Dynamic Pressure vs. Time and Distance, Project 1.11, Operation Teapot Report, WT-1110, Feb. 28, 1958. (Classified)
7. F. H. Shelton, The Precursor—Its Formation, Prediction, and Effects, Report SC-2850(TR), Sandia Corporation, July 27, 1953. (Classified)
8. M. L. Merritt, On the Effect of Slow Rise Times on the Blast Loading of Structures, Report AFSWP-460, Sandia Corporation, Sept. 25, 1953. (Classified)
9. F. G. Friedlander, The Diffraction of Sound Pulses, Proc. Roy Soc., A186: 322 (1946).
10. J. B. Keller and A. Blank, Diffraction and Reflection of Pulses by Wedges and Corners, Comm. Pure and Appl. Math., 4(1): 75-94 (June 1951).
11. E. V. Gallagher and T. H. Schiffman, Tests on the Loading of Building Equipment Shapes, Project 3.1, Operation Upshot-Knothole, WT-721, July 1955. (Classified)

12. L. J. Vortman and W. G. Francy, Effects of a Nonideal Shock Wave on Blast Loading of a Structure, Project 34.2, Operation Teapot. Report WT-1162, July 1, 1957. (Classified)
13. L. A. Schmidt, Study of Drag Loading of Structures in the Precursor Zone, Project 3.2, Operation Teapot Report, WT-1124, Jan. 30, 1959. (Classified)
14. G. W. Rollosson, Static and Dynamic Overpressure Measurements, Project 39.2, Operation Teapot Report, ITR-1192, 1955. (Classified)
15. E. Cohen and E. Laing, Response of Protective Vaults to Blast Loading, Project 30.4, Operation Plumbbob Report, ITR-1451, September 1957.

Tables and figures for Chap. 1 appear on pages 16 to 25.

TABLE 1.1 — PREDICTED AND MEASURED IMPULSE (OPERATION TEAPOT)

	Predicted impulse (assuming ideal wave shape), psi-sec	Measured impulse, psi-sec		Ratio of measured impulse to predicted impulse
Incident, free field	5.386	4.106		0.76
		Center band	End band	Center band
Front	7.983	16.16	12.760	2.025
Top	2.395	1.082	0.676	0.450
Back	3.257	1.344	0.692	0.413
Net translational	4.726	14.816	12.008	3.135

TABLE 1.2 — MEASURED IMPULSE (OPERATION TEAPOT, SHOT 12)

	Compacted desert soil	Loosened desert soil
Incident free-field impulse, psi-sec	6.25	6.25
Net translational impulse, psi-sec	8.4	9.6
Ratio	1.35	1.54

TABLE 1.3 — GAUGE LAYOUT FOR MEASURING INCIDENT SHOCK WAVE

Gauge code	Ground range, ft	Height above ground, ft	Gauge type	Gauge rating	Calibration pressure, psi
PGB-1150-0	1150	0	Pressure ground baffle (PGB)	100	75
Q-1150-3	1150	3	Pitot static tube (PST)	500	375
PGB-1700-0	1700	0	PGB	50	30
PGBU-1700-0	1700	0	PGB*	75	30
PGB-1800-0	1800	0	PGB	50	27
PGBU-1800-0	1800	0	PGB*	50	27
PGB-1900-0	1900	0	PGB	30	24
PGB-2000a-0	2000	0	PGB	30	21
PGB-2000b-0	2000	0	PGB	30	21
PGB-2100-0	2100	0	PGB	30	15
G-2000-3	2000	3	Greg	250	162
G-2000-10	2000	10	Greg	250	162
S-2000-3	2000	3	Snob	150	90
S-2000-10	2000	10	Snob	150	90
SS-2000-3	2000	3	Snob side-on	35	21
SS-2000-10	2000	10	Snob side-on	35	21
Q-2000-3	2000	3	PST	250	135
Q-2000-10	2000	10	PST	250	135
FP-2000-3	2000	3	Force plate		120

*Ultradyne pressure gauge.

TABLE 1.4—GAUGE LAYOUT FOR MEASURING PRESSURES ON TEST STRUCTURES

Gauge code	Ground range, ft	Height above ground, ft	Gauge type	Gauge rating	Calibration pressure, psi
		Project 30.4 Structure			
PMS-1	1144	0	Pressure	1000	600
PMS-2	1150	3	Pressure	1000	600
PMS-3	1150	7	Pressure	1000	600
PMS-4	1154	9⅔	Pressure	100	75
PMS-5	1158	9⅔	Pressure	100	75
PMS-6	1167¼	7⅞	Pressure	100	66
PMS-7	1167¼	1¾	Pressure	100	66
		Project 34.1 Structure			
PNC-1	2000	1	Pressure*	200	132
PC-2	2000	1	Pressure*	250	132
FPC-1	2000	1½	Force plate		120
PC-3	2000	2	Pressure	250	132
PC-4	2000	4	Pressure	250	132
FPC-2	2000	4½	Force plate		120
PNC-5	2000	5	Pressure*	200	132
PC-6	2000	5	Pressure*	250	132
PC-7	2000	5½	Pressure*	250	132
PC-8	2000½	6	Pressure*	50	21
PC-9	2001	6	Pressure*	50	21
PC-10	2001	6	Pressure*	50	21
PC-11†	2002	6	Pressure*	30	21
Y-C-1	2002	4	Pitch		
FPC-3	2003	6	Force plate		21
YP-C-1	2002	6	Yaw		(To ±45°)
PC-12	2004	6	Pressure	30	21
PC-13	2004	6	Pressure	30	21
PC-14	2005½	6	Pressure	30	21
PC-15	2006	5½	Pressure	30	15
PC-16	2006	5	Pressure	30	15
PC-17	2006	5	Pressure	30	15
PC-18	2006	4	Pressure	30	15
FPC-4	2006	3	Force plate	Not given	15
PC-19	2006	2	Pressure	30	15
PC-20	2006	1	Pressure	30	15
PC-21	2006	1	Pressure	30	15
PC-22	1986	0	Pressure	100	132
PC-23	1992½	0	Pressure	250	132
PC-24	1997	0	Pressure	250	132
PC-25	1999 + 7½ in.	0	Pressure	250	132

*Northam gauge.
†Not damped by manufacturer.

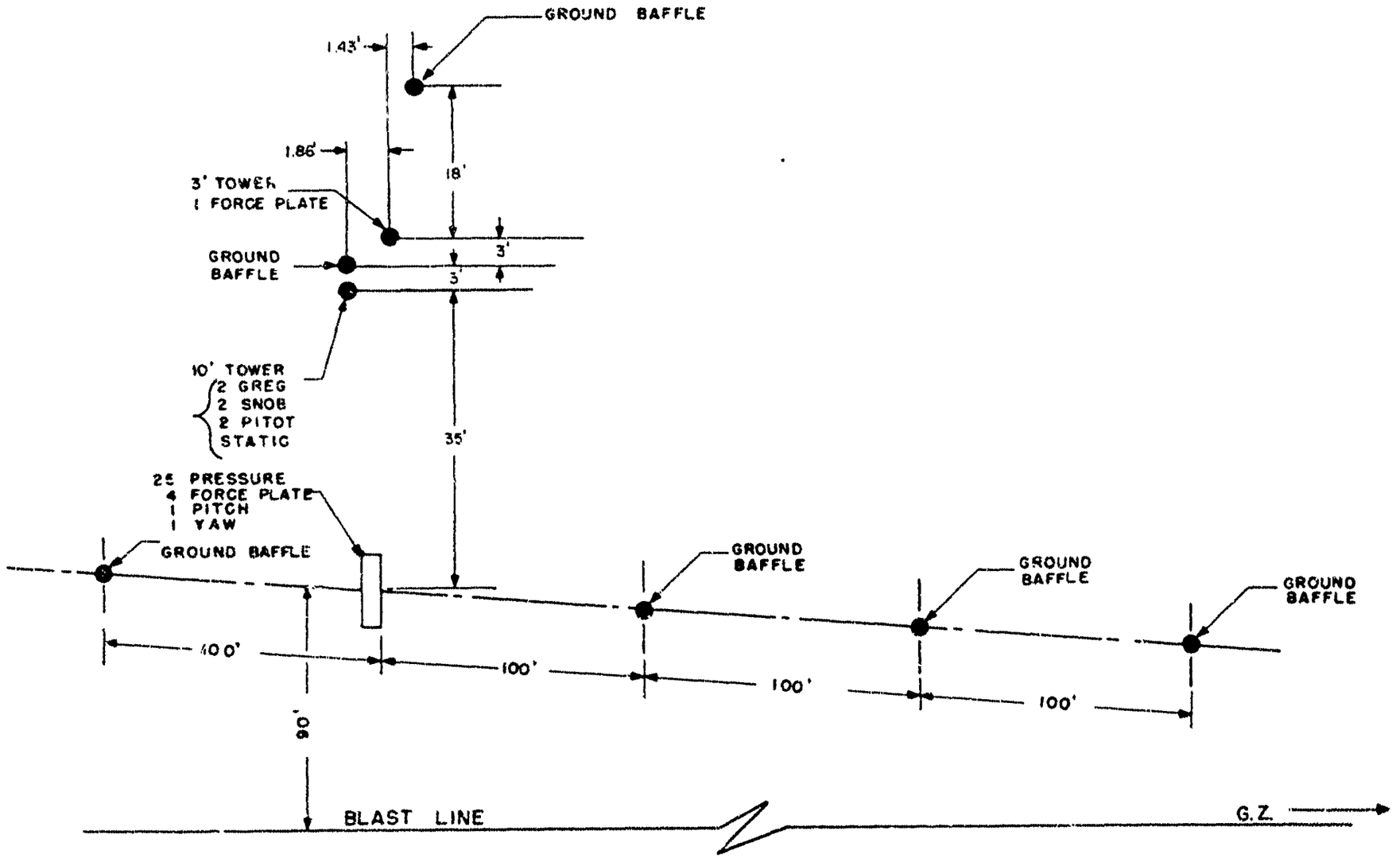

Fig. 1.1—Free-field gauges located at 2000 ft from GZ.

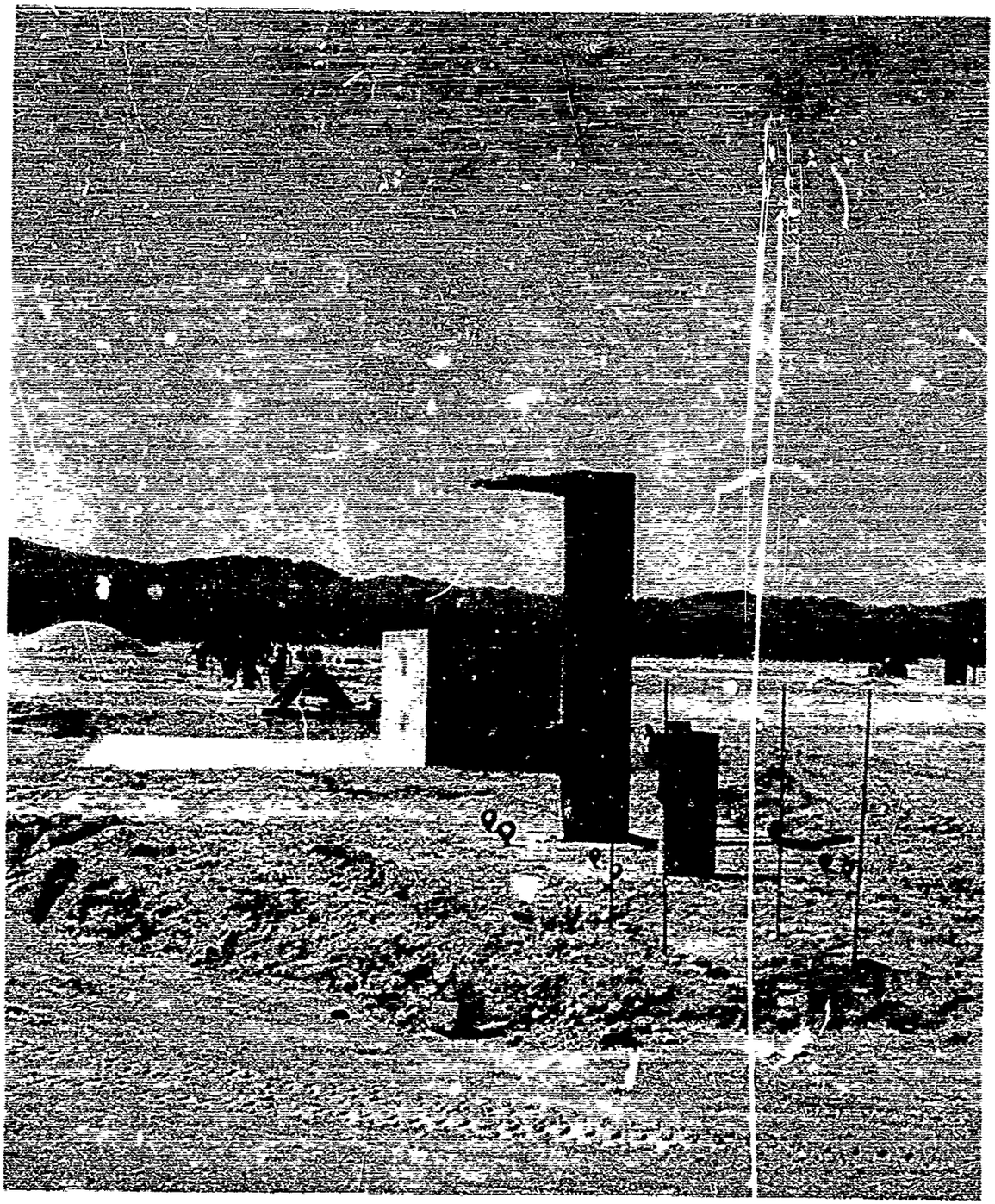

Fig. 1.2—The 6- by 6- by 20-ft test structure.

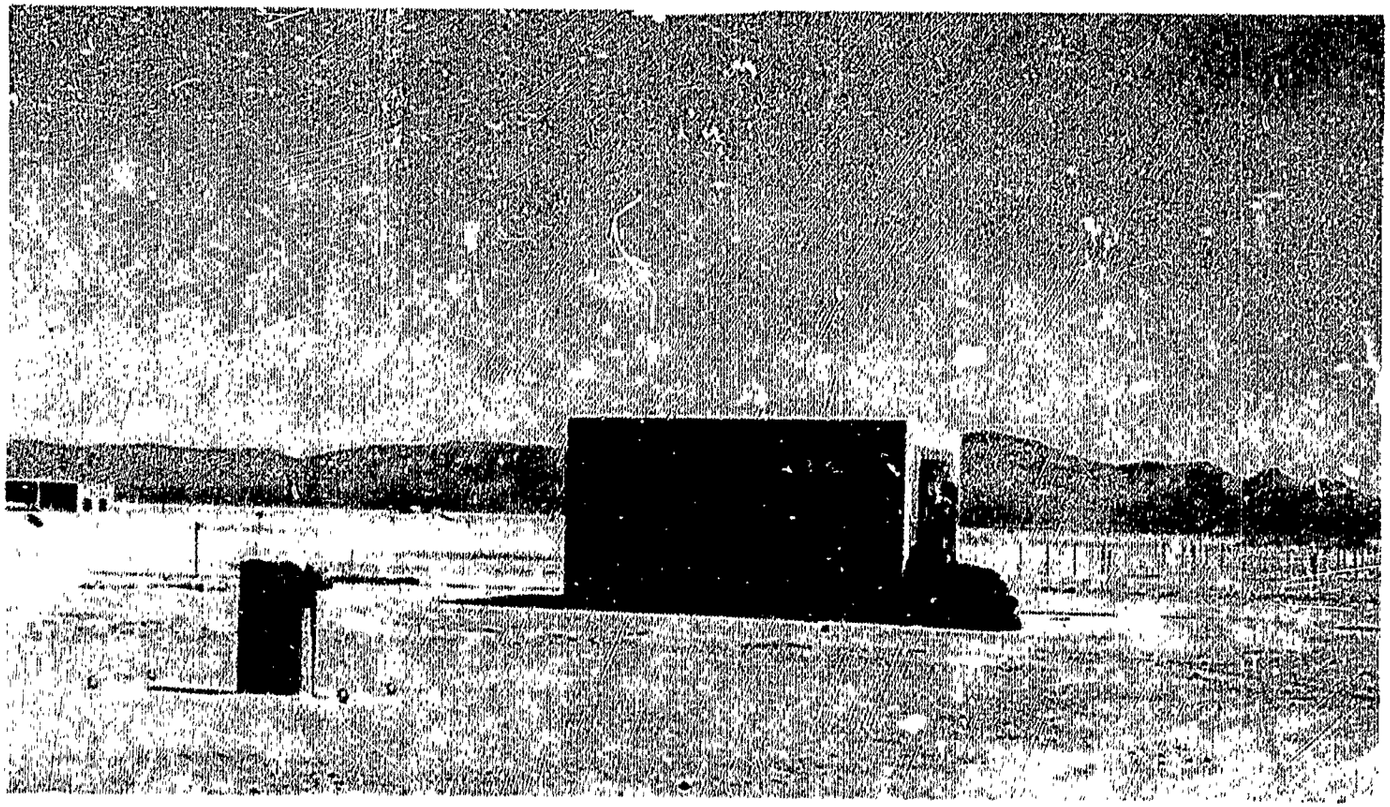

Fig. 1.3—Project 30.4 structure.

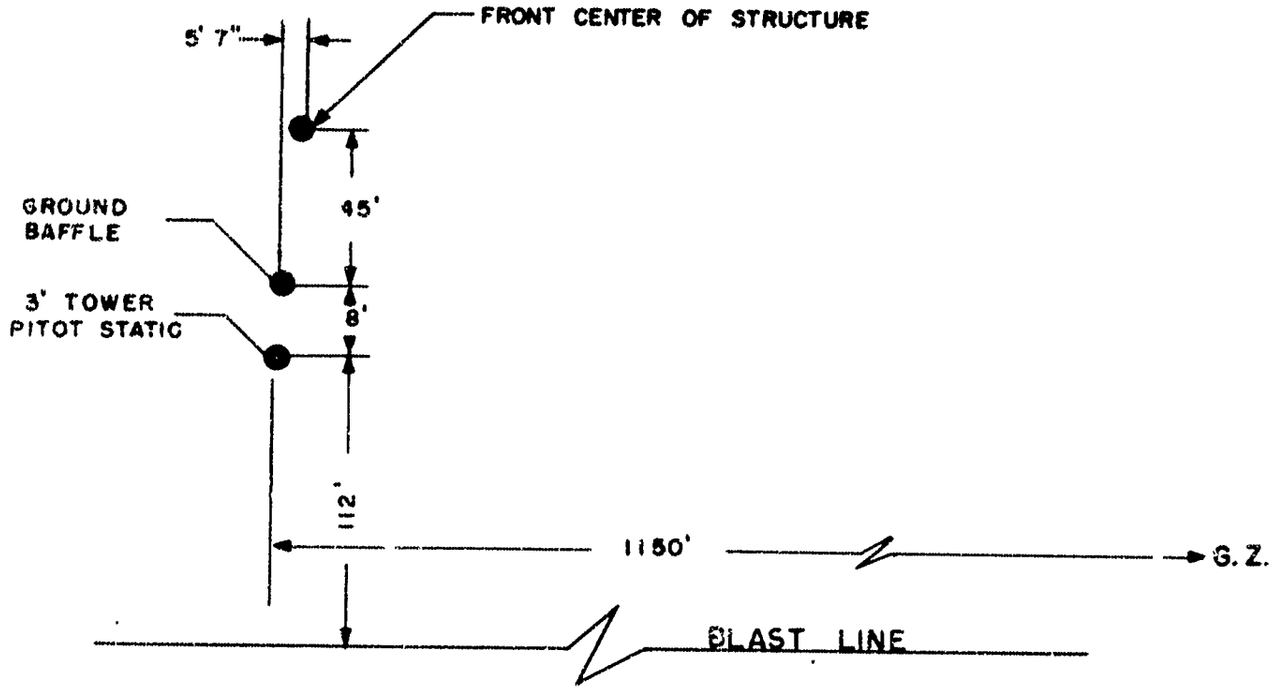

Fig. 1.4—Location of gauges for incident overpressure and incident dynamic-pressure measurements.

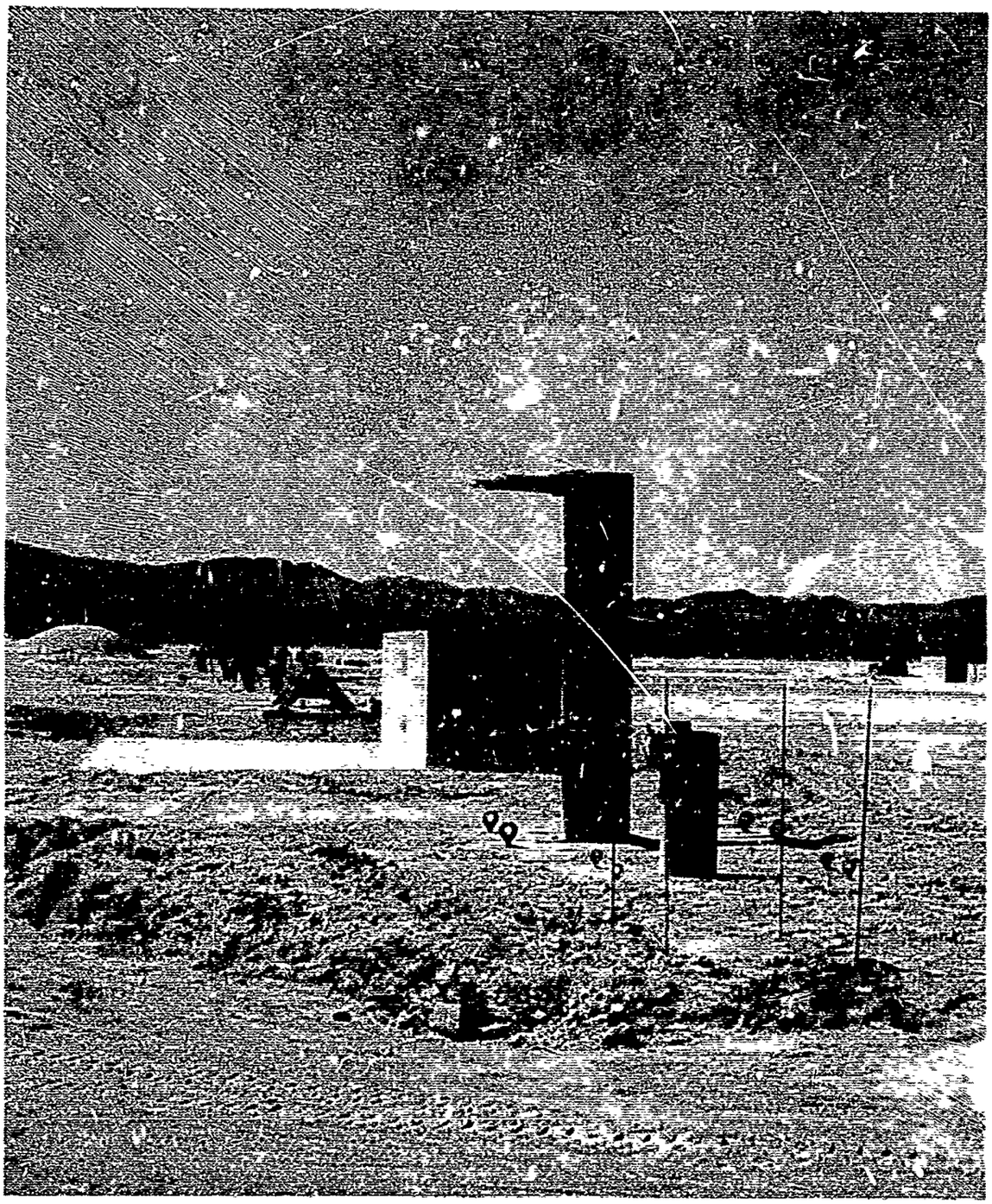

Fig. 1.2—The 6- by 6- by 20-ft test structure.

Fig. 1.6—Test structures.

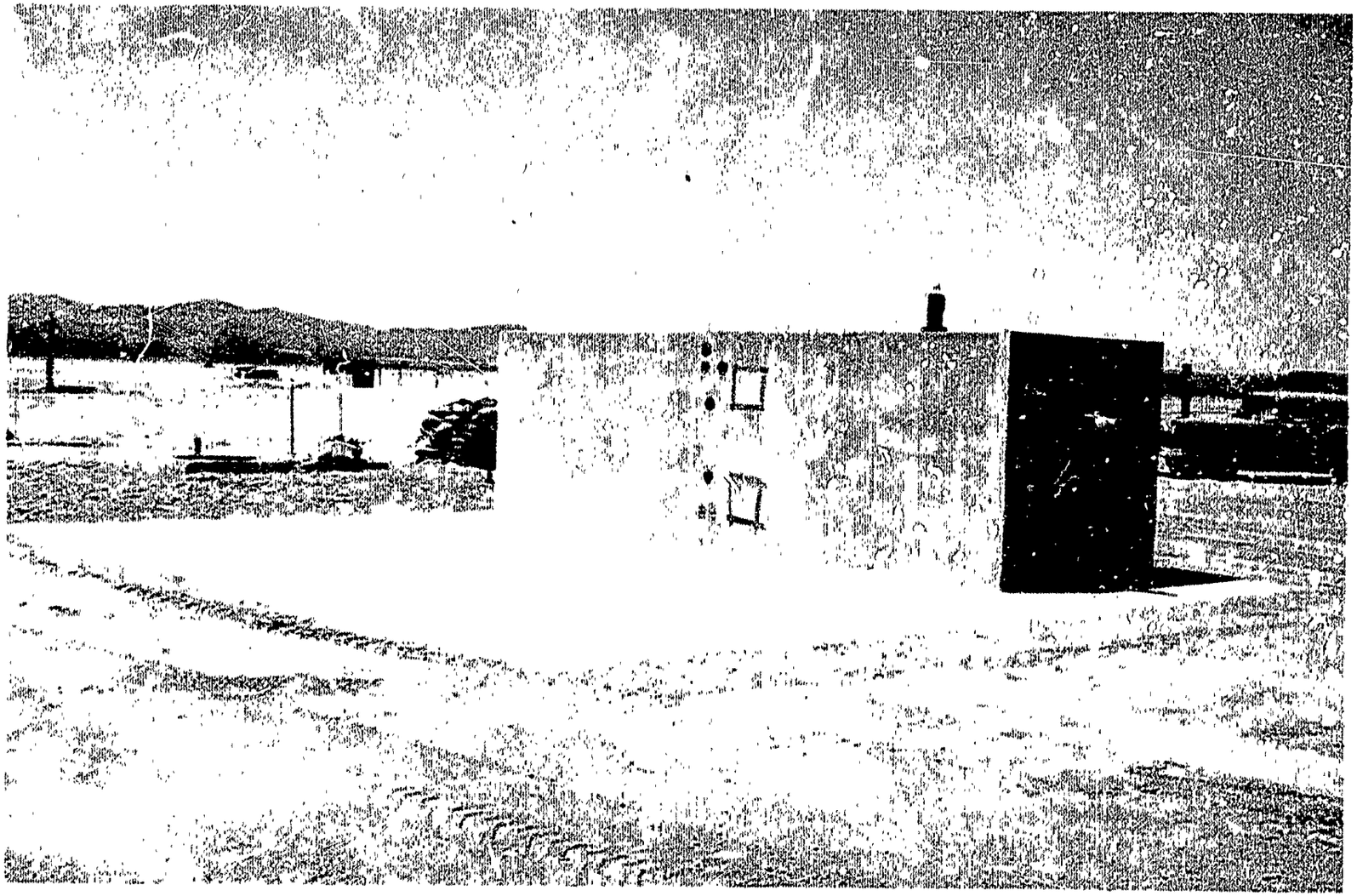

Fig. 1.6—Test structures.

FRONT, TOP, AND RIGHT END

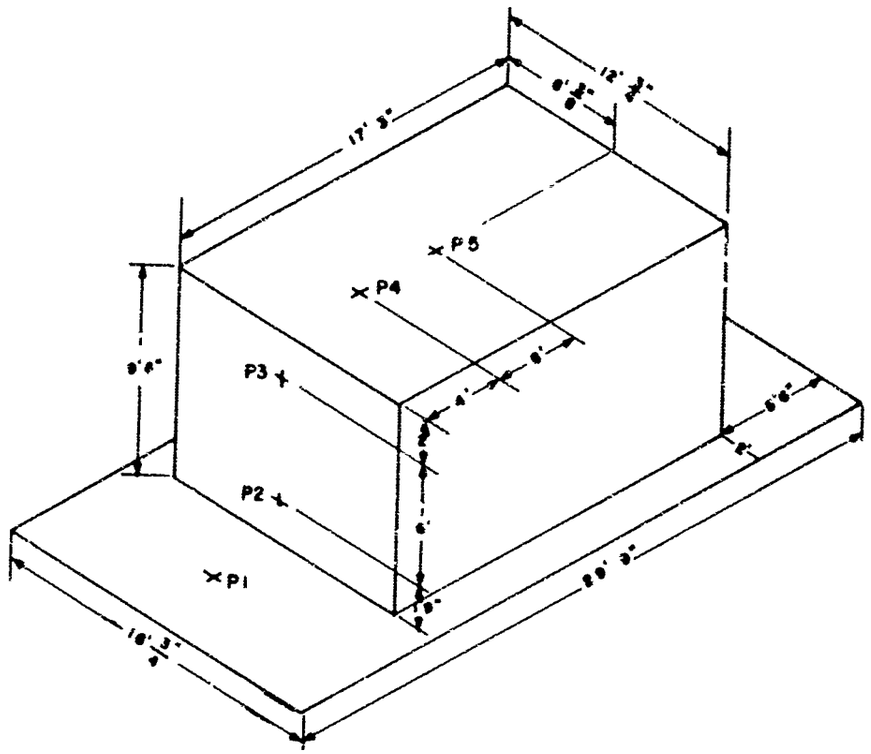

BACK, TOP, AND LEFT END

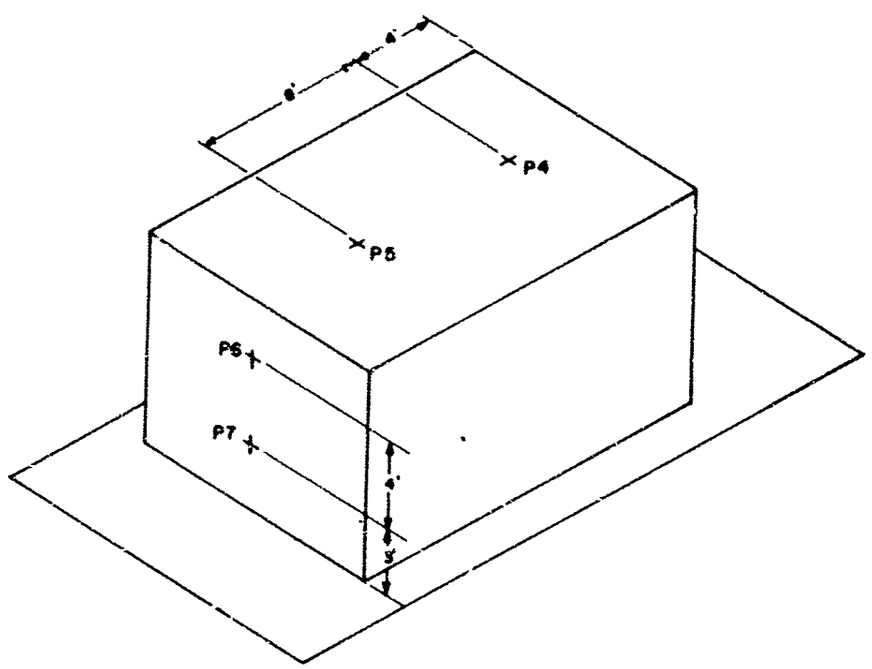

Fig. 1.8—Location of pressure gauges on Project 30.4 test structure.

Chapter 2

TEST RESULTS

2.1 STRUCTURAL DAMAGE

The 6- by 6- by 20-ft test structure experienced no damage other than scouring of the front face by dust and small rocks. Figures 2.1 and 2.2 show the physical appearance of the front of the structure. The most severe scouring appeared near the top of the front of the structure, suggesting higher velocity or greater momentum of particles near the top and demonstrating something of a boundary-layer effect.

Some structural damage to the front face was sustained by the Project 30.4 structure. (See Ref. 1 for a detailed report of damage to the Project 30.4 structure.) The damage is not believed to have had any significant effect on the pressure measurements made on the structure during the early times. There may have been a small effect at later times.

2.2 INCIDENT GAUGE RECORDS

All nine channels involved in the tower measurements performed satisfactorily through zero times. Some channels (e.g., the Greg gauges at the 3- and 10-ft levels and a Snob gauge at the 3-ft level) gave incomplete records; however, histories during most of the blast-wave passage were obtained. The reason for the failure of the instruments at the 3-ft level was an electrical failure, induced, in all probability, by vibration. At the 10-ft level, the entire nose probe of the Greg was removed by a large missile.

Arrival times, peak values, and times of peak value for the various special instruments are listed in Table 2.1.

Unfortunately no satisfactory wind-direction measurements were obtained. The yaw measure was lost because of recorder amplifier failure. A noisy, not overly credible pitch record was obtained. Records obtained are reproduced in Figs. 2.3 through 2.7.

The summary of gauge results for all gauges measuring free-field phenomena is given in Table 2.2. The summary includes arrival times, peak overpressures and the times they occurred, and positive-phase duration and impulse.

All ground-baffle pressure measurements showed expected wave shapes but gave values generally thought to be slightly low.

2.3 TEST STRUCTURE GAUGE RECORDS

Of 38 gauges on the structures, 1 was lost completely and 2 were impaired after giving all, or some part of, the record. Ten records show that the gauges filled with dust at or after the time of the peak over-pressure.

Gauge records obtained indicated that the set ranges were adequate and that no gauge was significantly overranged. Records from the gauges on the Project 30.4 structure are shown in

Figs. 2.8 and 2.9. Those from the gauges on the 6- by 6- by 20-ft structure are shown in Figs. 2.10 through 2.16. The results of the measurements are summarized in Table 2.3.

In lieu of the acoustic damping requested, the Wiancko gauges were mechanically damped with heavy grease by the manufacturer. This resulted in gross overdamping of all gauges supplied by the manufacturer. Overdamping has no serious effect so long as the pressure differential is reasonably large. The most deleterious effect to the records was the inaccurate recording of the positive-phase duration since the lag introduced by the grease made the durations appear longer than they actually were. So that the effect of overdamping on the over-all program would not be too serious, four acoustically damped gauges were incorporated. Three were placed in the ground baffles to give accurate positive-phase duration for the incident wave (1900, 2000, and 2100 ft). One such gauge (P-11) was placed on the top of the 34.1 test structure for the same reason.

Failure to provide for acoustic damping was probably the major factor contributing to the large amount of dust filling of some gauges.

2.4 MODIFICATION OF GAUGE RECORDS

Three types of problems were encountered which detracted from the value of certain of the gauge records. These were dust filling of gauges, induced electrical signal, and low gauge signal. To have discarded these records would have prejudiced the results. So that as much information as possible could be salvaged, certain modifications were made to the faulty gauge records. It should be kept in mind that, although the modifications were made to improve the value of the record, they must still be viewed with some skepticism.

The following gauges were dust filled: Q-1150-3, Q-2000-3, PMS-2, PMS-3, PC-3, PC-4, PC-6, PC-7, PC-22, PC-23, PC-24, and PC-25. The extent of dust filling of gauges PC-3, PC-4, PC-6, and PC-7 was evaluated by comparing values at various times with values at corresponding times from records from PC-1, PC-2, and PC-5, which did not dust fill. By this means the amount of dust filling with time was determined and subtracted from the record, giving the results shown in Fig. 2.17. A similar technique was used on gauges PC-22, PC-23, PC-24, and PC-25; but, because no gauge was completely free of dust filling, the modification was not as reliable as in the case of those discussed above. No suitable modification was found to correct for the dust filling in Q-1150-3, Q-2000-3, PMS-2, and PMS-3 although an estimate was made of their impulses.

Gauge PMS-6 (Fig. 2.9) picked up an induced 60-cycle signal from electric equipment installed for Project 30.4. Based on the average amplitude of the 60-cycle signal before and after the shock signal, the effect of the 60-cycle signal was arithmetically filtered out, resulting in the pressure vs. time curve shown in Fig. 2.18.

As shown in Fig. 2.9, the amplitude of PMS-7 was less than one-fourth that of PMS-6, although both gauges were located on the back wall of the structure. Impulses of gauges on the back of the 6- by 6- by 20-ft structure showed considerable scatter but gave no conclusive evidence of an impulse gradient with height above the ground even though there was an appreciable gradient on the front. It is assumed that the same lack of impulse gradient holds true for the back of the Project 30.4 structure. Although no mechanical or electrical error could be found, one is suspected; therefore the amplitude of PMS-7 has been arbitrarily increased by 4.7 so that its positive-phase impulse is equal to that of PMS-6. The results indicate, when compared with the record from PMS-6 without the 60-cycle signal, that, except for amplitude, PMS-7 is a credible record (see Fig. 2.18).

2.5 DATA REDUCTION

The magnetic tapes were played back on oscillograph paper. When the paper records were read, all upper and lower peaks were read, as well as one or more points between. Since high-frequency pressure changes are of little significance to loading, the records were arithmetically smoothed before plotting.

REFERENCE

1. E. Cohen and E. Laing, Response of Protective Vaults to Blast Loading, Project 30.4, Operation Plumbbob Report, ITR-1451, September 1957.

TABLE 2.1 — MAXIMUM VALUES OF FREE-FIELD TOWER MEASUREMENTS (2000 FT WEST OF GZ)

Instrument	Elevation, ft	Arrival time, sec	First maximum		Second maximum		Remarks
			Value, psi	Time, sec	Value, psi	Time, sec	
Greg	3	0.486	140 (spike to 165)	0.661	145 (spike to 167)	0.764	Gauge damaged after blast-wave passage
	10	0.486	170	0.625	145	0.743	Gauge damaged after second maximum
Snob	3	0.487	42	0.545	65	0.753	Gauge damaged after second maximum
	10	0.487	120	0.635	93	0.748	
Pitot-static tube	3	0.486	48	0.521			Gauge plugged after maximum
	10	0.485	140	0.632	108	0.755	
Force plate	3	0.485	117 (spike to 129)	0.662	110 (spike to 117)	0.746	
Snob side-on	3	0.482	17	0.554	25	0.798	
	10	0.486	24	0.591	36	0.795	

TABLE 2.2 — SUMMARY OF FREE-FIELD GAUGE RESULTS

Distance, ft	Gauge	Location	Calibration pressure, psi	Time of arrival, msec	First peak overpressure, psi	Time of arrival of first peak, msec	Second peak overpressure, psi	Time of arrival of second peak, msec	Positive-phase duration, msec	Positive-phase impulse, psi-msec
1150	PGB-1150-0	Ground baffle	75	222	17	268	87	312	462	8.14
1150	Q-1150-3	3 ft	375	223	518	305				
1700	PGB-1700-0	Ground baffle	30	369	9.3	485	31.8	592	598	4.86
1700	PGBU-1700-0	Ground baffle	30	369	14	467	37.2	594	806	7.21
1800	PGB-1800-0	Ground baffle	27	401	8.6	465	23	653	720	4.5
1800	PGBU-1800-0	Ground baffle	27	402	12.6	444	23	653	540	4.48
1900	PGB-1900-0	Ground baffle	24	438	10.4	463	27.3	713	619	4.7
2000	PGB-2000a-0	Ground baffle	21	483	19.2	663	25.8	805	552	5.17
2000	PGB-2000b-0	Ground baffle	21	484	11.8	645	24.2	822	578	4.05
2100	PGB-2100-0	Ground baffle	15	524	15.1	538	12.6	883	578	3.75
2000	G-2000-3		162	486	140 (spike to 165)	661	145 (spike to 167)	764	Gauge damaged after blast-wave passage	
2000	G-2000-10		162	486	170	628	145	743	Gauge damaged after second maximum	
2000	S-2000-3		90	487	42	545	65	753	Gauge damaged after second maximum	
2000	S-2000-10		90	487	120	635	93	748		
2000	SS-2000-3		21	482	17	554	25	798		
2000	SS-2000-10		21	486	24	591	36	795		
2000	Q-2000-3		135	486	48	521			Gauge plugged after maximum	
2000	Q-2000-10		135	486	140	632	108	755		
2000	FP-2000-3		120	485	117 (spike to 129)	662	110 (spike to 117)	746		

TABLE 2.3—SUMMARY OF RESULTS OF GAUGES LOCATED ON TEST STRUCTURES

Gauge	Location	Calibration pressure, psi	Time of arrival, msec	First peak overpressure, psi	Time of arrival of first peak, msec	Second peak overpressure, psi	Time of arrival of second peak msec	Positive-phase duration, msec	Positive-phase impulse, psi-sec
				Project 30.4, 1150 ft					
PMS-1	Footing	600	219	277	309			Failed at 533 msec	
PMS-2	Front	600	222	410	313				24.0* (Dust filled)
PMS-3	Front	600	221	668	300				42.3* (Dust filled)
PMS-4	Top	75	225	20	270	66	316	400	5 43
PMS-5	Top	75	227	15.5	252	60	319	342	4 97
PMS-6	Back	66	227	18	259	39	345	363	4.36
PMS-7	Back	66	231	4.6(21.3)*	250	6.2(28.8)*	356	334	0 92(4.32)*
				Project 34.1, 2000 f					
PNC-1	Front	132	478	61	625	59	785	636	12 86
PC-2	Front	132	478	81	629	57	787	533	12.6.
FPC-1	Front	120	478	69	617	65	786	Failed at 617 msec	
PC-3	Front	132	481	45	626	56	789		13.6* (Dust filled)
PC-4	Front	132	480	102	624	69	783		14.8* (Dust filled)
FPC-2	Front	120	481	104	626	138	783	622	21.86
PNC-5	Front	132	481	166	626	90	783	712	18.66
PC-6	Front	132	481	166	624	72*	783*	781*	17.8* (Dust filled)
PC-7	Front	132	481	175	625	71	762	343*	16.2* (Dust filled)
PC-8	Top	21	484	14.1	543	6.6	915	599	0 36
PC-9	Top	21	484	14.3	546	5.4	925	696	0 69
PC-10	Top	21	484	9.7	537	5.3	925	628	0.46
PC-11	Top	21	485	10.9	547	6.1	904	558	1.02
PFC-3	Top	21	482	13.7	630	3.5	923	509	0 75
YP-C-1	Right end	45*	487	16.5* up	490	27.7* down	892		
PC-12	Top	21	485	9.6	547	5.8	953	700	1.76
PC-13	Top	21	484	11.1	549	6.6	944	682	1.59
PC-14	Top	21	484	8.8	550	6.2	949	685	1.79
PC-15	Back	15	484	6.23	531	6 5	943	799	1.53
PC-16	Back	15	485	4.9	533	5.1	941	727	1.22
PC-17	Back	15	485	6.9	510	6.3	944	705	1.25
PC-18	Back	15	486	6.8	513	7.4	897	810	1.62
FPC-4	Back	15	484	9.7	492	11.8	836	692	1.76
PC-19	Back	15	486	7.8	514	7.2	954	706	1.52
PC-20	Back	15	487	9.5	492	8.2	899	686	1.09
PC-21	Back	15	487	6.6	514	6.2	900	707	1.39
PC-22	Front footing	132	474	17.1	620	24.2	796	575*	5.93* (Dust filled)
PC-23	Front footing	132	476	14	508	33	787	708* (Dust filled)	5.75*
PC-24	Front footing	132	481	26	538	37.4	786	575*	6.45* (Dust filled)
PC-25	Front footing	132	483	45.6	650	42	788	555* (Dust filled)	8.88*

*Estimated by correction.

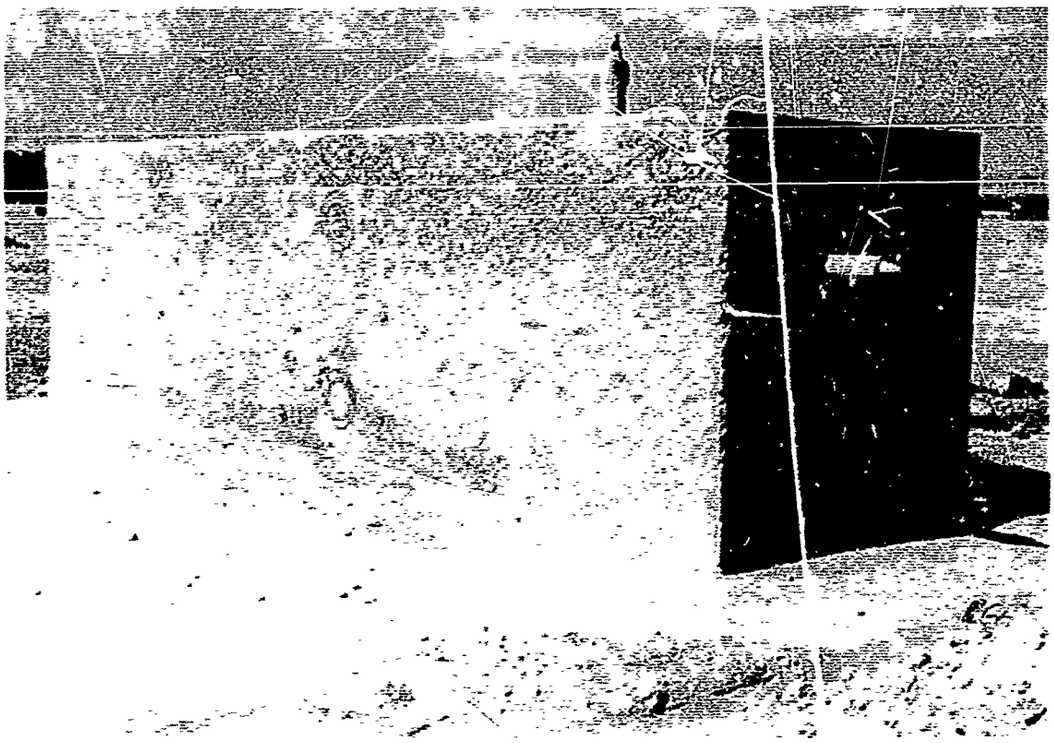

Fig. 2.1—Front face of the 6- by 6- by 20-ft test structure.

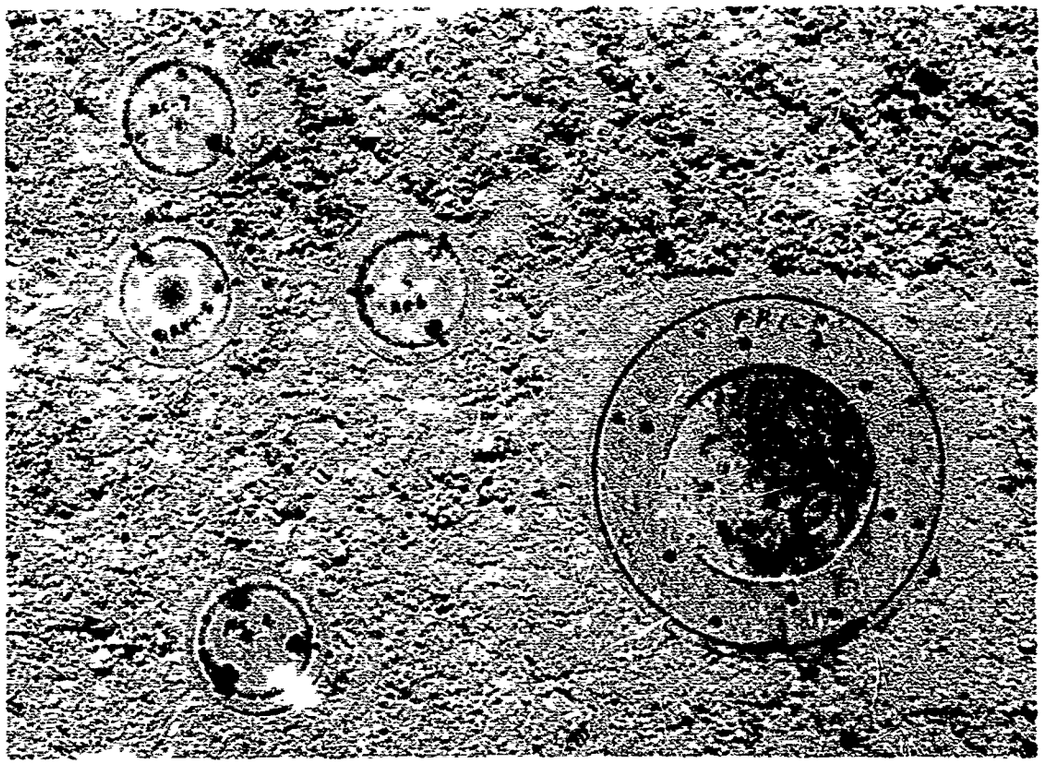

Fig. 2.2—Close-up of the front face of the 6- by 6- by 20-ft test structure.

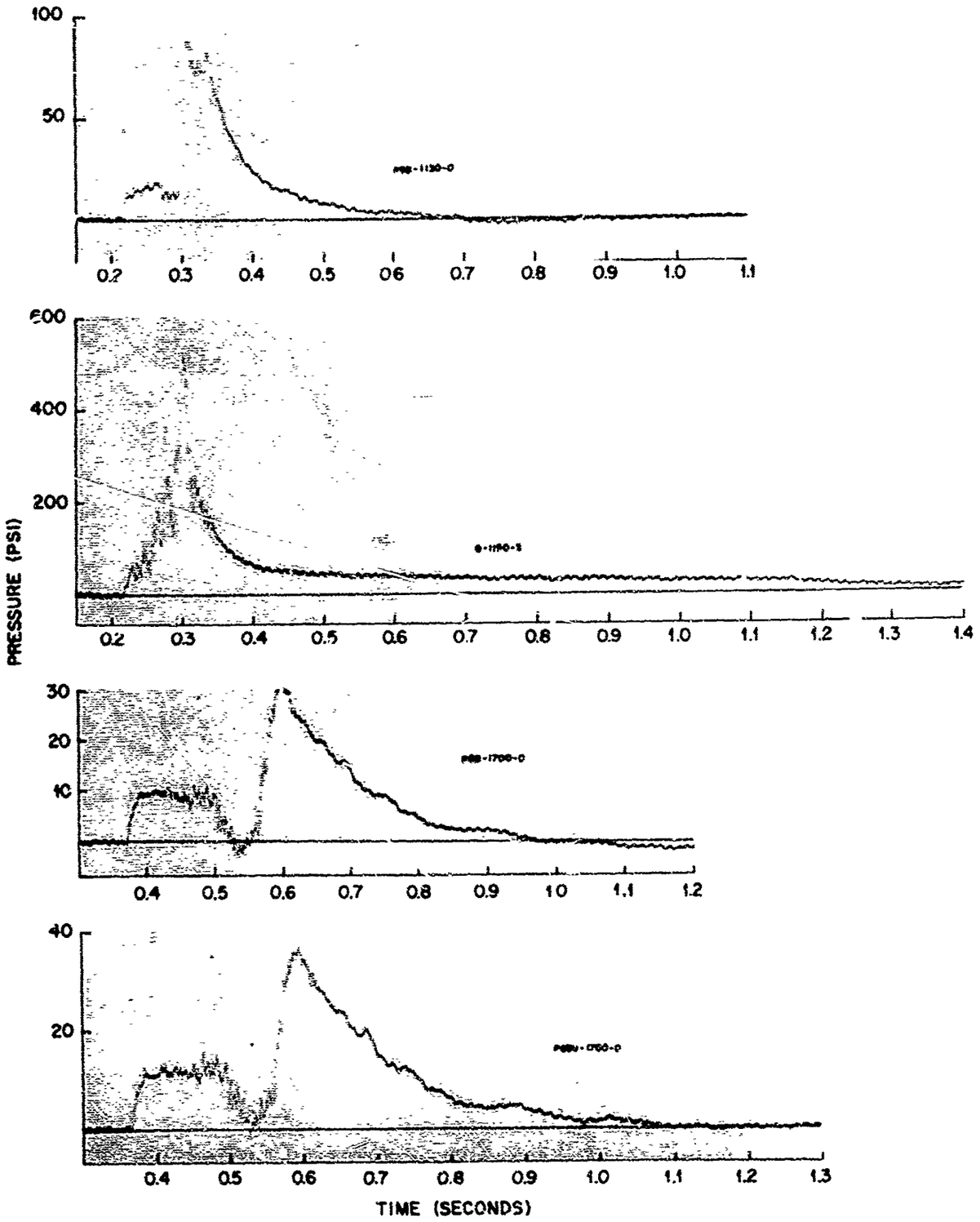

Fig. 2.3—Incident gauge records.

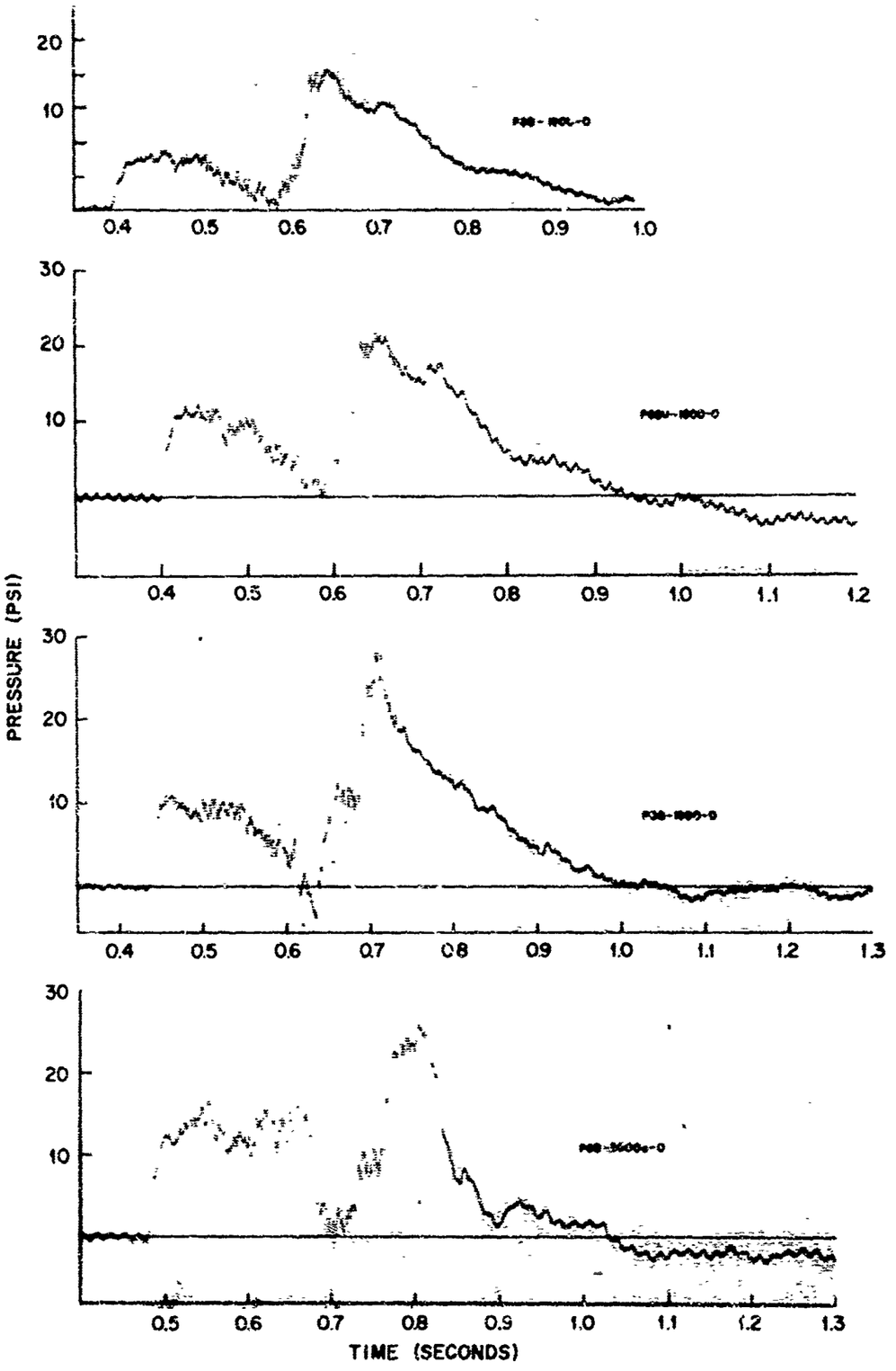

Fig. 2.4—Incident gauge records.

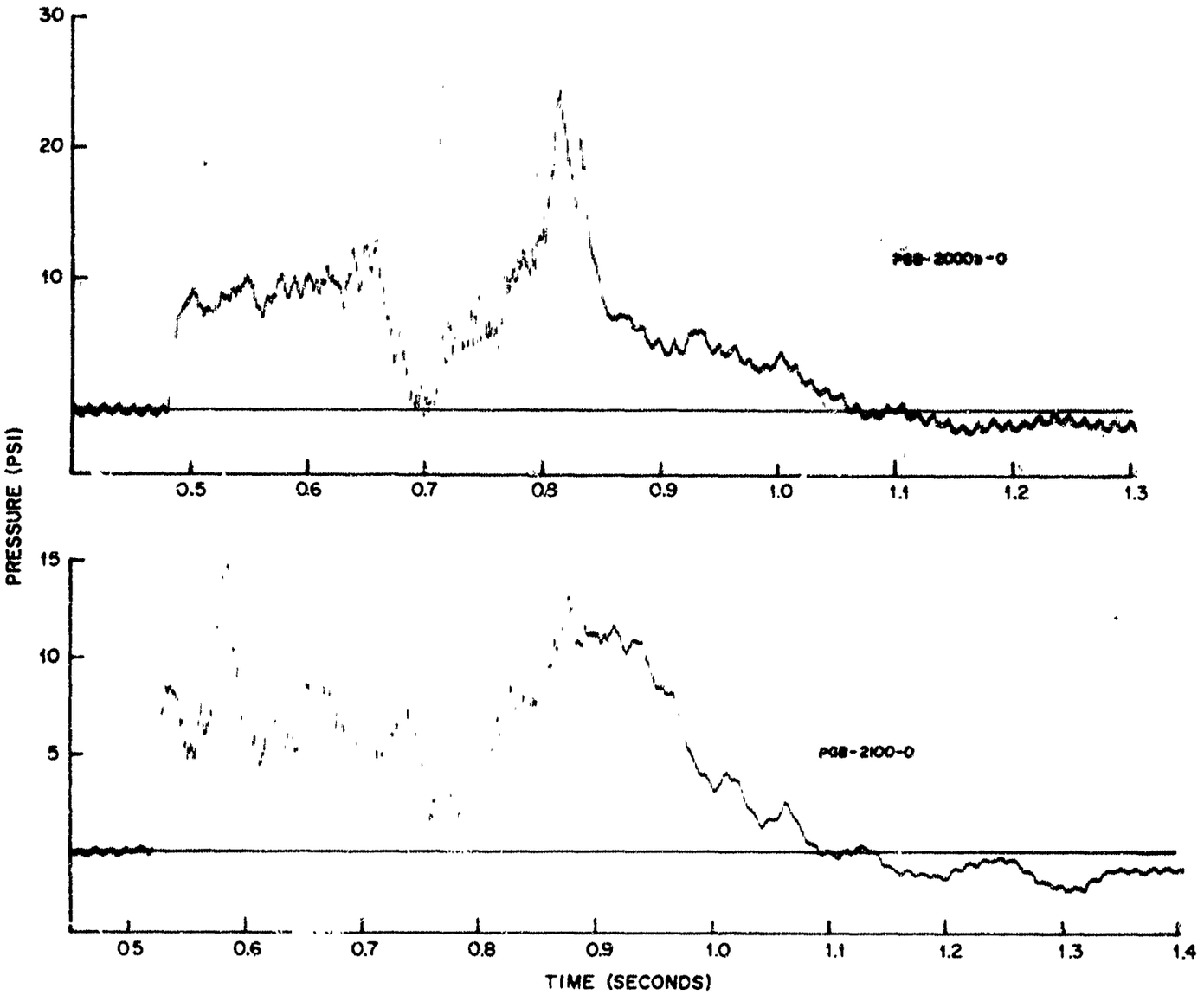

Fig. 2.5—Incident gauge records.

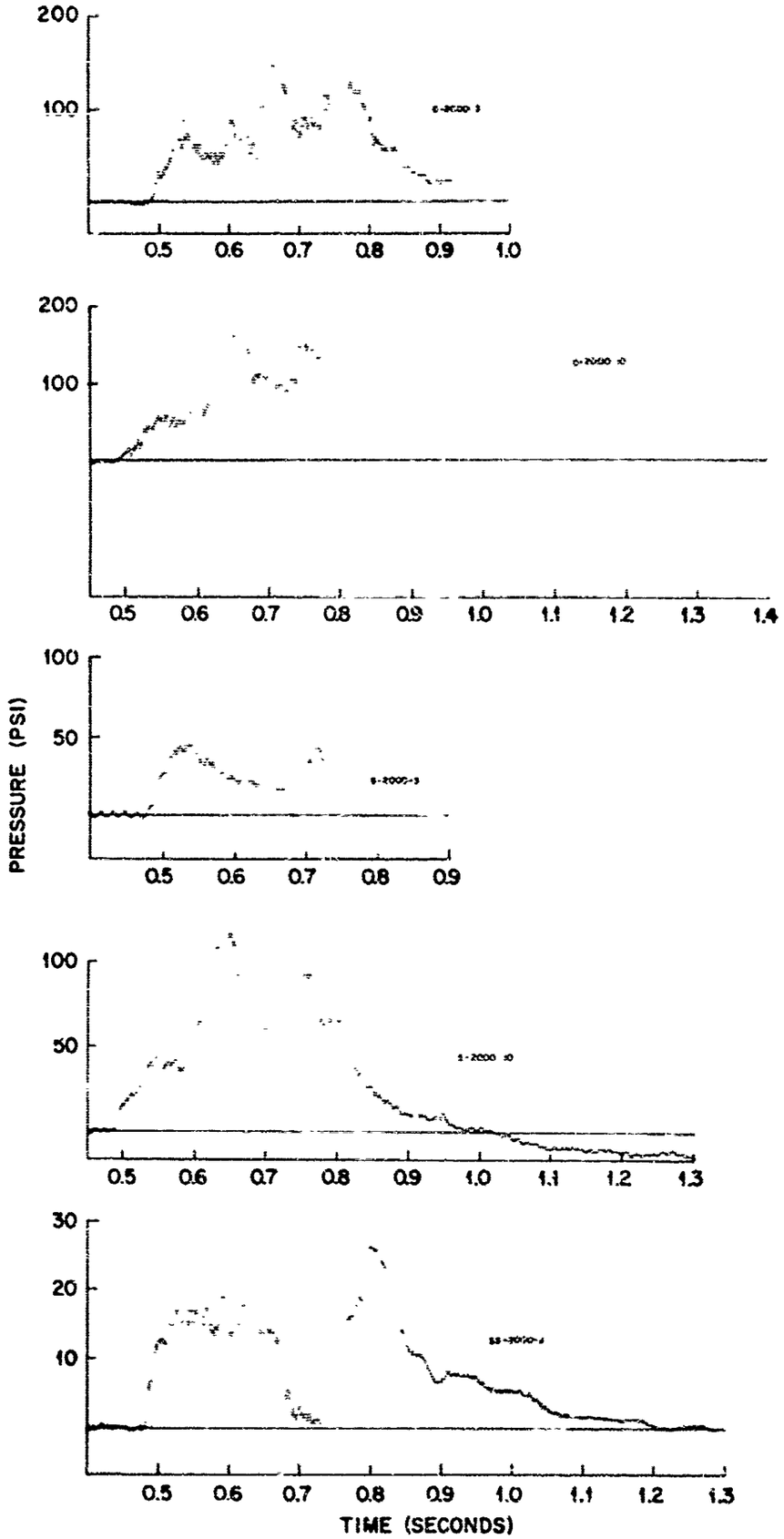

Fig. 2.6—Incident gauge records.

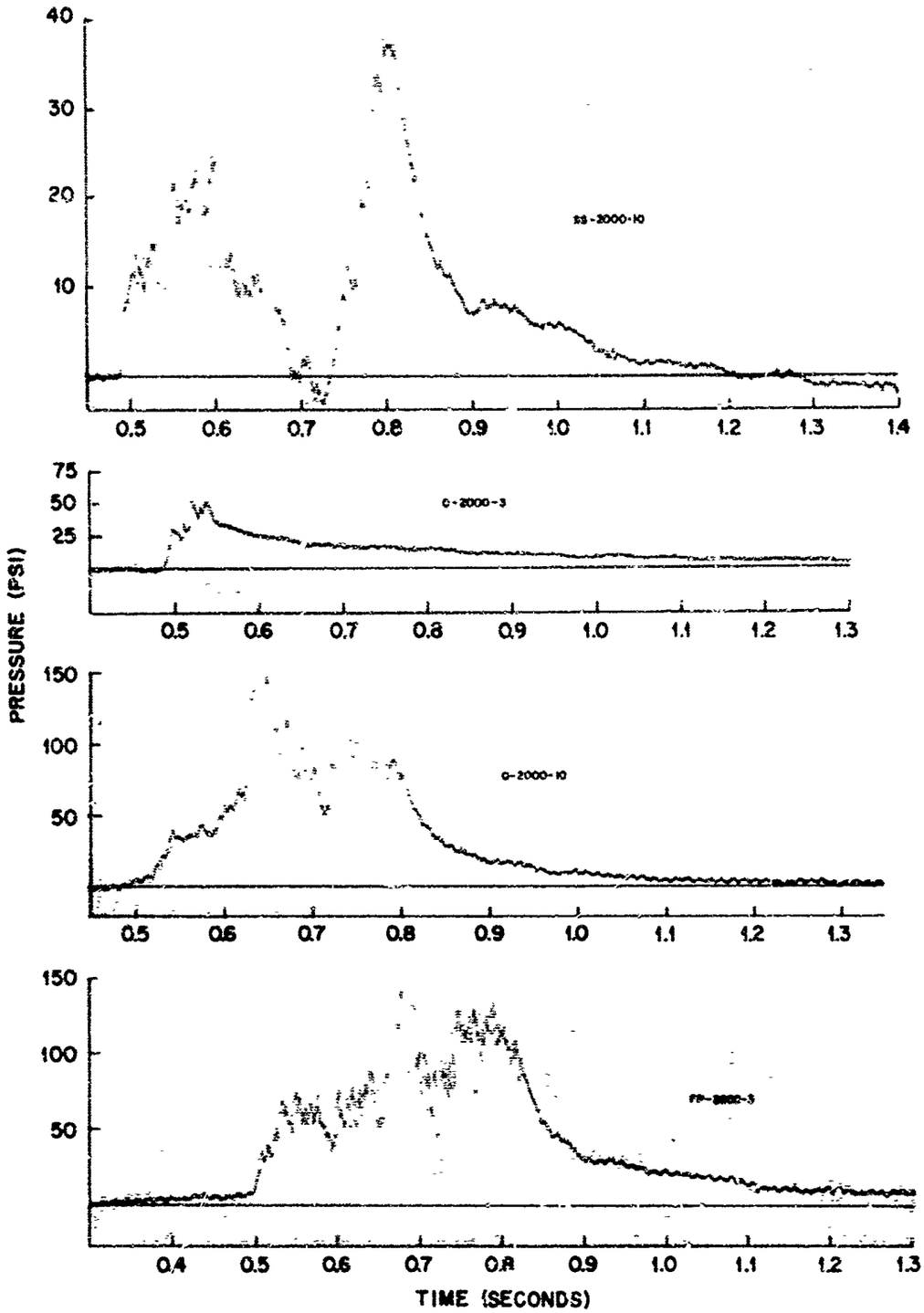

Fig. 2.7—Incident gauge records.

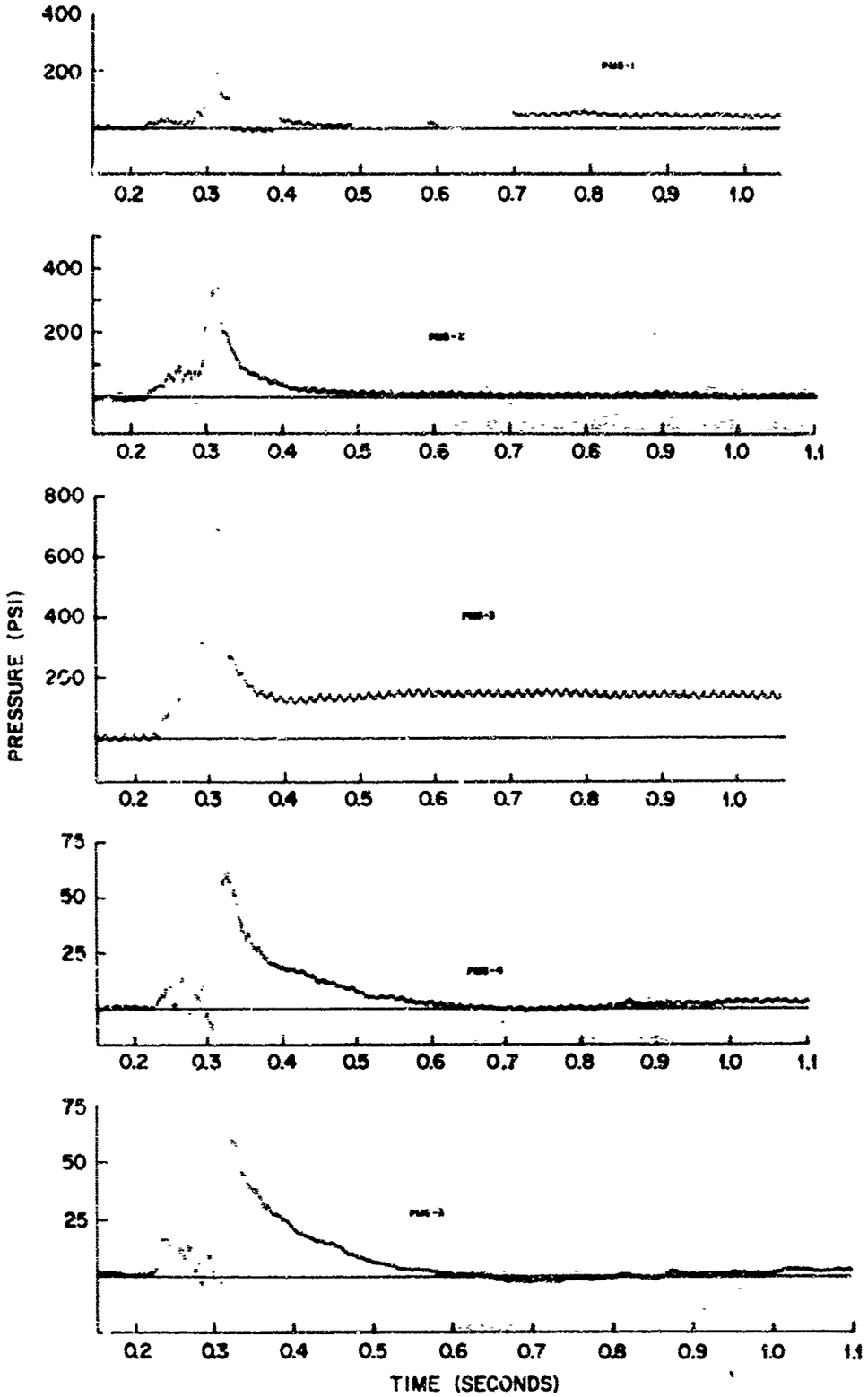

Fig. 2.8—Project 30.4 structure gauge records.

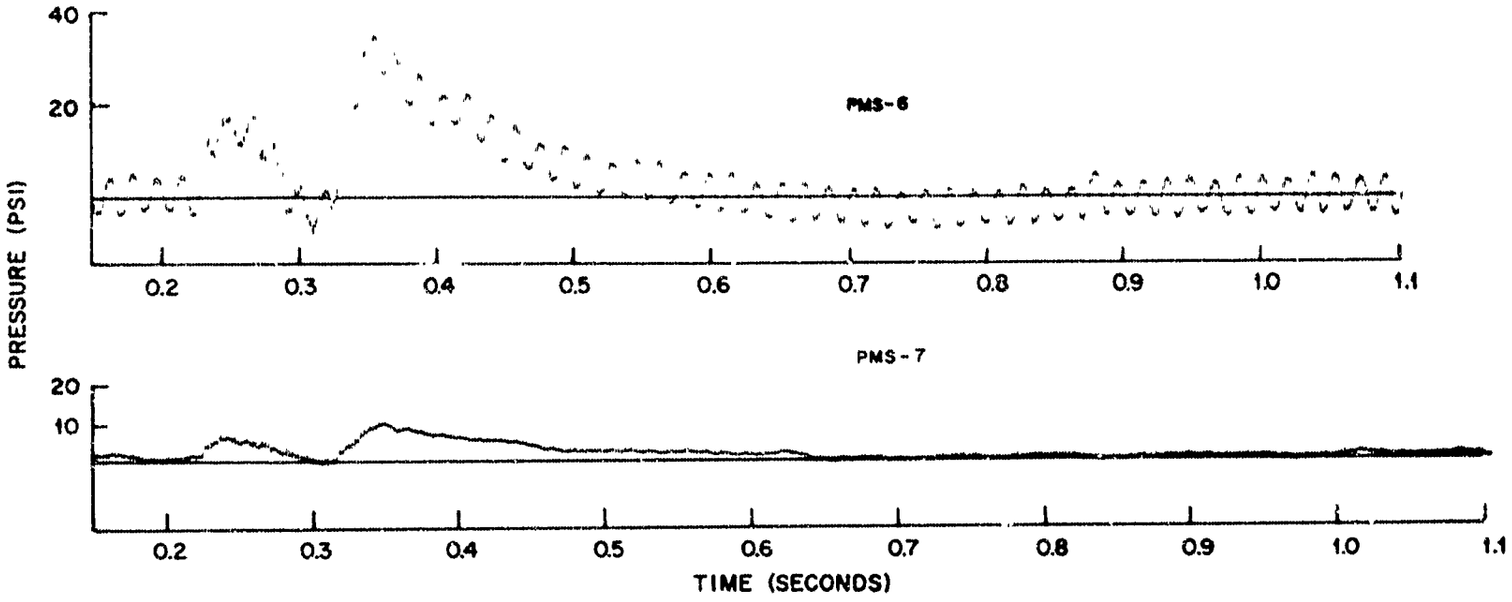

Fig. 2.9—Project 30.4 structure gauge records.

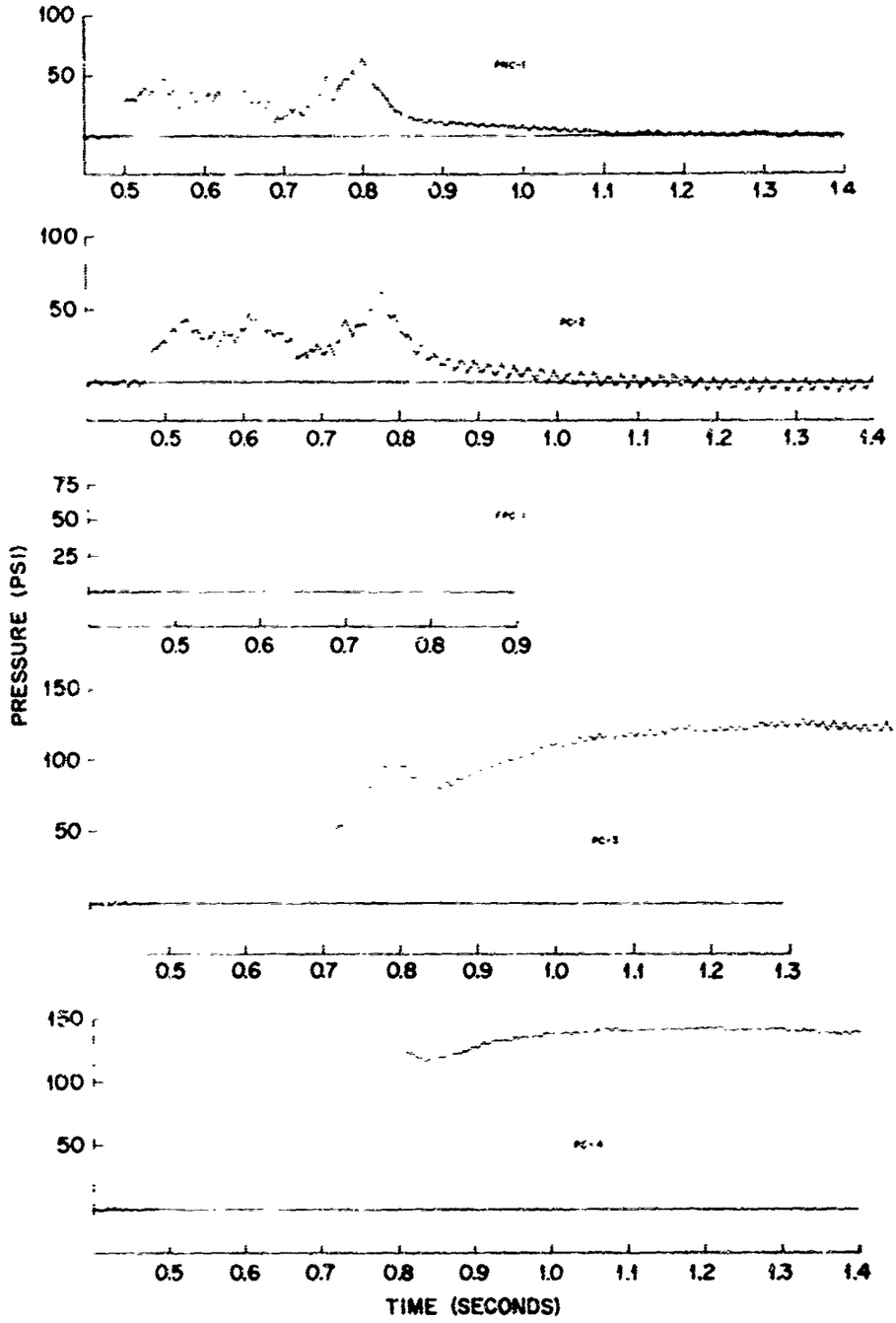

Fig. 2.10—Project 34.1 structure gauge records.

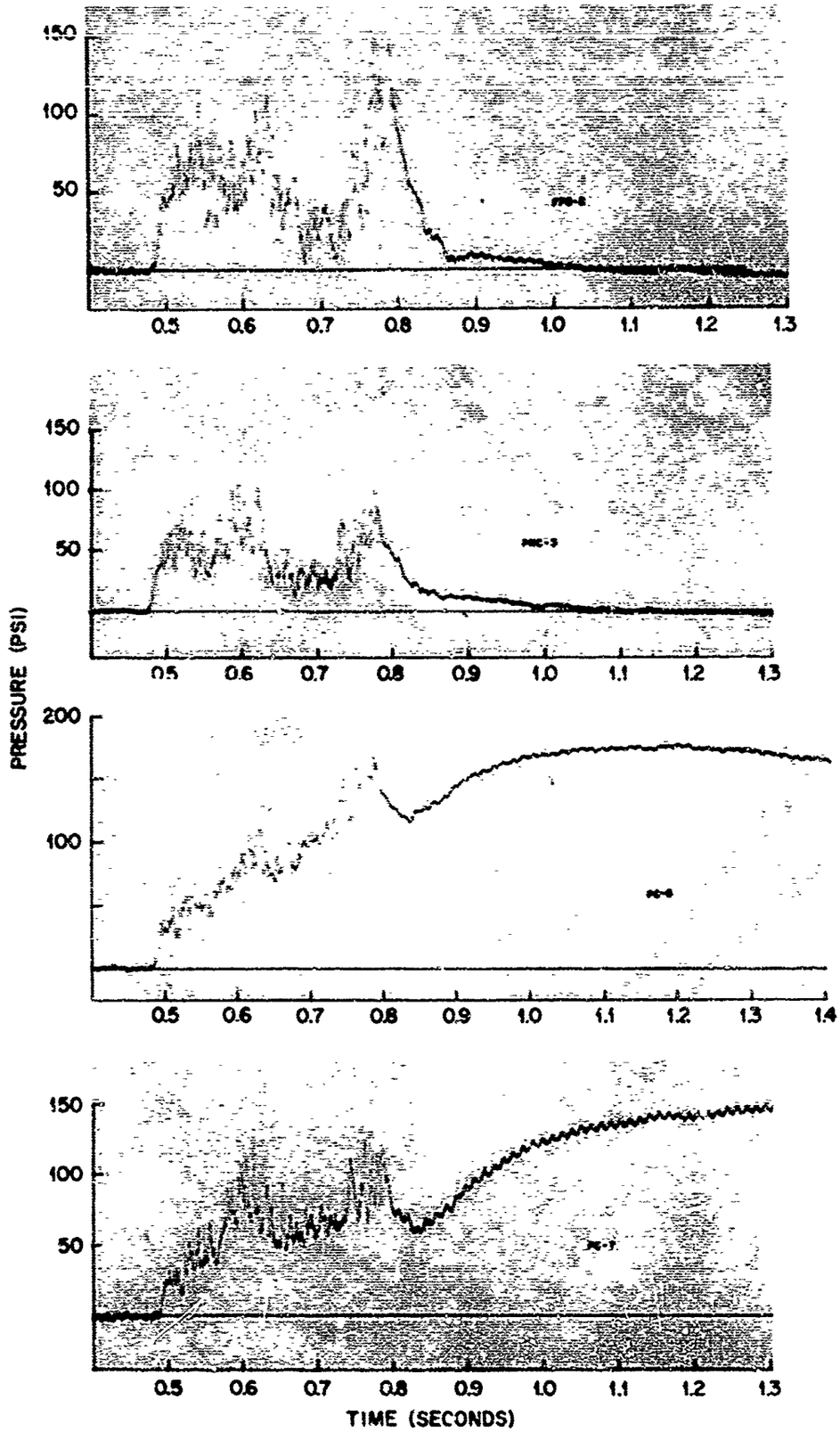

Fig. 2.11—Project 34.1 structure gauge records.

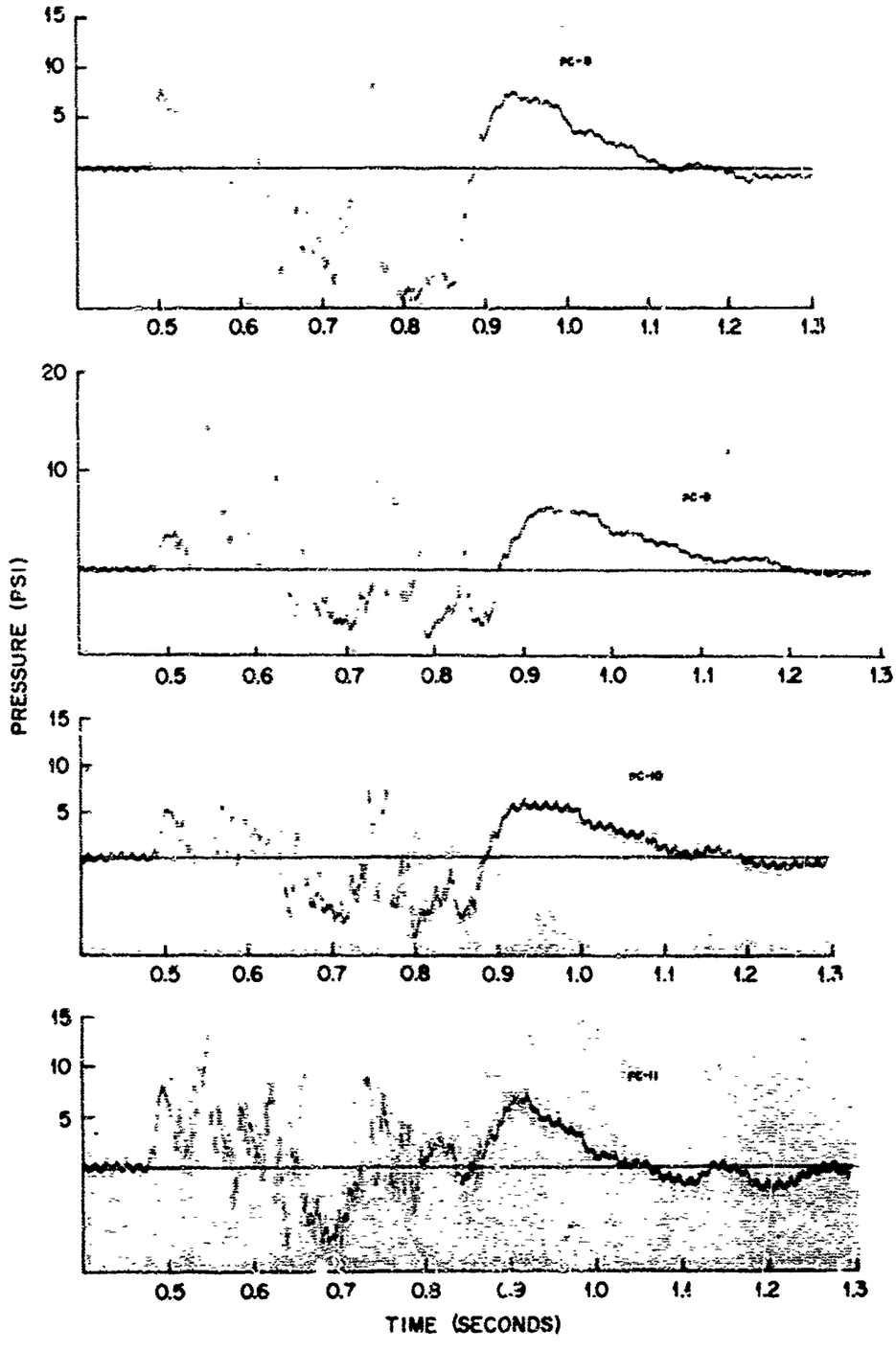

Fig. 2.12—Project 34.1 structure gauge records.

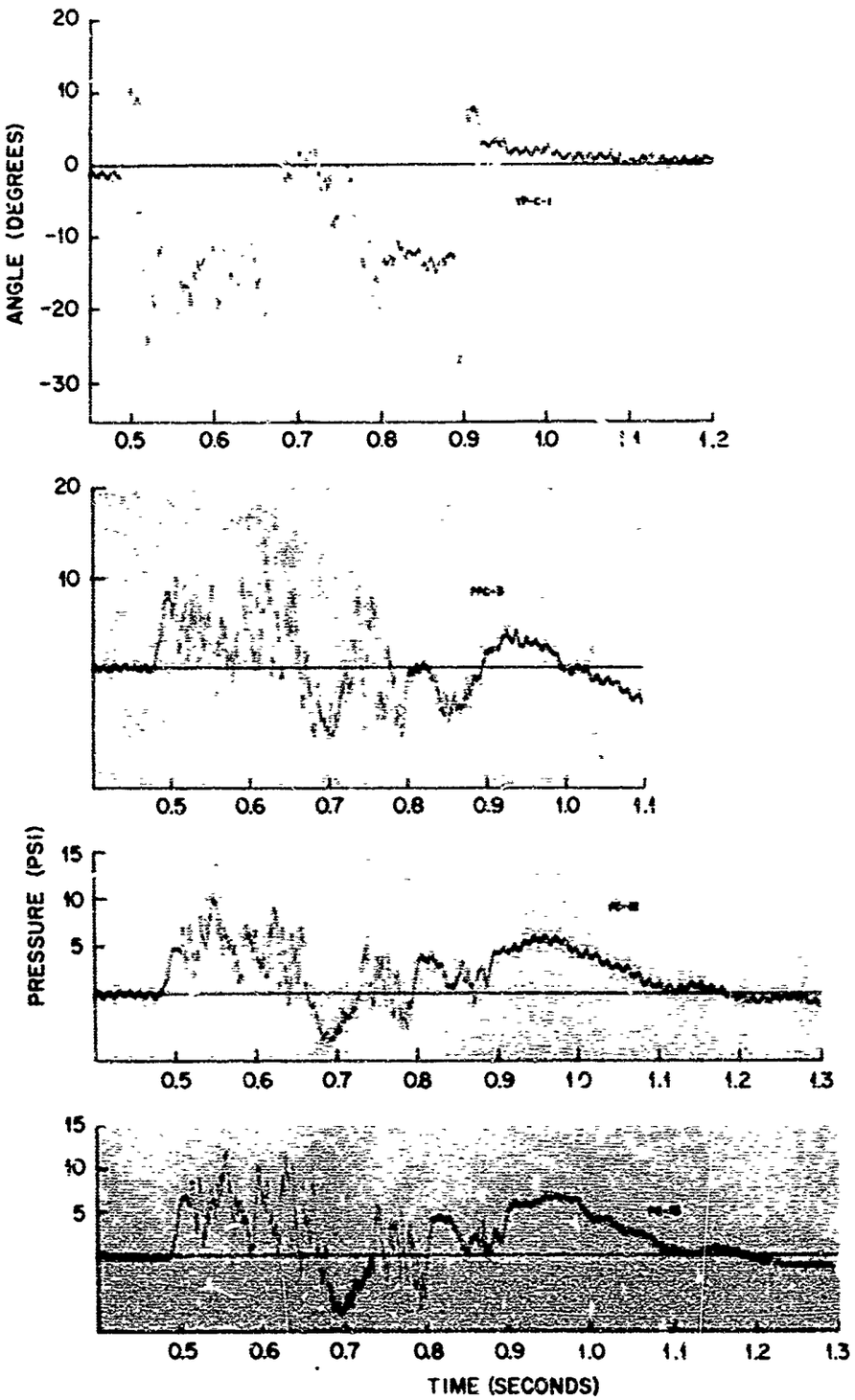

Fig. 2.13—Project 34.1 structure gauge records.

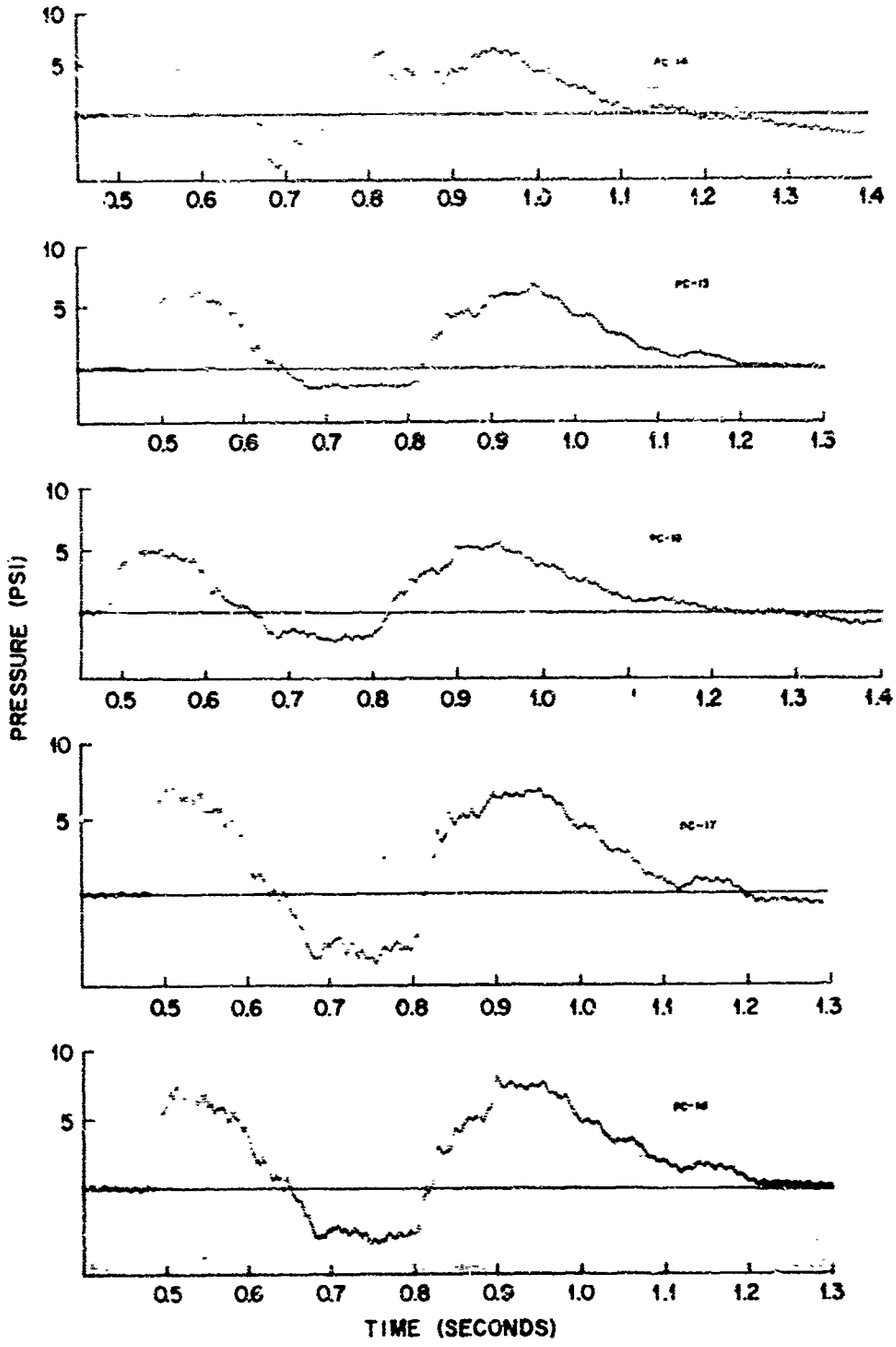

Fig. 2.14—Project 34.1 structure gauge records.

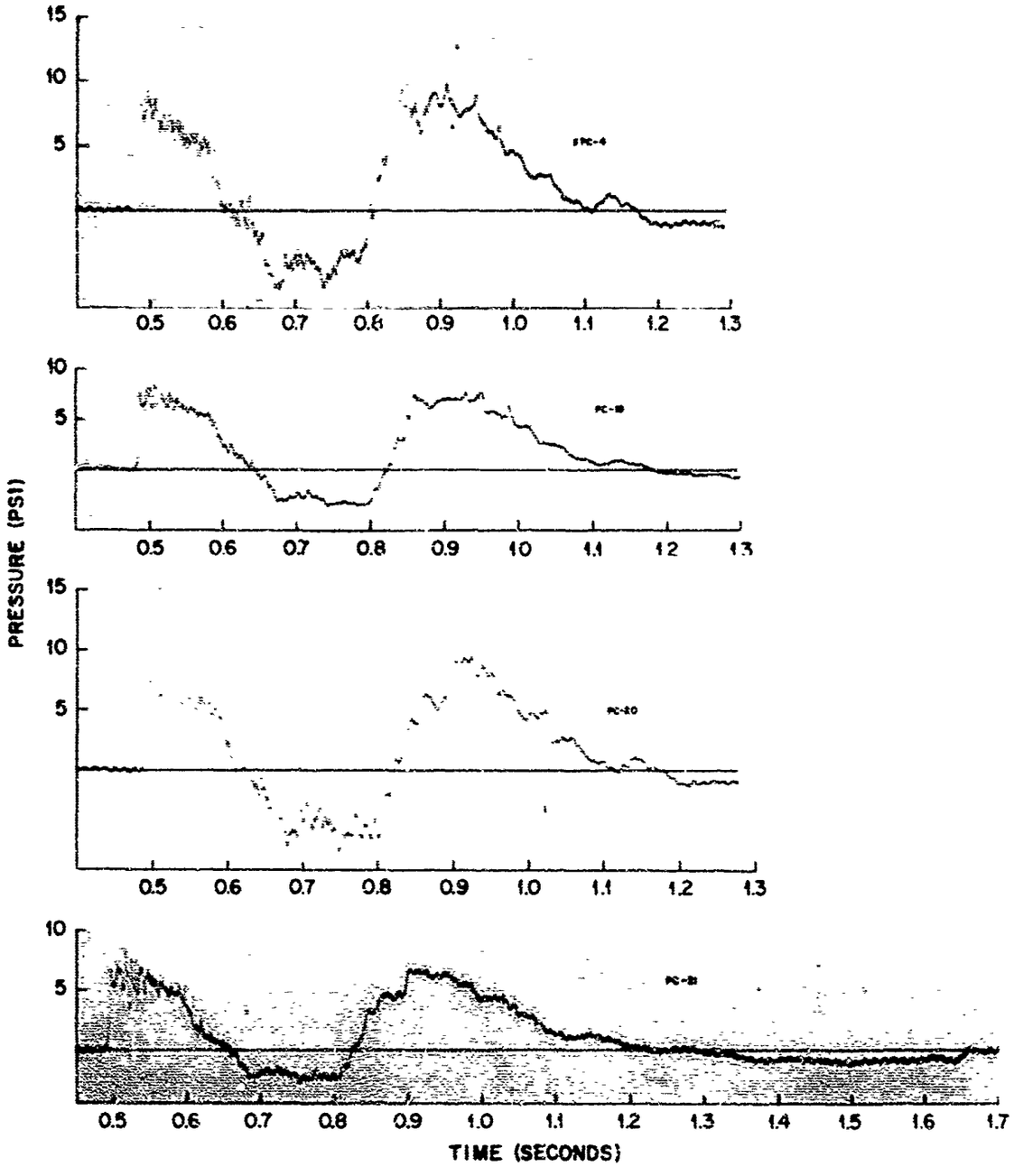

Fig. 2.15—Project 34.1 structure gauge records.

Fig. 2.16—Project 34.1 structure gauge records.

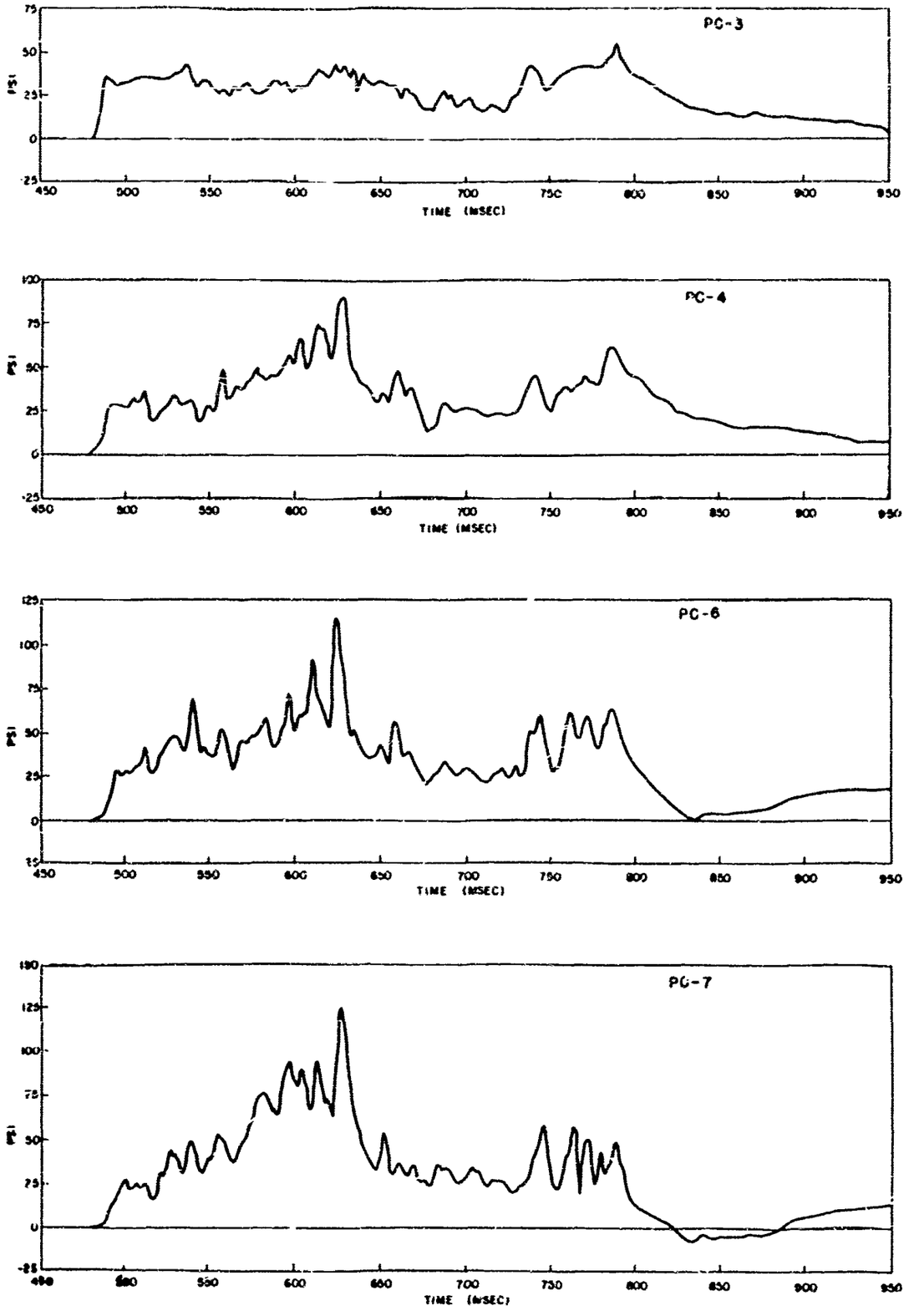

Fig. 2.17—Records corrected for dust filling of gauges.

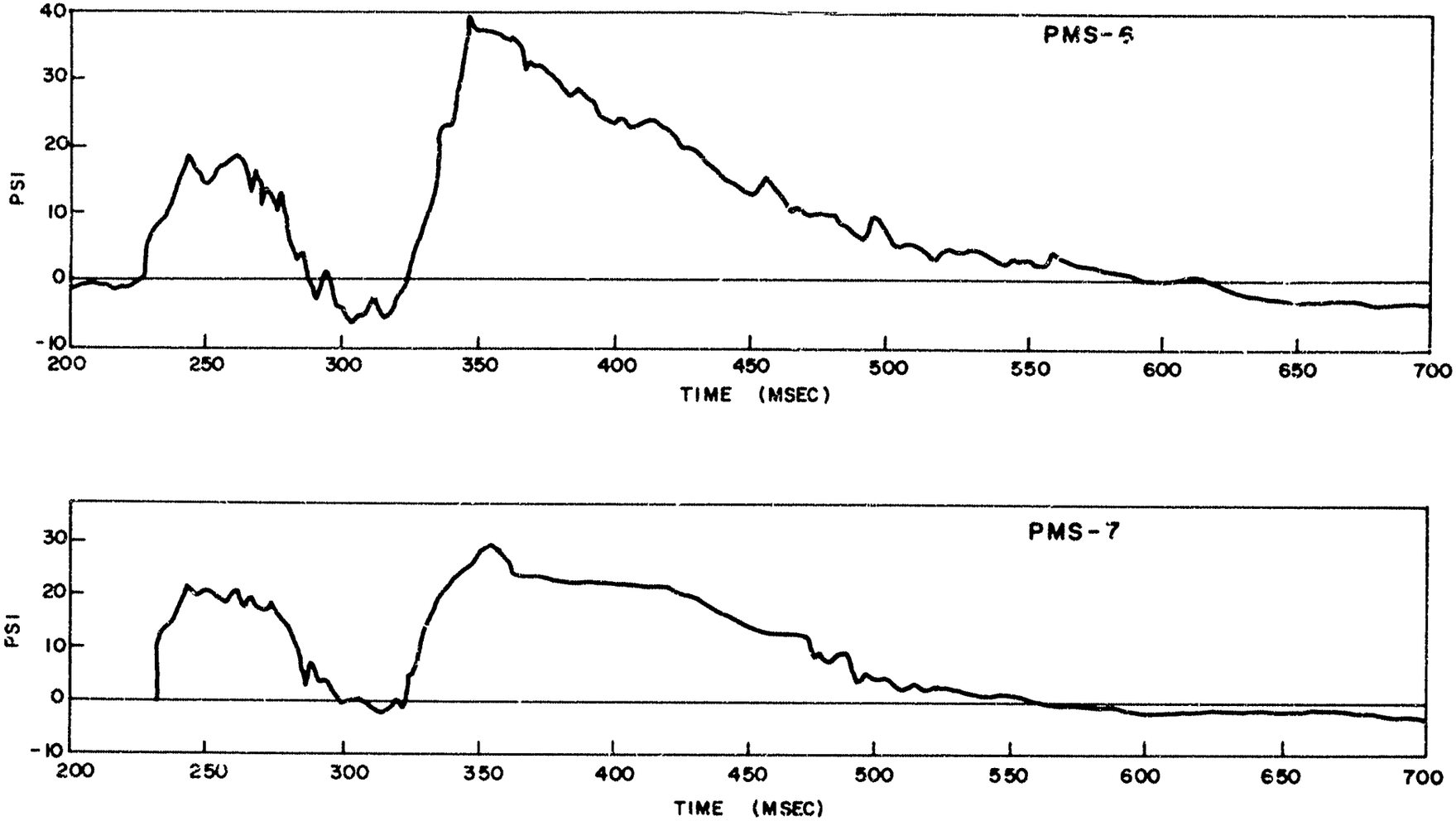

Fig. 2.18—Correction of gauges PMS-6 and PMS-7.

Chapter 3

DISCUSSION

3.1 FREE-FIELD MEASUREMENTS

Before attempting correlation of the free-field measurements with loads on the cubical, we shall first examine the phenomenon history that these measurements and the parameters derivable from them imply. Such a detailed study is worth while since we may compare our conclusions with those obtained in previous field experiments using the same instrumentation.

Both Greg and Snob gauges register the stagnation pressure of air; but the Greg also responds to the momentum flux of dust, which the Snob ignores. The difference between the two is the dust momentum flux ($\rho_d \mu_d^2$ or ϕ_d); whereas the uncorrected air dynamic pressure (q_{ac}) is the difference between the Snob stagnation pressure and the side-on pressure measurements. Air-flow Mach number (M) and the corrected air dynamic pressure (q_a or $\frac{1}{2} \rho_a \mu_a^2$) can be computed from the ratio of stagnation pressure. Finally, the ratio of suspended dust to air density can also be calculated if the air and dust are assumed to be in velocity equilibrium. Such an assumption is well justified at Frenchman Flat since dust particles require only milliseconds to be accelerated.

Raw records for the Snob, Greg, force plate, and Pitot-static tube, as well as side-on pressure measurements, are displayed in Figs. 2.6 and 2.7. Smoothed records of these same instruments are shown in Figs. 3.1 and 3.2. Derived quantities based on the smoothed curves are displayed in Figs. 3.3 through 3.6.

The head-on instruments registering some part of dust momentum flux, all except the Snob, show similar records at the 3- and 10-ft elevations. The general shape of the Snob records at the 10-ft elevation resembles that of the other instruments, but at the 3-ft elevation there is a marked departure since the Snob's response is depressed for a considerable period of time. One's first reaction is that the Snob at the lower level was plugged during part of the blast-wave passage, but more careful examination does not confirm this because in the depressed period turbulence is fully evident on the record. On the other hand, it is obvious that the Pitot-static tube at the lower elevation was completely plugged after 540 msec.

There are other significant differences between the measurements at the 3- and 10-ft levels. Records at both elevations show a gradual increase with time after the shock-wave arrival with a couple of minor peaks during this rise. These records show two marked peaks in the second half of the blast wave which are separated in time by about 100 msec. At the 10-ft elevation, however, the marked peaks begin more sharply and earlier than those measured at the lower elevation. This is particularly true of the first peak where the maximum values are achieved 35 msec earlier at the higher elevation. Furthermore, the first peak has a greater amplitude at this level; whereas the two peaks have about the same value at the lower elevation.

An examination of the derived quantities suggests the reason for this difference. The period of the first peak (625 to 700 msec after time zero) was a time of high dust concentration (Fig. 3.7) and low mass velocity at the lower elevation; whereas the mass velocities at

the 10-ft elevation were very high. These conditions imply that the origin of the first peak is a high air velocity, first observed at the 10-ft elevation. The high velocity was only gradually and incompletely transmitted by turbulence to the lower elevation. The turbulent coupling was comparatively weak because of the marked difference in the effective densities at 3 and 10 ft. On the other hand, the second peak came when the densities at the two elevations were comparable; therefore the stagnation pressure records at the two elevations are more nearly identical. The other derived quantities, such as air dynamic pressure, emphasize but do not cross-check this conclusion. Air dynamic pressure, both corrected and uncorrected, is high at the 10-ft elevation and low at the 3-ft elevation during the first peak; the two have about the same value during the second peak. The dust momentum flux shows a gradual rise during the blast-wave passage. This rise coincides with observations made during previous experiments. At the lower elevation, however, there is a marked peak. The air-flow Mach number was found to exceed 1 at both elevations. At the higher elevation, this number remained slightly below 2 during the passage of the two peaks. At the 3-ft elevation, the number stayed below 1 until the second peak, when it achieved a value of over 1.5. These high values of Mach number imply high velocities of materials, although, owing to the lack of temperature or density data, precise values cannot be specified. If the temperatures were comparable with those measured during the Teapot 12 shot, the peak velocity at the 10-ft elevation probably was about 3000 ft/sec and over 2000 ft/sec at the 3-ft elevation.

Thus far the force-plate results have been considered in only a superficial manner. The function of this instrument is to determine the effect of obstacle size on the registration of dust momentum flux. The typical stagnation length for a Frenchman Flat particle at 1000 ft/sec is about 10 cm or 4 in. This distance is long compared to the critical dimensions of the Greg and Snob gauges; but it is less than the diameter of the force plate. If an incompressible air flow is assumed, one would assert that the registration of the dust momentum flux should approach that of air and be about one-half the actual value of the dust momentum flux. In fact, this assertion seemed experimentally confirmed for the rather light dust loads of the desert line on shot 12 of Operation Teapot. In this experiment, on the other hand, the stagnation pressure registered by the force plate lies closer to the Greg stagnation pressure than to the Snob, except in the early stages where the test is not definitive. The air-stream lines before the force plate were probably compressed, allowing a higher registration of momentum flux. In the second peak, some basic difference seems to exist between the Greg and the force-plate records since the force plate indicates a longer peak with less amplitude than the Greg.

A comparison of the Greg, Snob, and Pitot-static tube at the 10-ft level can be made. After the first peak the Pitot-static tube seemed to register about half the dust momentum flux. Before the first peak the Pitot-static record lies below both the Snob and Greg records. This discrepancy probably represents a pitch or yaw of the early flow. It is emphasized that the coefficient we have ascribed to the Pitot-static tube should not be taken as a general result but should be applied only to the dust, material velocities, and dust concentrations observed in this test.

Figure 3.8 displays the four side-on pressure measurements taken in the tower vicinity. The pressure record obtained at the ground baffle between the towers and the Snob side-on record are remarkably similar; whereas the pressure record of the ground baffle located 21 ft north of this location indicates a considerably lower amplitude and a different shape. As is usually the case, the 3- and 10-ft-level records agree only in general. The amplitudes are higher and show more fluctuation at the 10-ft level than at the 3-ft level. It is hopeless to try to correlate side-on pressure with the dynamic pressure. The first dynamic-pressure peak comes as the side-on pressure is decreasing from its first peak; whereas the second dynamic-pressure peak comes just before the peak side-on pressure is obtained. This pattern displayed by the second peak was also observed in Operation Teapot measurements.

Since dust momentum flux and related data were obtained in Operation Teapot, we can compare these present results with those, remembering that the Plumbbob location scales to 1660 ft on Met (Shot 12), whereas measurements were made on the Operation Teapot shot at 2000 and 2500 ft. Air dynamic pressures, dust momentum fluxes, etc. are all naturally higher at this closer scaled distance. The sums of air dynamic pressure and dust momentum flux at

the 3- and 10-ft elevations are commensurate with an extrapolation of the Operation Teapot data. From the particulate dynamics standpoint, the most remarkable difference is the considerably greater relative contribution of dust to stagnation pressures at the 3-ft level. Dust and air contributions to stagnation pressure were about equal at 2000 and 2500 ft in Operation Teapot, but the dust contribution at times exceeded that of air by a factor of over 10 in Operation Plumbbob. At the 10-ft level in the later stages, the dust momentum flux contribution also exceeded that of air dynamic pressure; but the excess is not marked and is, indeed, comparable to the Operation Teapot results. In fact, from the effects point of view, the contribution of dust at the 10-ft elevation is not at all remarkable because the earlier peak had higher stagnation pressures brought about mostly by air.

One may ask whether or not the observation of such proportionately higher dust momentum fluxes reopens the question of exploring dust more fully in future tests. From a phenomenological standpoint, the answer still seems negative. This latest experiment seems to confirm that dust is a symptom and not a cause of high dynamic pressures per se. Rather, these high values of dynamic pressure seem to be caused by high mass velocity. In fact, this test has confirmed that these velocities feed through from the upper to the lower layers. Furthermore, it should also be mentioned that the area in front of the station was considerably more loosened by construction and traffic in this test than it was in the Operation Teapot experiment. This condition may have caused an artificial enhancement of the dust concentrations.[1]

3.2 INCIDENT PRESSURES

At the 6- by 6- by 20-ft structure, the precursor of the incident wave was quite pronounced (gauges P-2000a-0 and P-2000b-0; Figs. 2.4 and 2.5) and lasted for approximately 225 msec. The precursor peak overpressure occurred about 180 msec after arrival and was followed by a general decline in overpressure to nearly ambient pressure 40 msec after the peak. This minimum was followed by a gradual rise to the second peak overpressure.

At the Project 30.4 structure, the precursor had a duration of 75 msec. The main shock wave was more pronounced and was not preceded by the marked return to ambient pressure as at the more distant station.

Figure 3.9 shows the pressure-distance curves for Operation Upshot-Knothole shots 1 and 10, Operation Teapot Apple II, and IBM Problem M, all scaled to 37 kt. Superimposed on Fig. 3.9 are the first and second peak overpressures of the measured incident pressure waves. Both first and second peak overpressures behaved in an erratic manner with respect to the earlier shots. Second peaks were higher than the first (precursor peaks) except at the most distant station.

Figure 3.10 shows the positive-phase impulse vs. distance for the free-field gauges of this project. Included in the figure are values[2] for impulse measured by Stanford Research Institute (SRI) as a part of Project 1.3. In a personal communication the authors of Ref. 2 have indicated to us those values they believe to be low owing to a gauge or calibration discrepancy; these have been noted separately on the figure. There is no serious disagreement between those they believe to be true and those they believe to be low except at their most distant station. With the exception of the Ultradyne gauge at 1700 ft, all our impulse values are low by comparison with all the Project 1.3 values. The Ultradyne gauges were not mechanically overdamped, and it is interesting to note that, although the Ultradyne gauge at 1700 ft gave agreement with the Project 1.3 data, the one at 1800 ft gave a value almost identical with the Wiancko gauge. Very real asymmetries in overpressures and wave forms have been observed frequently at the same radial distances on different radii. It is impossible to resolve conclusively whether the differences observed here are due to asymmetries or to mechanical overdamping of the gauges. In view of the asymmetry that appears between the structure and the free-field gauges only 35 ft away, it is not surprising to note asymmetries between two sets of pressure gauges about 100 ft apart.

Figure 3.11 shows shock arrival time vs. distance for the free-field gauges. If the peak overpressure vs. shock velocity relation presented by Shreve[3] for Upshot-Knothole 1 is assumed to hold for shot Priscilla with its larger yield and higher burst height, the overpressures of the first peaks would be as shown by the dashed line in Fig. 3.9. The overpressure values

thus deduced from arrival times are in reasonable agreement with experimental data of other shots. For his calculation Shreve used the first peak immediately following the precursor shock arrival; whereas we have read in all cases the maximum overpressure occurring any time between arrivals of the precursor and the main shock. This lends evidence to the suspicion that our lower of two values for first peaks at 1700 and 1800 ft and the value at 1150 and 1900 ft are much too low.

3.3 PRESSURE ON THE 6- BY 6- BY 20-FT STRUCTURE

Peak overpressures measured by gauges on the front were about as expected. Unfortunately only three of the seven pressure gauges gave second peaks and impulses in which confidence could be placed since the remaining gauges filled with dust to such an extent that the Bourdon tube was prevented from following accurately the pressure vs. time history. It appears that the first peaks were not as seriously affected by the dust loading of the Bourdon tubes as were the second peaks.

The difference between the PNC-5 and the force-plate FPC-2 records may be due to the differences in their response to dust. PNC-5 was a Northam gauge unaffected by dust. It exhibited a higher second peak than the corrected PC-6; this occurrence might be construed as a measure of the effect of overdamping and dust on the remaining gauges. Agreement between the PNC-1 and PC-2, the former a Northam gauge, gives reliability to the measurement of both. Of the gauges placed on the front of the structure, all except PNC-1, PC-2, and PNC-5 were overdamped and dust filled; and when the modification mentioned earlier was made, all four remaining gauges were weighted heavily by the assumption that PNC-5 was correct. Thus if the value for PNC-5 was high, values of records of all gauges above PNC-1 and PC-2 are high by amounts that increase with their height on the structure. Accordingly average overpressure and average impulse for the front would be overestimated. Also if heavy reliance is placed on FPC-2, the modified pressures and impulses would have even higher values especially after 750 msec. The fact that the record from the force plate (FPC-2) was even higher than that of PNC-5 lends support to a belief that PNC-5 was not too high, although the difference between the PNC-5 record and that of the force plate may be due to the differences in their response.

Peak overpressures on the top and back of the structure agree with the peak overpressures expected. Wave shapes on the front resemble those of the incident overpressure, and wave shapes on the top and back are generally alike; but front and incident wave shapes are quite different from those of the top and back. The negative pressure occurring on the top and back lasts from 150 to 330 msec after shock arrival, followed by more than 260 msec of positive pressure. On the incident and front records, a dip begins at 150 msec after arrival, followed by a large maximum pulse that occurs during the latter part of the interval during which pressures on the top and back are negative. It is interesting to note that this difference is qualitatively the same as that of the Teapot Turk Galloping Domino even though the Operation Plumbbob structure was not destroyed.

Since the incident pressure vs. time curves shows a return to ambient between the precursor and the main shock, it is not unexpected to see the dip carried over the measurements made on the top and back. In each case however, the pressure went well below ambient, averaging −5.6 psi on the top and −3.7 psi on the back. A similar excursion below ambient observed from the Turk shot has been attributed to the movement of that structure. Now it is clear that such excursions are typical of precursor blast loading; they are caused by the negative pressure contribution of high dynamic pressure at a time when overpressure is quite low.

The results of impulse measurements are given in Table 3.1. Values are from the average overpressure vs. time curves for the front, top, and back of the structure, which are shown in Fig. 3.12. The net translational (front minus back) average overpressure vs. time curves are shown in Fig. 3.13. Impulse vs. time from the same curves is shown in Fig. 3.14. The force plates on the front showed greatly different overpressures after about 0.75 sec, the greater overpressure being indicated for the uppermost force plate. If the force-plate records alone are used, the result is as shown by the dashed lines in the three figures. The lower overpressures on the lowermost gauges is a strong indication of a boundary-layer effect.

For the impulse comparison c. Table 3.1, the lower value of gauge PGB-2000b-0 has been chosen as the most accurate value for incident impulse (see Fig. 3.10). The relatively closer to GZ Priscilla data with a higher value for incident impulse give about the same ratios to incident for the top and back as the more distant (and lower pressure) Turk shot. The front and consequently the net translational give smaller values than those obtained for Turk. This can be taken as evidence of smaller values of dynamic pressure relative to overpressure than existed on the earlier shot.

The records from gauges on the front and back of the structure do not display the unusual oscillation that appeared on the records from the Operation Teapot Met and Turk shots and on those from the Operation Upshot-Knothole Project 3.1 structure. Those on the top do show an oscillation of about 25 cycles/sec. Those of three earlier shots, Upshot-Knothole 10, Teapot Met, and Teapot Turk, oscillated 100 cycles/sec, 13 to 14 cycles/sec, and 16 to 30 cycles/sec, respectively. It was postulated earlier that the oscillation was somehow related to the failure of the structure.[4] The existence of the oscillation on the top of this structure, which did not fail, would seem to refute the earlier postulate. Since oscillation does not occur on the top of structures subjected to nonprecursor blast loading, either full-scale or in the shock tube,[5] one is left with the conclusion that it is peculiar to precursor blast loading. There is evidence of a correlation between the frequency of the oscillation and the peak overpressure in the incident wave, but the data are too sparse for a conclusive finding. If more information is obtained in future experiments, it would be interesting to see if such a suggestion is confirmed.

3.4 PRESSURE ON THE PROJECT 30.4 STRUCTURE

The records from gauges on the front of the structure indicated that PMS-3 was filled with dust. PMS-2 may have been dust filled but to a much lesser extent. Records from both gauges show wave forms and peaks that are characteristic of those of the incident dynamic-pressure record rather than of the incident-overpressure record.

The wave shapes recorded by gauges on the top and back of the structure agree with those of the incident-overpressure wave but show a dip below ambient pressure at the end of the precursor just before arrival of the main shock wave even though the incident-overpressure wave had no such excursion below ambient. This phenomena is a further verification of the behavior observed on the 6- by 6- by 20-ft structure and on the Galloping Domino. No oscillation of the pressure wave as described for the other structures was evident.

The record of the single gauge on the forward footing of the structure indicates that the gauge was disturbed or damaged by a mechanical blow, probably from a rock, 0.11 sec following arrival of the shock wave.

The results of impulse measurements are given in Table 3.2, and their ratios to incident overpressures may be compared with those from the more distant station. Values are not for the impulse of the average pressure vs. time curves as at the more distant station but are arithmetic averages of impulses of individual overpressure vs. time records.

3.5 FOOTING LOADING

It has been the practice of structural designers to provide a wide toe on the forward footing of a structure. This practice was based on the assumption that the reflected pressure on the front of the structure occupied a volume at the front in such a manner that the reflected pressure rather than the incident pressure acted downward on the toe of the footing in a way that helped to prevent overturning. Figure 3.15 shows the spacial distribution of impulse across the toe of the front footing in terms of the impulse of the incident wave. The incident impulse from both gauges has been used. In this case it can be seen that only the 4 ft immediately in front of the structure contribute significantly to the stability of the structure. The impulse values cited were estimated by eliminating what was thought to be the contribution to recorded pressure due to the dust filling of the gauges.

Since the gauge on the toe of the footing of the Project 30.4 structure failed after 111 msec, a similar comparison could not be made. It was possible, however, to show the comparison us-

ing the impulses of only the first 111 msec of the records from the incident, the toe, and the lower front gauge; and this has been added to Fig. 3.15. The situation at the foot of the 30.4 structure was not analogous to that at the foot of the 34.1 structure owing to the ground effect.

It might be expected that the spacial extent and amplitude of the reflected pressure would bear some relation to the smaller of the structure height or the half width and the Mach number. The height of the Project 34.1 structure was 6 ft. and the half width of the Project 30.4 structure was also 6 ft. Six feet in front of the Project 34.1 structure there is only about 10 per cent more impulse on the footing than in the incident wave. On the closer structure, for the first 111 msec at least, the impulse on the footing 6 ft in front is nearly twice that of the incident wave. Since the ratio had not approached 1 by a point 6 ft in front of the structure, it might be concluded that structure dimensions alone do not account for the spacial extent and that Mach number must also be considered.

Figure 3.15 also gives an indication of the extent of the nearly stationary air and dust in front of the structure which oncoming air and dust must penetrate to effect a momentum transfer before loading the structure.

3.6 CORRELATIONS BETWEEN FREE-FIELD AND STRUCTURE MEASUREMENTS

Either casual or detailed examination reveals a dismaying fact when the forward-face cubicle pressure measurements are compared with free-field stagnation pressure. The two sets of data show internal consistency and yet disagree with each other. This difference is confined mostly to the second half of the blast wave. Here, the free-field measurements indicate two distinct peaks of stagnation pressure, confirmed by three channels at the 10-ft elevation and two channels at the 3-ft elevation. On the other hand, the cubicle pressure gauge and force-plate data deny entirely the existence of the first peak and show considerable internal disagreement over the magnitude of the second peak. Therefore, the seven pressure channels and the two force-plate channels that are on the cubicle show a different wave shape than that of the seemingly well-confirmed free-field measurements. The only feasible conclusion seems to be that both sets of data are right and that there was a real difference between the precursor wave in a separation of only 30 ft.

Such discrepancies over such short distances have been discovered before [a perusal of the comparisons in ITR-1153 (Ref. 6) will furnish several examples]. Usually the data were obtained by two different agencies at adjacent locations. The comparison was less severe because the instruments were of different types; however, in this project similar instruments (the Greg and the force plate and the Pitot-static tube and the pressure gauges) gave different reports at adjacent stations. Some difference might be expected because of the obstacle size in dusty flow, but the difference encountered is much too great to be accounted for by this single factor.

Whether or not such discrepancies in wave form are commonplace, it is unfortunate that such a difference appears here. It allows us only to compare the first portion of the blast wave, and even here we are in the awkward position of calculating drag coefficients, knowing that the marked difference of the second half of the blast may well imply lesser difference in the early history. Merris[7] found that diffraction effects would be noticeable but small at 24 ft from a structure such as the one in this project and would have disappeared before reaching 48 ft. Thus a move closer to the structure to reduce asymmetric anomalies would have introduced diffraction anomalies in the free-field measurements.

Now that this discrepancy has been emphasized, a correlation of the free-field measurements with the pressure measurements on the cubicle will be attempted. Three such correlations seem reasonable as well as useful for loading estimates. The first and most obvious is a comparison of the free-field measurements of stagnation pressure with those observed on the cubicle face. The second is a comparison of the average net translational force per unit area of the cubicle with the air dynamic pressure and dust momentum flux to specify effective drag coefficients for air and dust. The final correlation is a comparison of combinations of air dynamic pressure and dust momentum flux with the departures from side-on pressure recorded at the top and back of the cubicle.

The air-pressure measurements on the front face of the cubicle were discussed in detail in Sec. 3.3. In general, the wave shapes are consistent except that the Northam gauge PNC-5 and the upper force plate FPC-2 show a considerable variation in the value of the peak at the end of the blast wave, although their impulses differ by only 15 per cent. In general, the peaks are later, weaker, and broader in observations made further down the cubicle face. This is a trend that would be expected from the free-field measurements, which suggest a downward transfer of momentum by turbulence from the high-flow region above. A comparison of the stagnation-pressure results is shown in Fig. 3.16. Here the average stagnation pressure on the cubicle face and force-plate data taken on the cubicle face have been plotted, along with the smoothed Greg, Snob, and force-plate records at the 3-ft elevation. The derived quantity of the Greg data minus half the dust momentum flux also is plotted. This calculated parameter is the stagnation pressure that would be predicted from incompressible theory when the stopping length of the particle (10 cm) is small compared to the obstacle size (183 cm). In the early stages of the blast wave (first 80 msec), the average cubicle stagnation pressure, according to the pressure gauges, lies closest to the values recorded by the Snob. At the end of this period, it approached the derived parameter $G-(\phi_d/2)$, where it remained for about 20 msec. Following this the average pressure exceeded the derived parameter and assumed a value about midway between it and the Greg record. This departure could represent the change of flow pattern as the dust concentration increases. Following this analysis further is not practical, however, since the cubicle force-plate average gives a different picture of this variation. The force-plate data are obtained by averaging the data from the two instruments on the front face which were centered about the 3-ft level. They agree with the Greg record until the arrival of the 640-msec peak in the free field. This behavior suggests that the incompressible theory of dust loads is not applicable and that the streamlines were pressed toward the obstacle surface, allowing dust to register with a higher coefficient than one-half. It may be mentioned at this point that the pressure measurements taken in front of the cubicle suggest a similar result since it is at only a short distance in front of the cubicle that significant departures from side-on pressure are observed. Little or no agreement exists after the first free-field peak at 640 msec. Free-field measurements register higher values than those observed in the early blast waves; whereas the cubicle measurements show a low in stagnation pressure during the first peak. The second peak is not comparable except for the force-plate measurements, which approach the values of $G-(\phi_d/2)$ during the second peak.

In Fig. 3.17 the new force according to the pressure gauges has been plotted, as well as the net force according to force-plate data. Along with these measured net force vs. time records, the sum of the dust momentum flux and the air dynamic pressure and one-half the dust momentum flux, as well as air dynamic pressure alone, have been plotted. The drag parameter curves would not be expected to agree with the new force curves unless, fortuitously, the drag coefficient happened to be 1 for a parameter we have chosen. Such is certainly not the case for the net translational force as specified by pressure gauges. The new force per unit area at first lies close to derived parameters $Q_a + (\phi_d/2)$ but finally approaches the full sum of air dynamic pressure and dust momentum flux. No comparison is possible except in the first half of the blast wave. The net translational force, according to the cubicle force plates, is always comparable with the sum of corrected air dynamic pressure and the dust momentum flux until the first peak.

In the first half of the blast wave, there seems to be sufficient correspondence between the free-field measurements and those of the cubicle to allow computation of a dust-drag coefficient. This is accomplished by the use of the following arbitrary expression where F is net translational force per unit area:

$$F = Cq_a + K\phi_d$$

The air-drag coefficient, C, is sensitive principally to Mach number for this case since the Reynolds number is always large. The dust drag coefficient, K, is expected to be a function of the ratio of dust momentum flux to air-stagnation pressure and dust size; it is intended then to account not only for the force exerted by the dust, but also for changes of the air-flow pattern

brought about by dust deceleration. Rather than attempt to explore the variation of K with the ratio of dust momentum flux to air stagnation pressure, we shall compute an average value for this parameter under these field circumstances. Figure 3.18 is a histograph of the values of K calculated in the interval 530 to 640 msec by the use of net force values according to pressure data as well as to the force plate. The fluctuation is considerable when the new force based on pressure data is used. The average value of K is about 0.65. The value of K is much more stable if the net force based on the force plates, which has an average value of 1.07, is used. Practically it would seem better to use the force-plate data for loading estimates since the dust momentum may have been considerable at the cubicle surface and since the response of pressure gauges to this flux is uncertain.

A comparison of the departures of side pressure on the top and back of the cubicle with the various dynamic parameters [q_a, $q_a + (\phi_d/2)$, and $q_a + \phi_d$] and net cubicle translational force according to the pressure gauges and force plates is plotted in Fig. 3.17.

At low Mach numbers and large Reynolds numbers (>1000), this departure would be expected to be about proportional to air dynamic pressure for the clean-air case, but this is obviously not the case in the dusty field conditions of this project. The departure is nearly proportional to $q_a + \phi_d$ until 640 msec after zero when the gross difference in wave shape appears. This would seem to correlate with the diffusion effect observed in dust-tunnel experiments.

The departures from side-on pressure at the top and back of the cubicle are about the same, suggesting a flow separation at the cubicle forward edge with a nearly uniform wake. The departure confirms the existence of the second peak at the cubicle and shows no indication of the first peak at this location.

REFERENCES

1. L. A. Schmidt, Study of Drag Loading of Structures in the Precursor Zone, Project 3.2, Operation Teapot Report, WT-1124, Jan. 30, 1959. (Classified)
2. L. M. Swift, D. C. Sachs, and F. M. Bauer, Air-blast Phenomena in the High-pressure Region, Project 1.3, Operation Plumbbob Report, ITR-1430, Oct. 11, 1957. (Classified)
3. J. D. Shreve, Jr., Air Shock Pressure-Time vs. Distance for a Tower Shot, Project 1.1c-1, Operation Upshot-Knothole Report, WT-712, April 1955. (Classified)
4. L. J. Vortman and W. G. Frany, Effects of a Nonideal Shock Wave on the Blast Loading of a Structure, Project 34.2, Operation Teapot Report, WT-1162, July 1, 1957. (Classified)
5. Charles H. Kingery and John H. Keefer, Comparison of Air Shock Loading on Three-dimensional Scaled and Full-size Structures. Part II. Structure 3.1a., Report AFSWP-775, Ballistic Research Laboratories Technical Note N-976, January 1955. (Classified)
6. H. K. Gilbert and E. B. Doll, Technical Summary of Military Effects, Programs 1-9, Operation Teapot Report, WT-1153, February 1960. (Classified)
7. W. E. Morris, Shock Diffraction in the Vicinity of a Structure, Project 3.1a, Operation Upshot-Knothole Report, WT-786, August 1959. (Classified)

TABLE 3.1 —MEASURED IMPULSES (6- BY 6- BY 20-FT STRUCTURE)

	Turk shot		Priscilla shot	
	Impulse, psi-sec	Ratio	Impulse, psi-sec	Ratio
Incident	4.11		4.05	
Front (av.)	16.16		13.4	
Front/incident		3.93		3.31
Top (av.)	1.08		1.36	
Top/incident		0.26		0.34
Back (av.)	1.34		1.47	
Back/incident		0.33		0.36
Net translational average	14.82		11.9	
Net/incident		3.60		2.94

TABLE 3.2 —MEASURED IMPULSES (PROJECT 30.4 STRUCTURE)

	Impulse, psi-sec	Ratio
Incident	8.14	
Front	33.15	
Front/incident		4.07
Top	5.20	
Top/incident		0.64
Back	4.34	
Back/incident		0.53
Net translational	28.81	
Net/incident		3.54

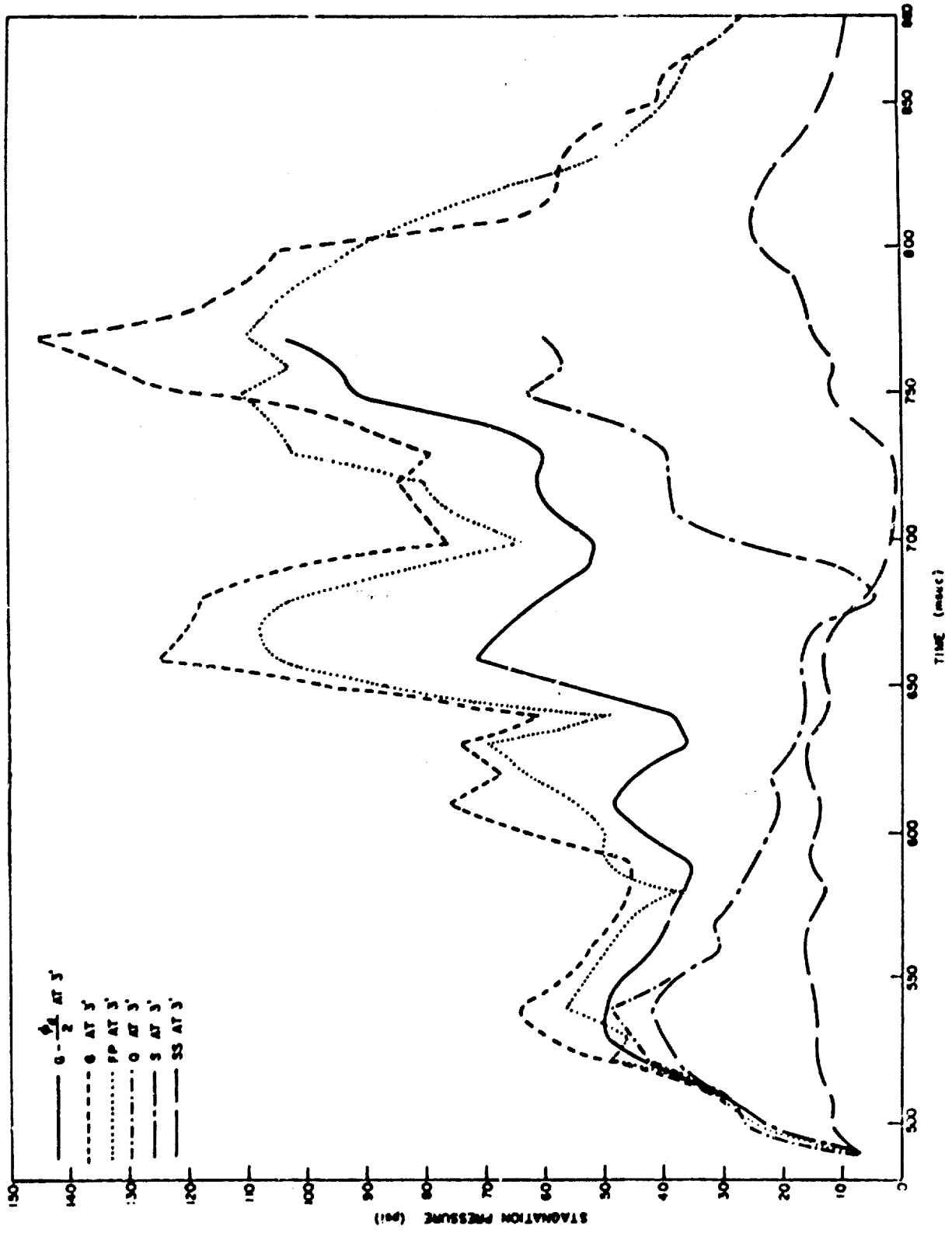

Fig. 2.1—Comparison of the stagnation pressures for the 3-ft-level free-field measurement at 2000 ft from GZ.

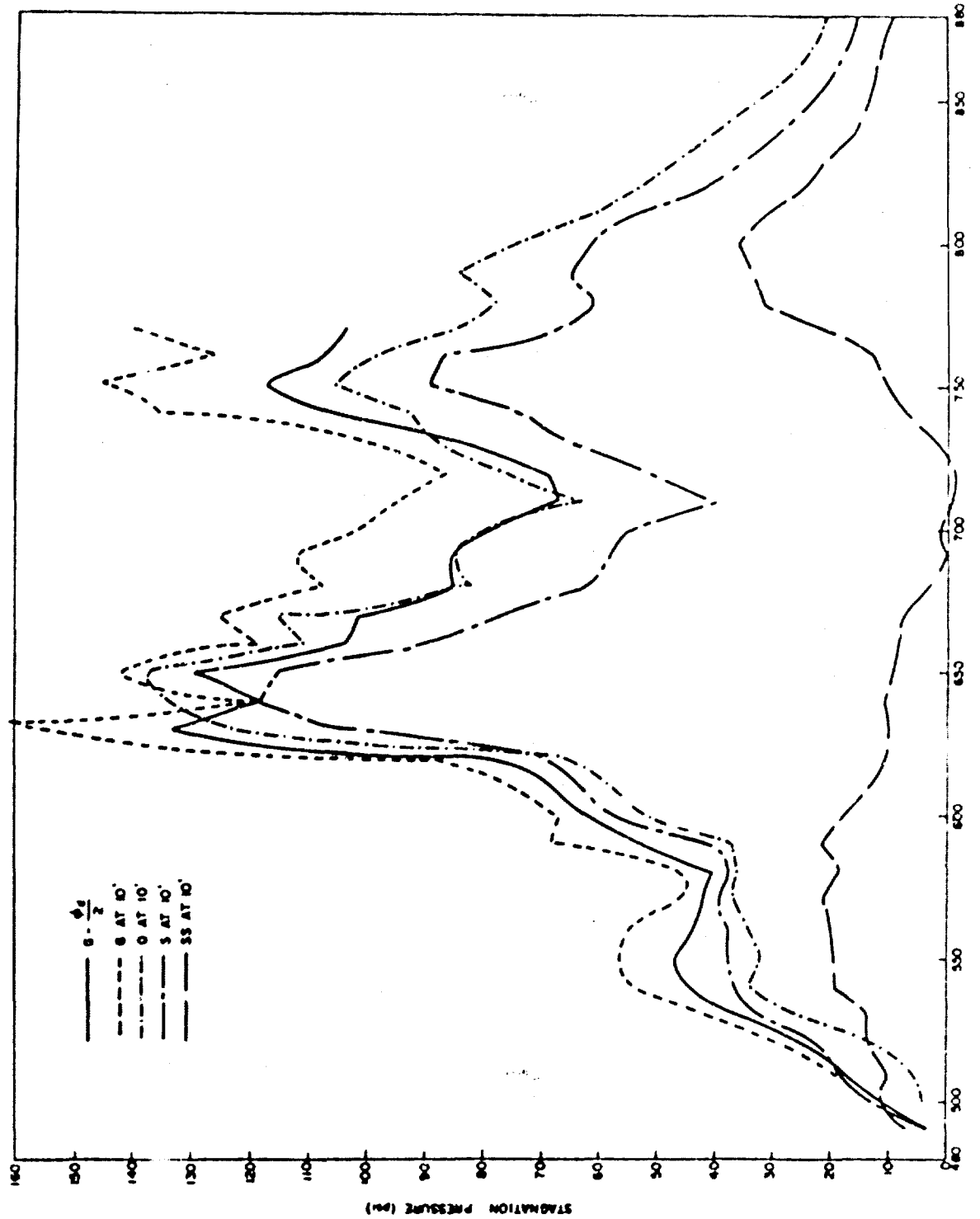

Fig. 1.3—Comparison of the stagnation pressures for the 10-ft-level free-field measurement at 2000 ft from GZ.

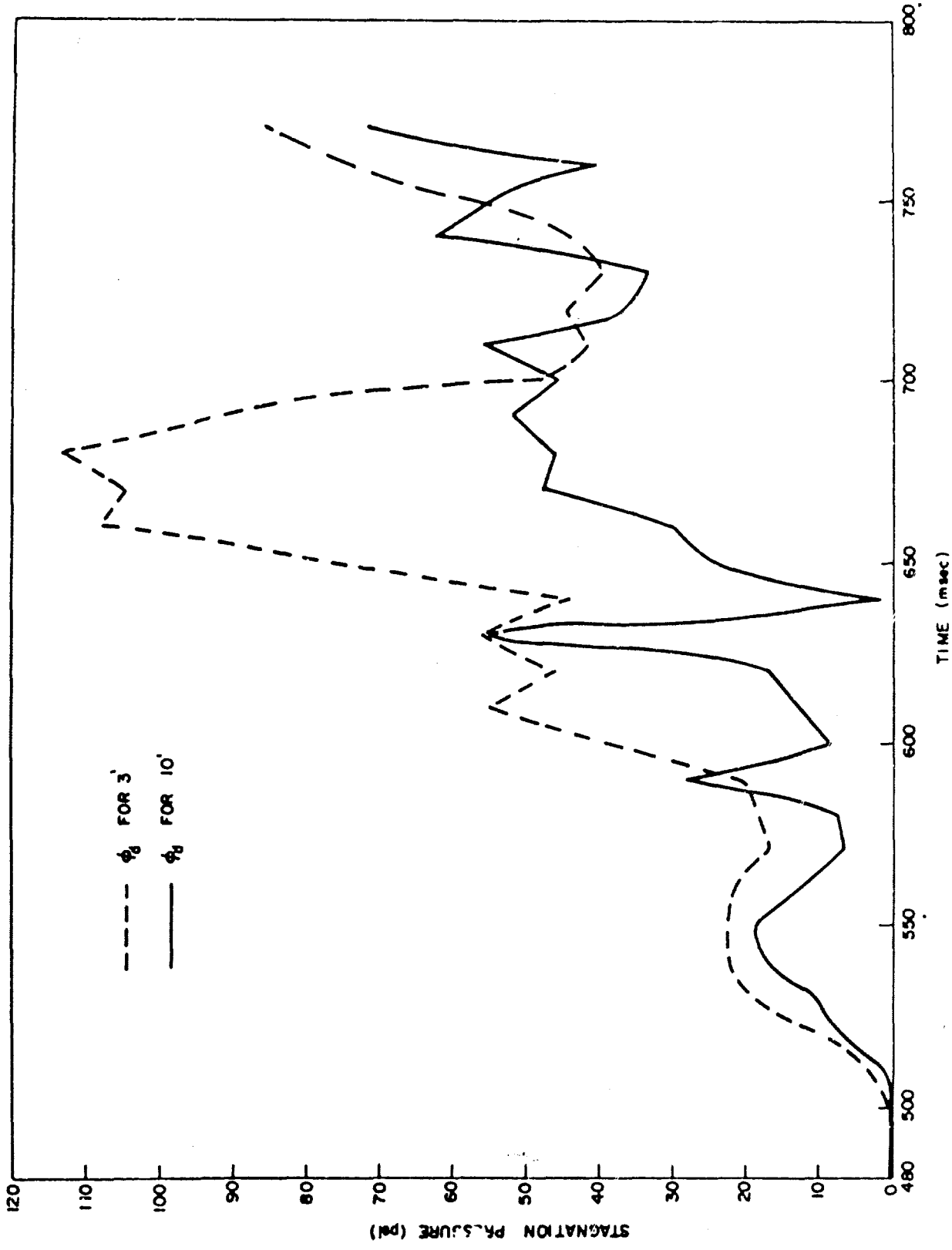

Fig. 3.3—Dust momentum flux Φ_d at the 3- and 10-ft levels.

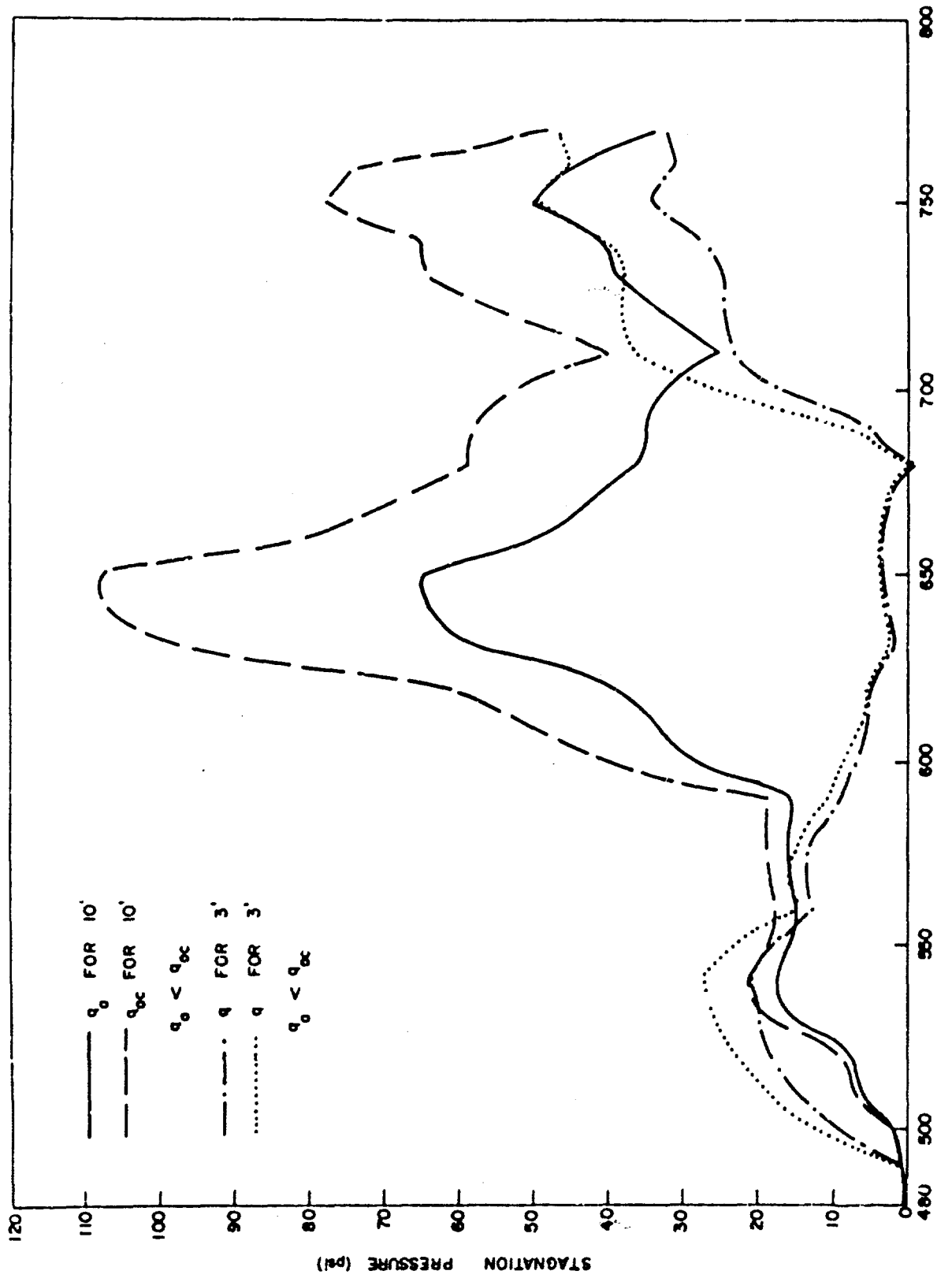

Fig. 3.4—Corrected (q_o) and uncorrected (q_{oc}) air dynamic pressures for the 3- and 10-ft levels.

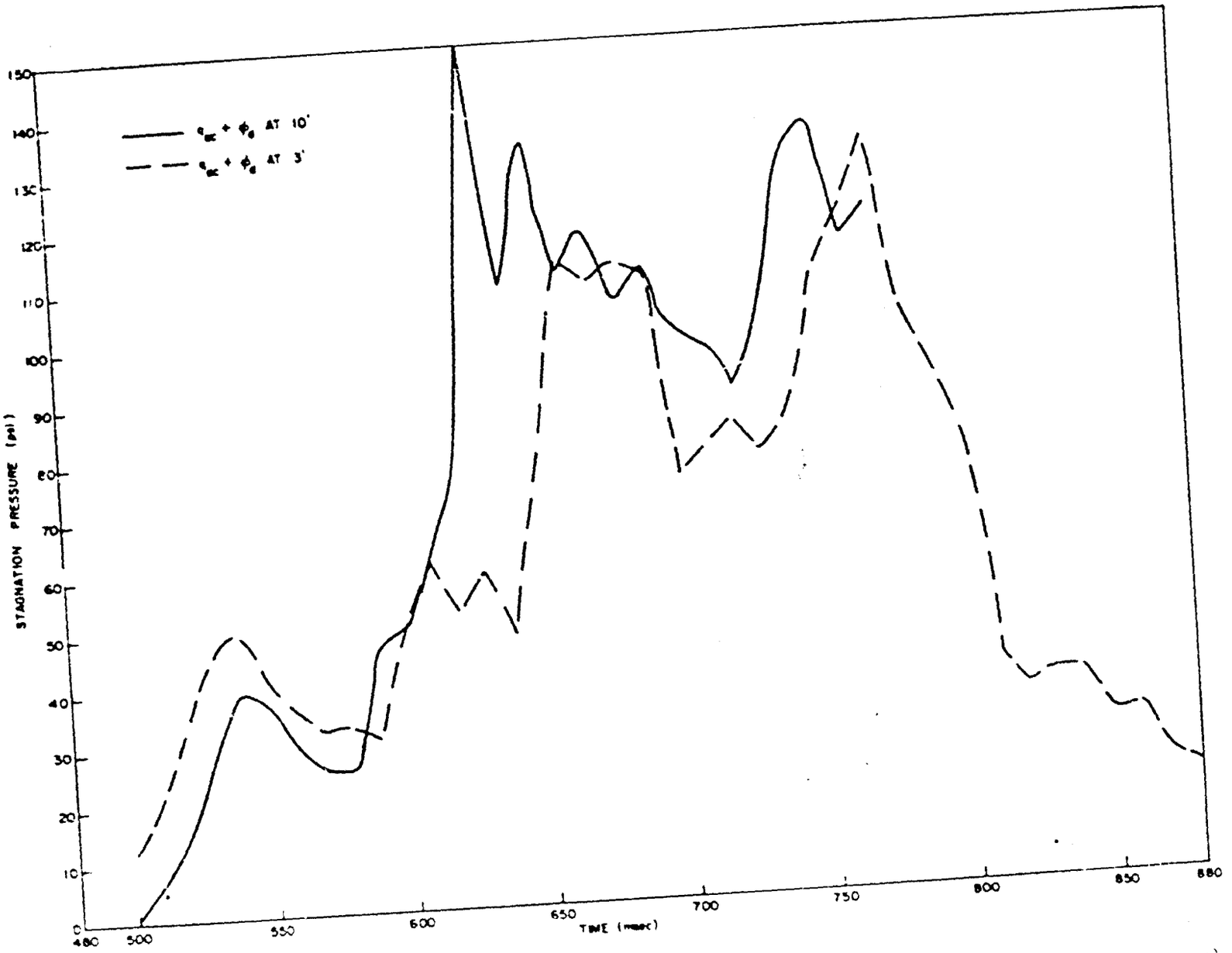

Fig. 3.5—Sum of uncorrected air dynamic pressure and dust momentum flux at the 3- and 10-ft levels (Greg gauge minus Sneb side-on gauge).

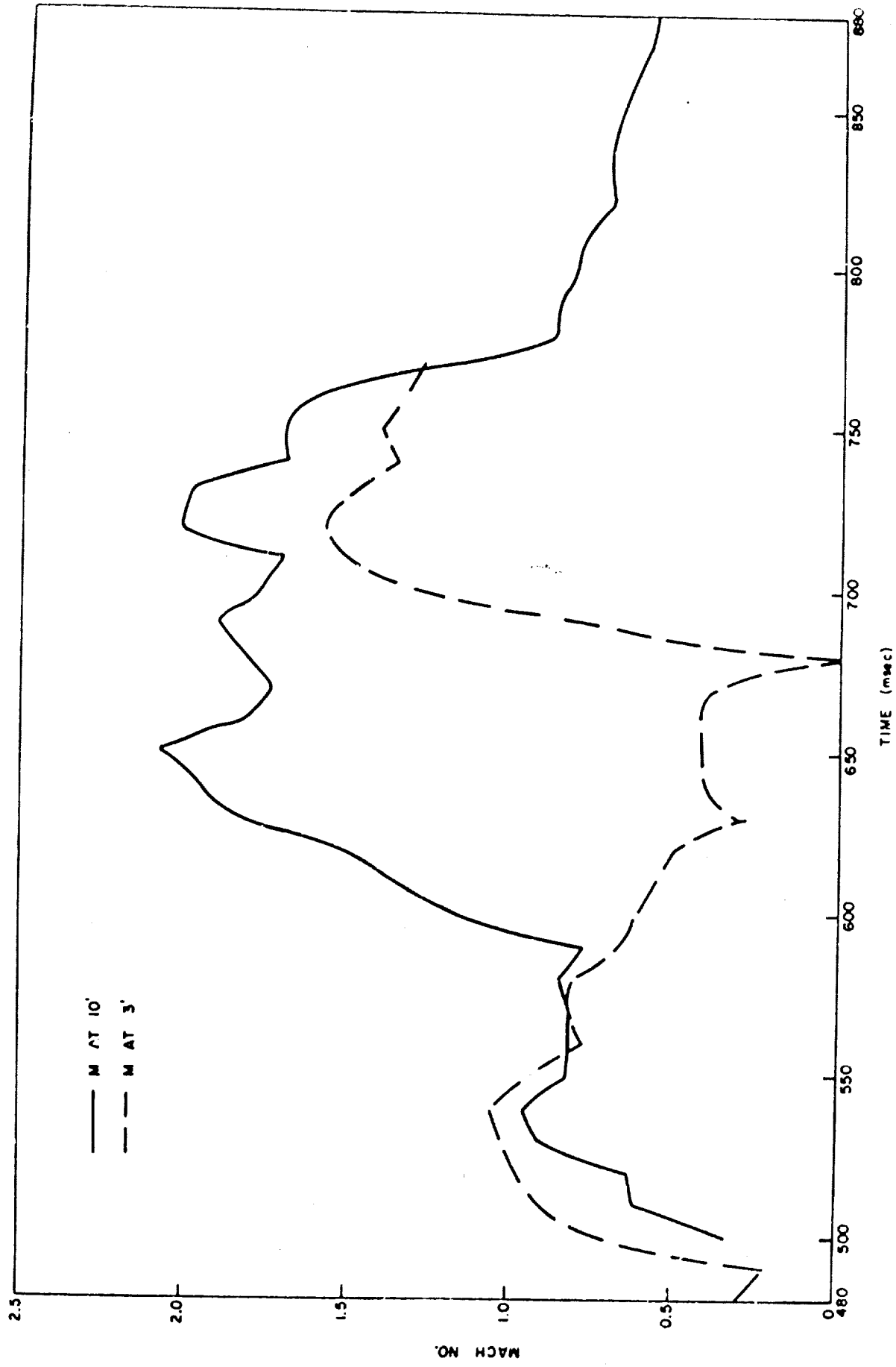

Fig. 3.6—Air-flow Mach number at the 3- and 10-ft levels.

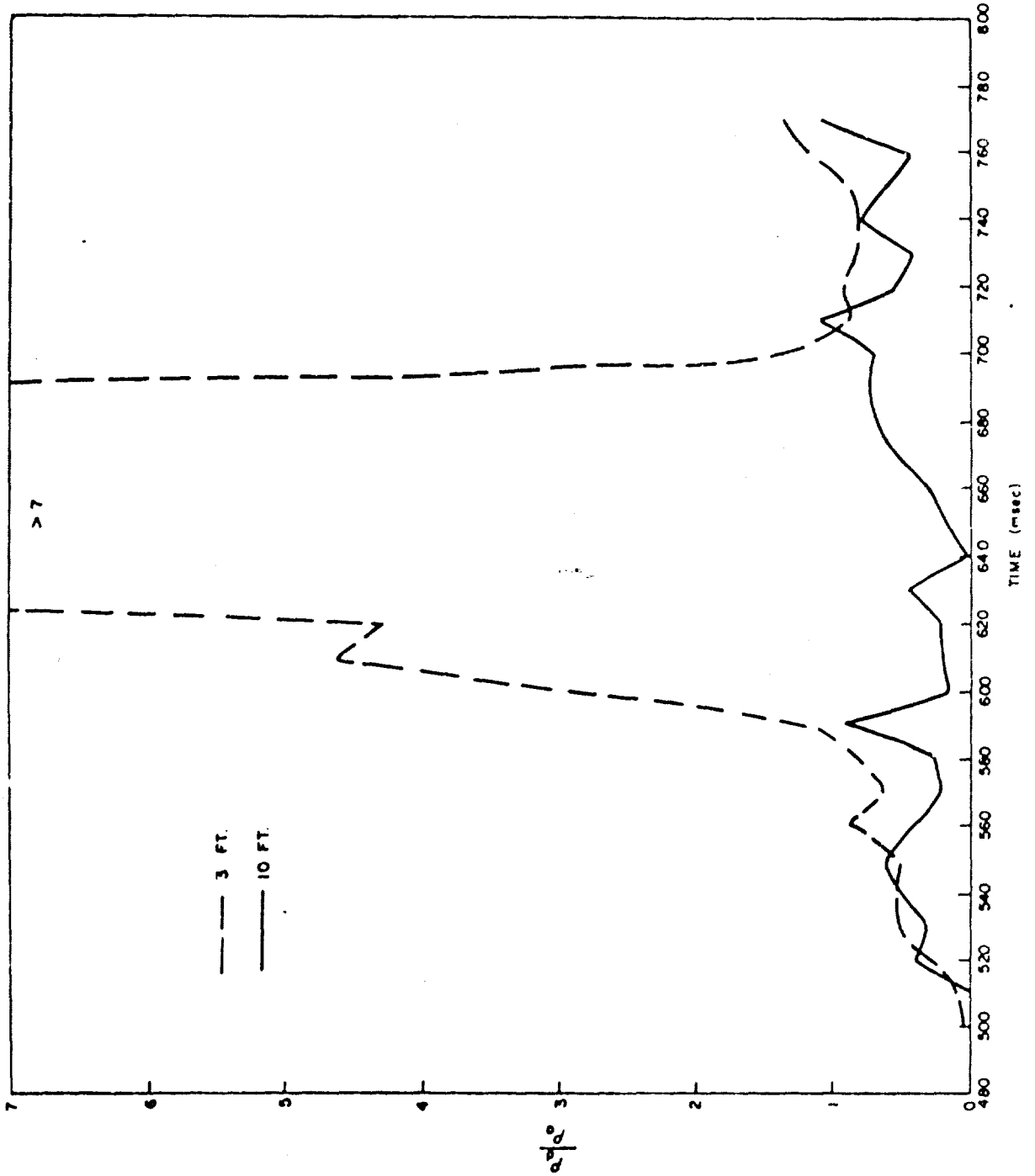

Fig. [illegible] — Ratio of suspended dust density to air density (ρ_d/ρ_a) at the 3- and 10-ft levels.

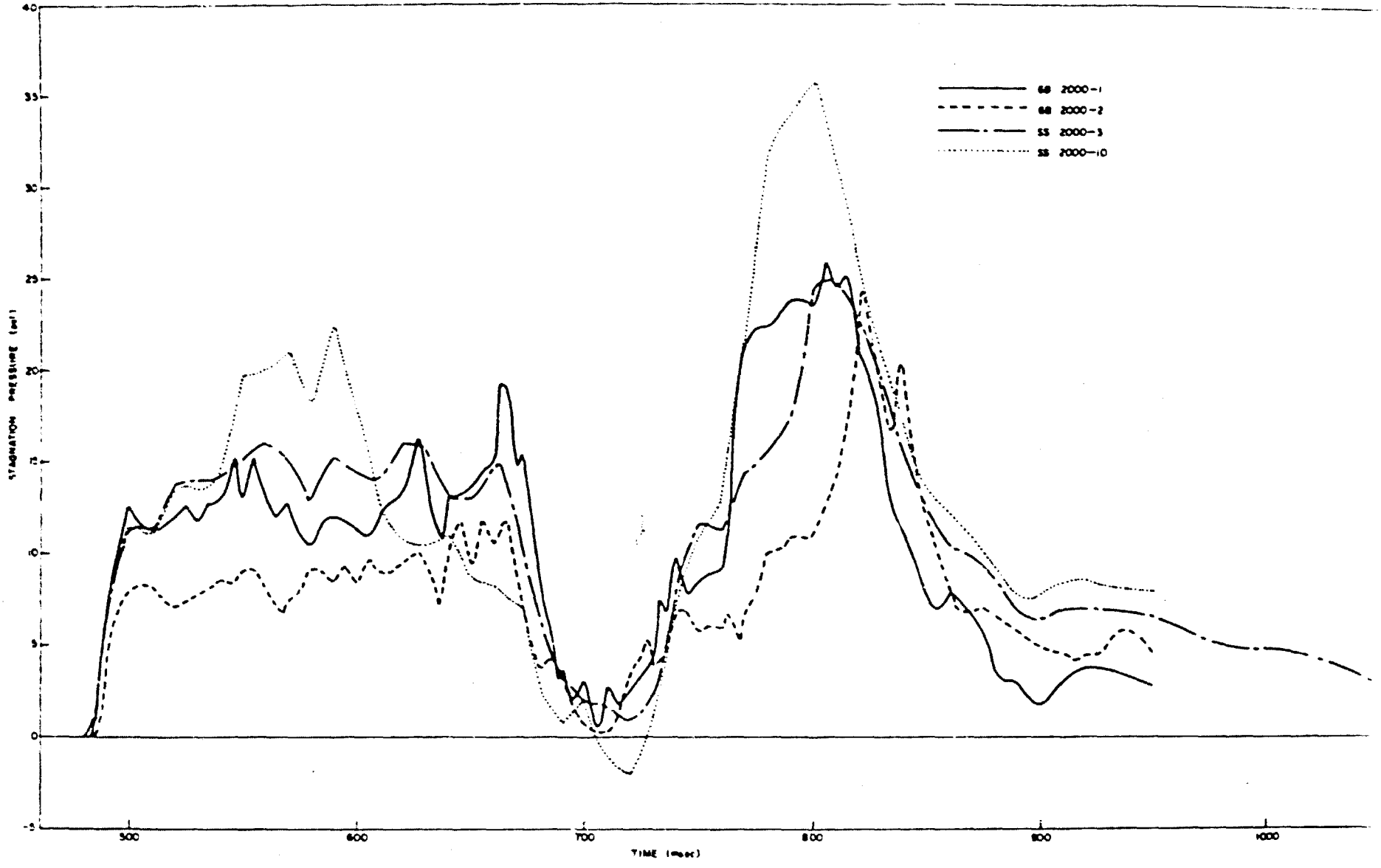

Fig. 3.8—Comparison of overpressure at ground baffles with the tower measurements.

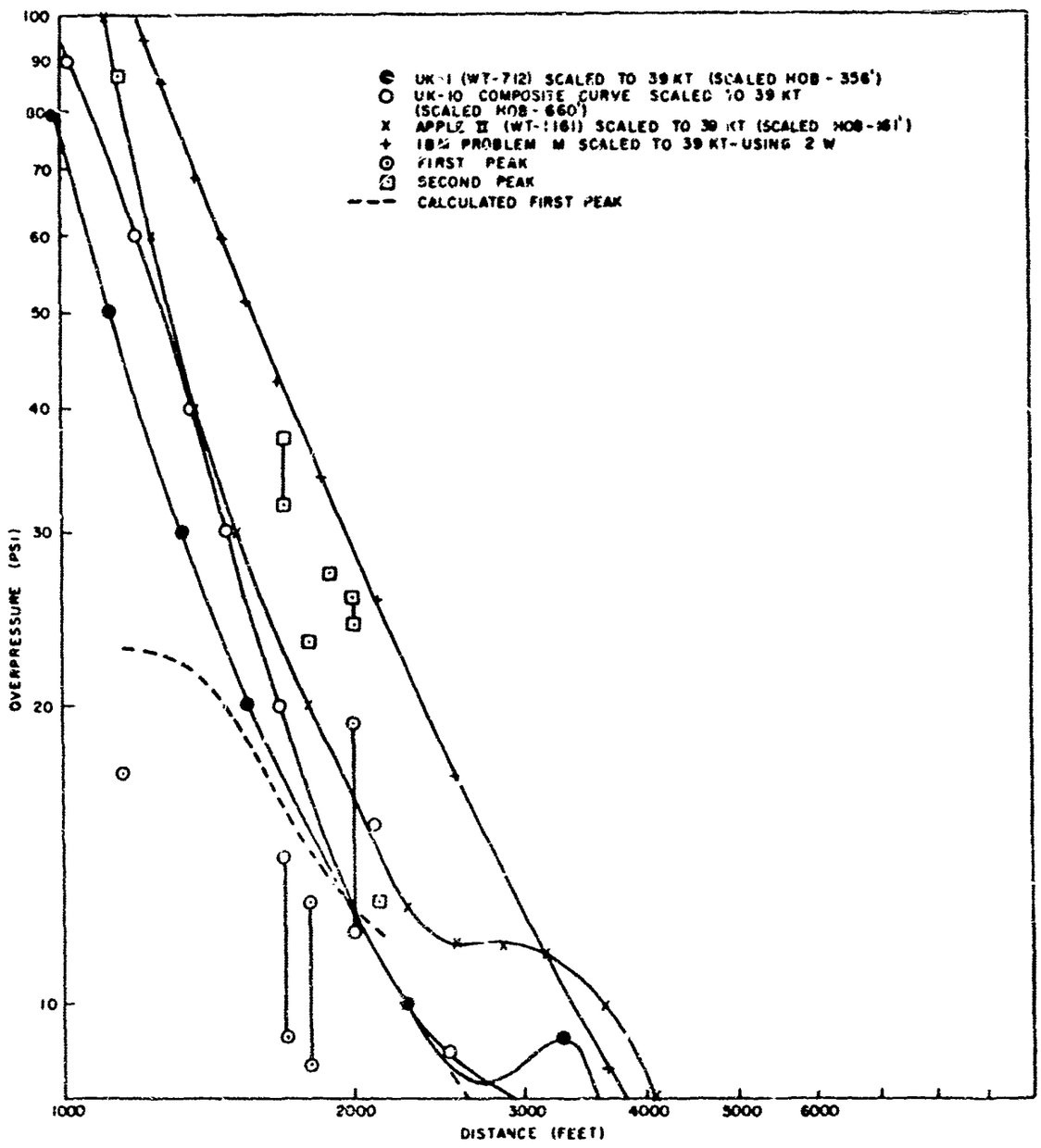

Fig. 3.9—Comparison of Project 34.1 peak overpressures with those from other events.

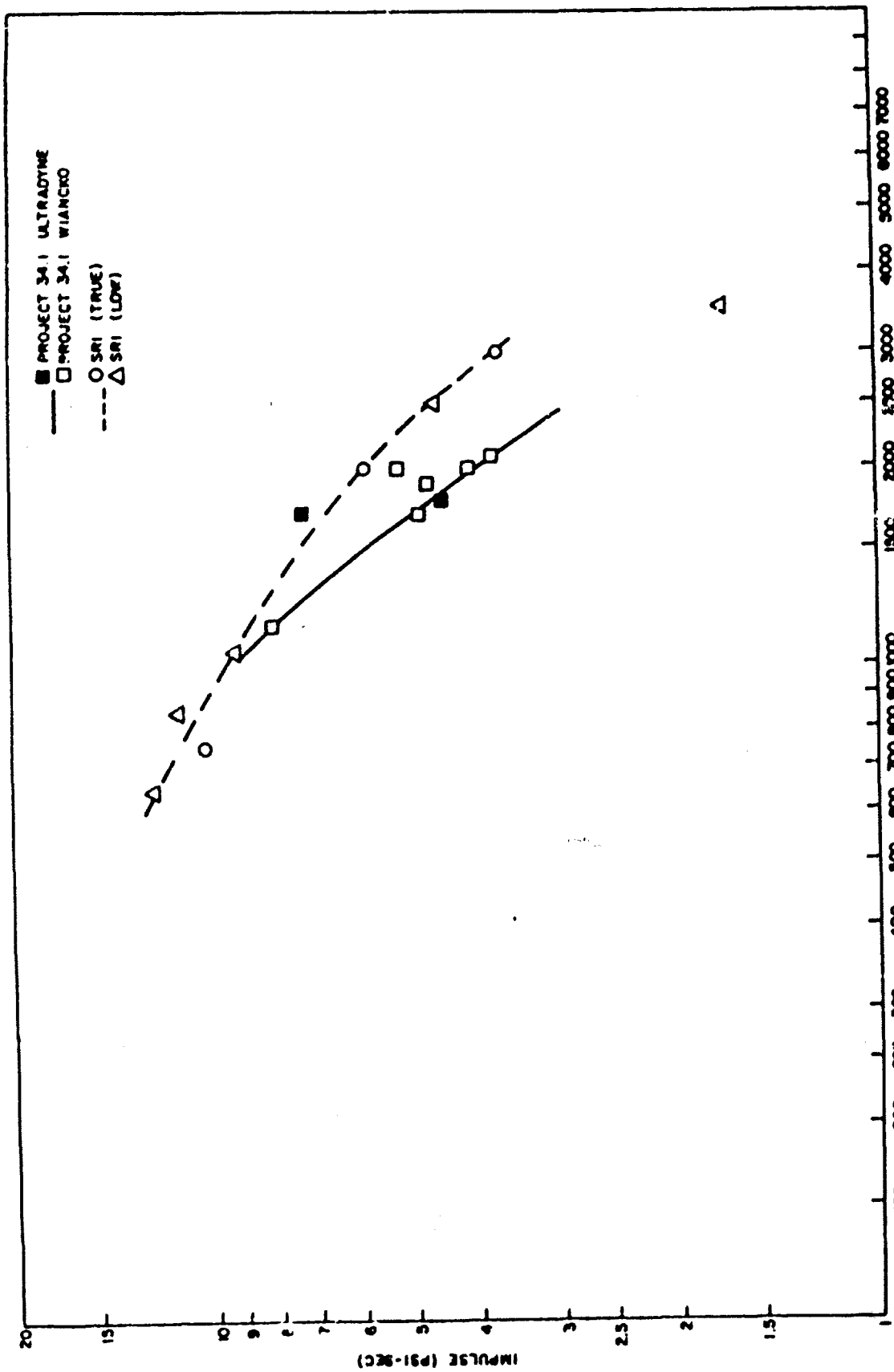

Fig. 3.10—Measured impulses.

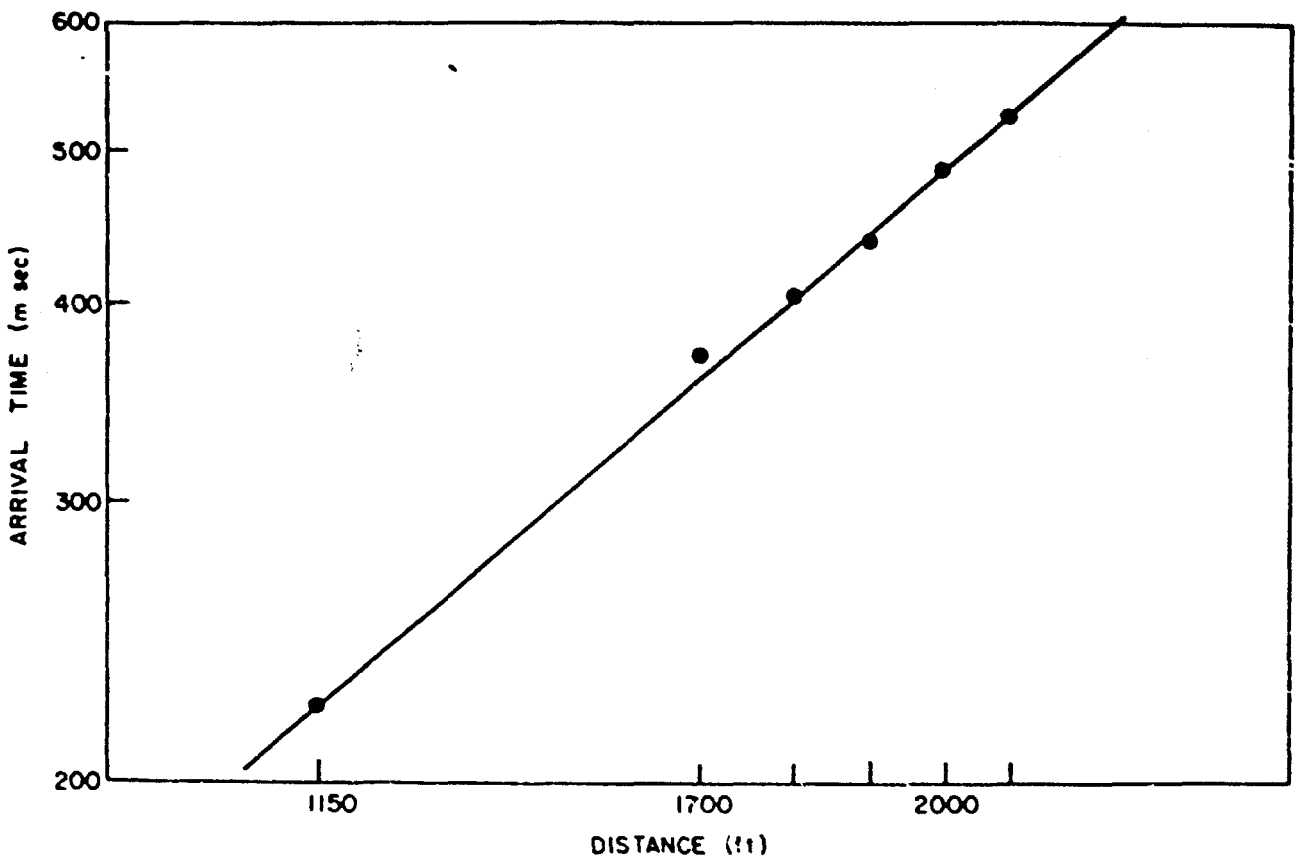

Fig. 3.11—Measured arrival times.

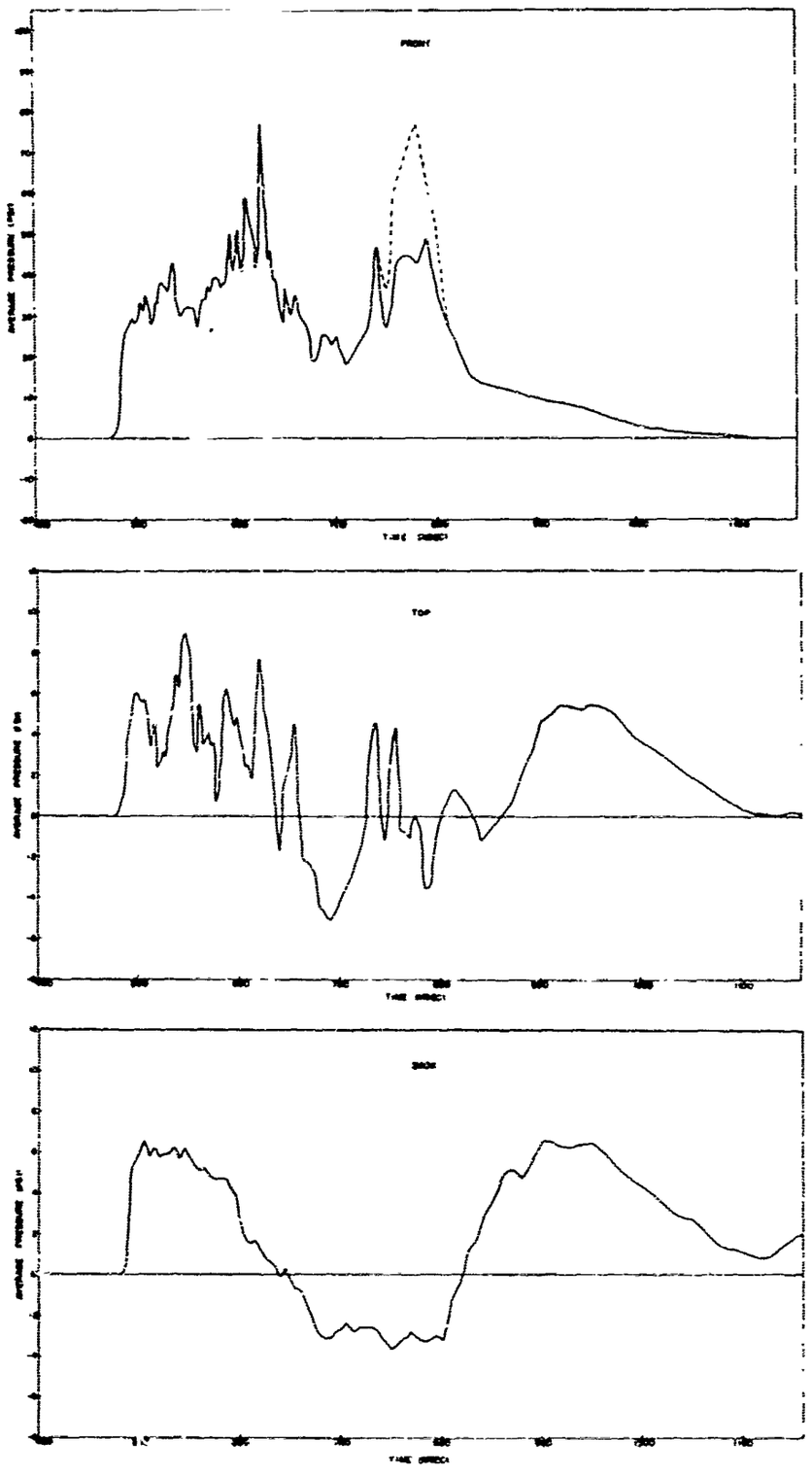

Fig. 3.12—Average pressure vs. time measured on front, top, and back of the 6- by 6- by 20-ft test structure.

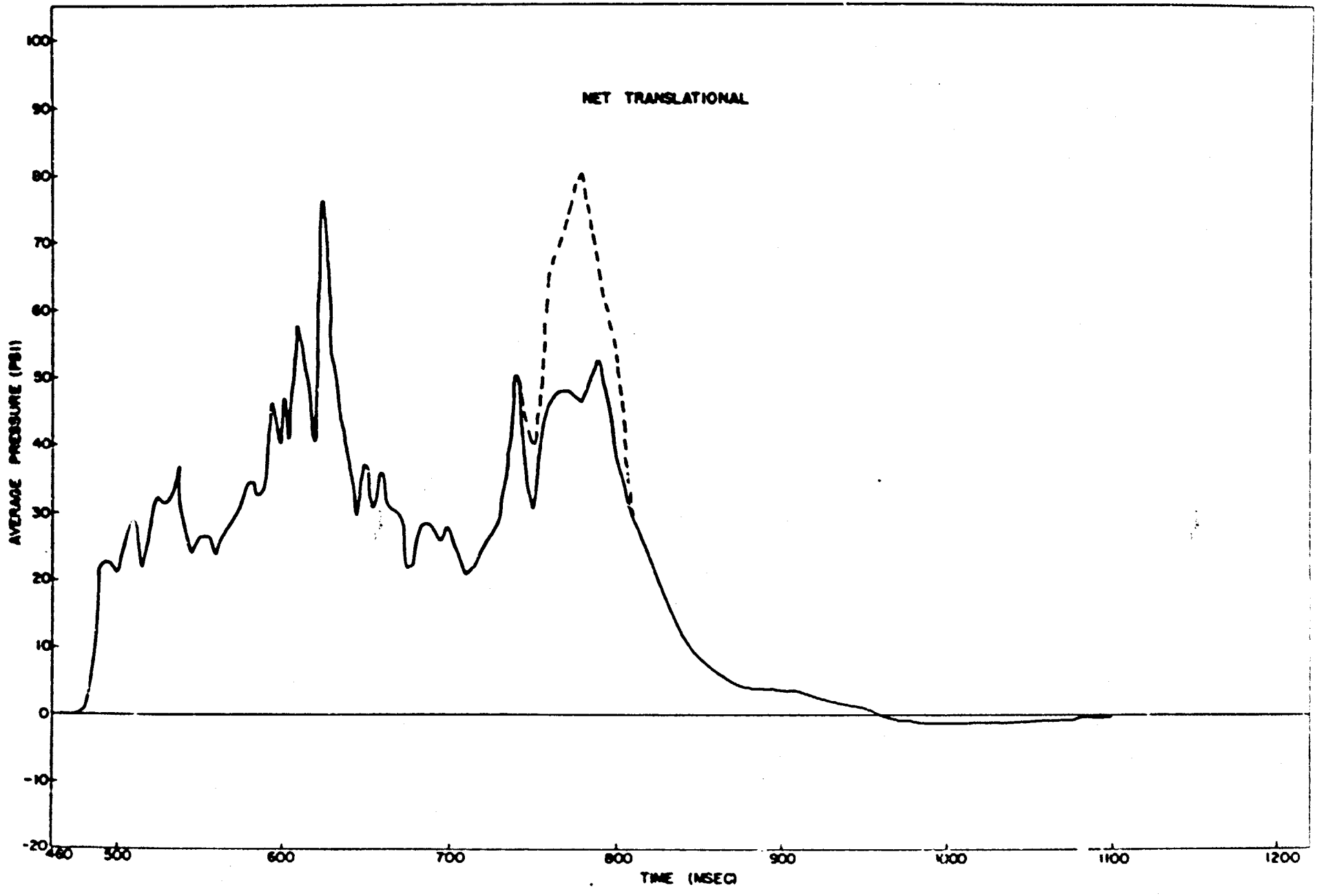

Fig. 3.13—Net translational pressure vs. time for the 6- by 6- by 20-ft test structure.

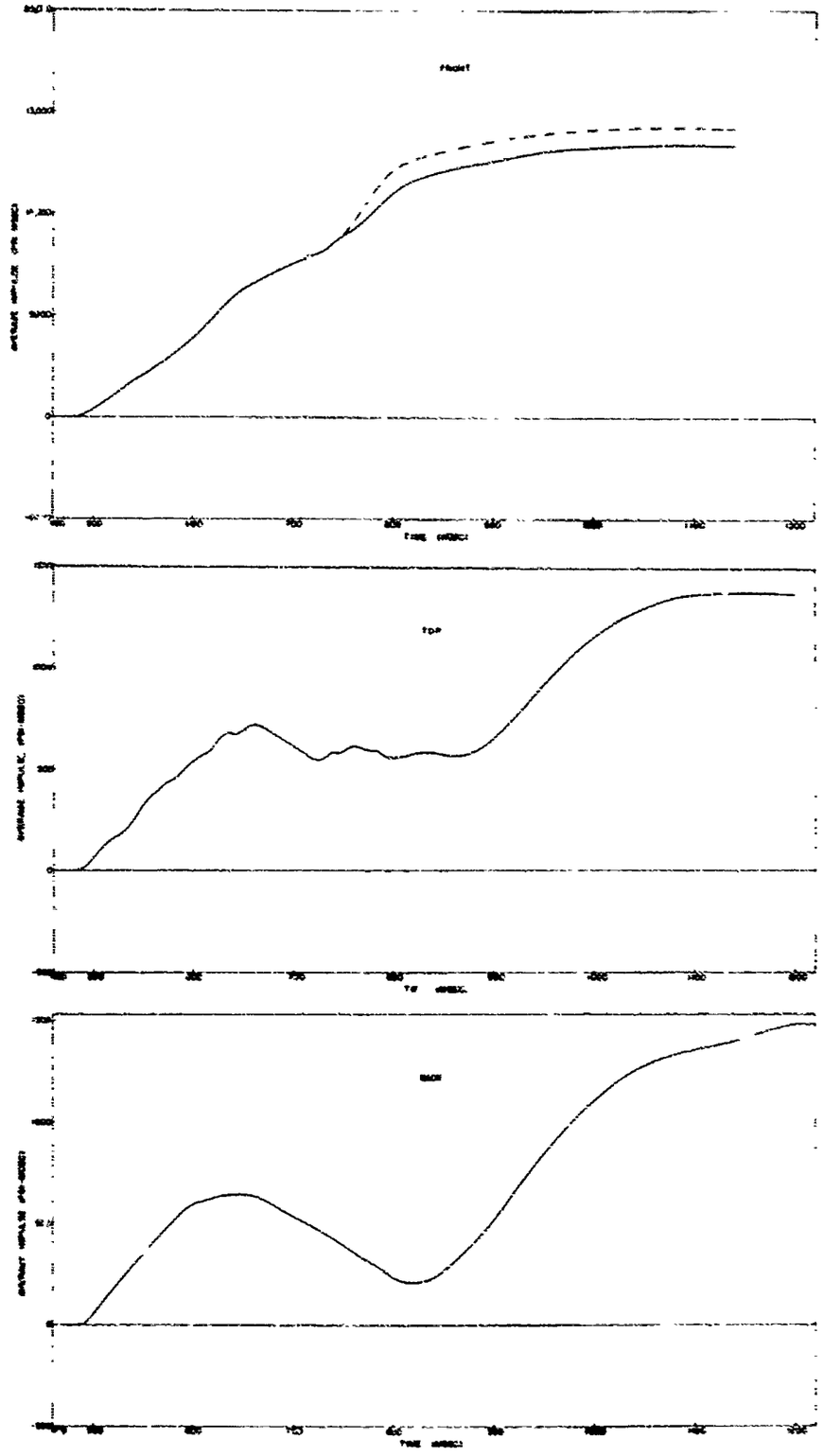

Fig. 3.14—Average impulse vs. time for front, top, and back of the 6- by 6- by 20-ft test structure.

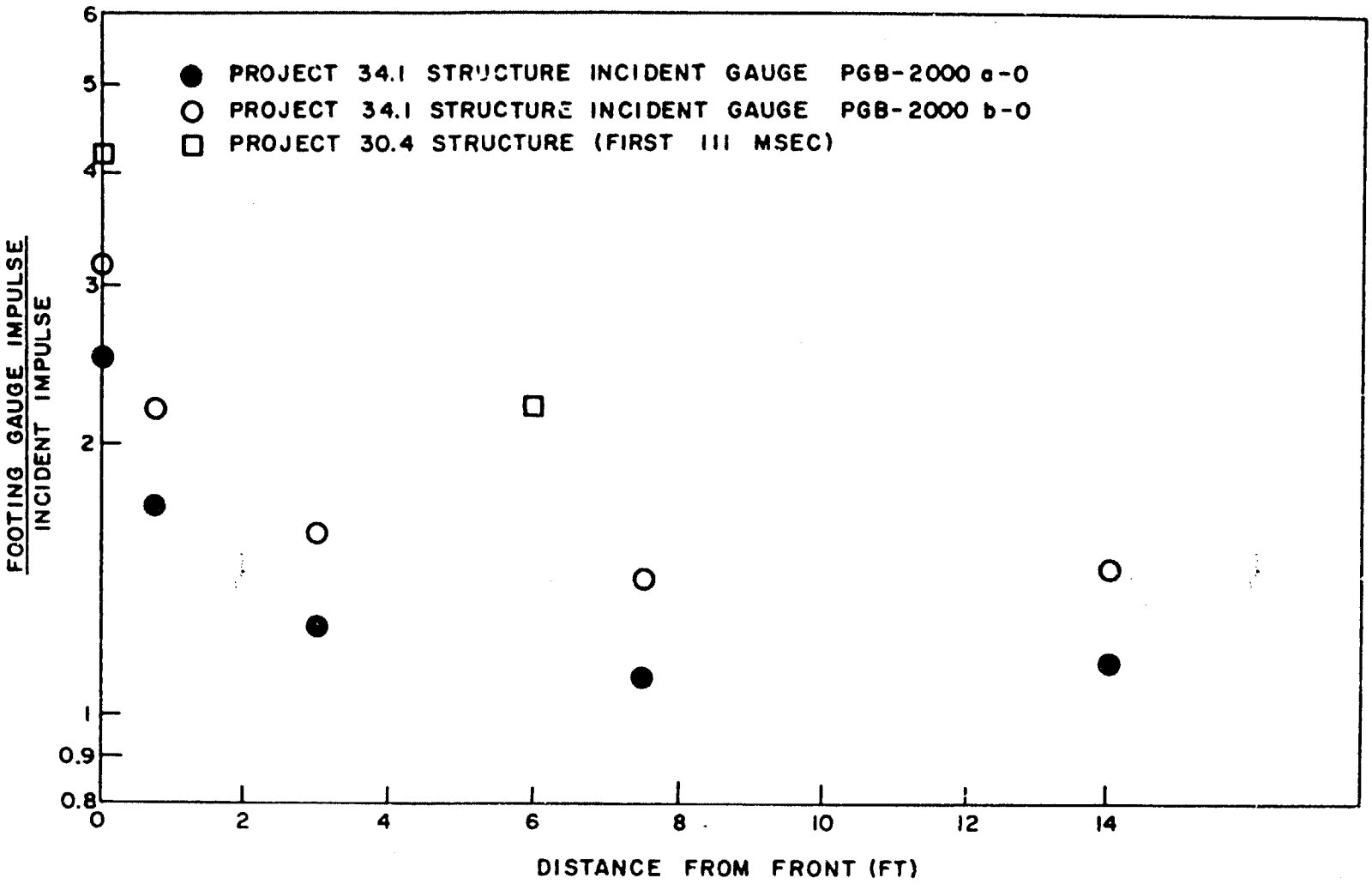

Fig. 3.15—Footing gauge impulses as a function of distance in front of the test structure.

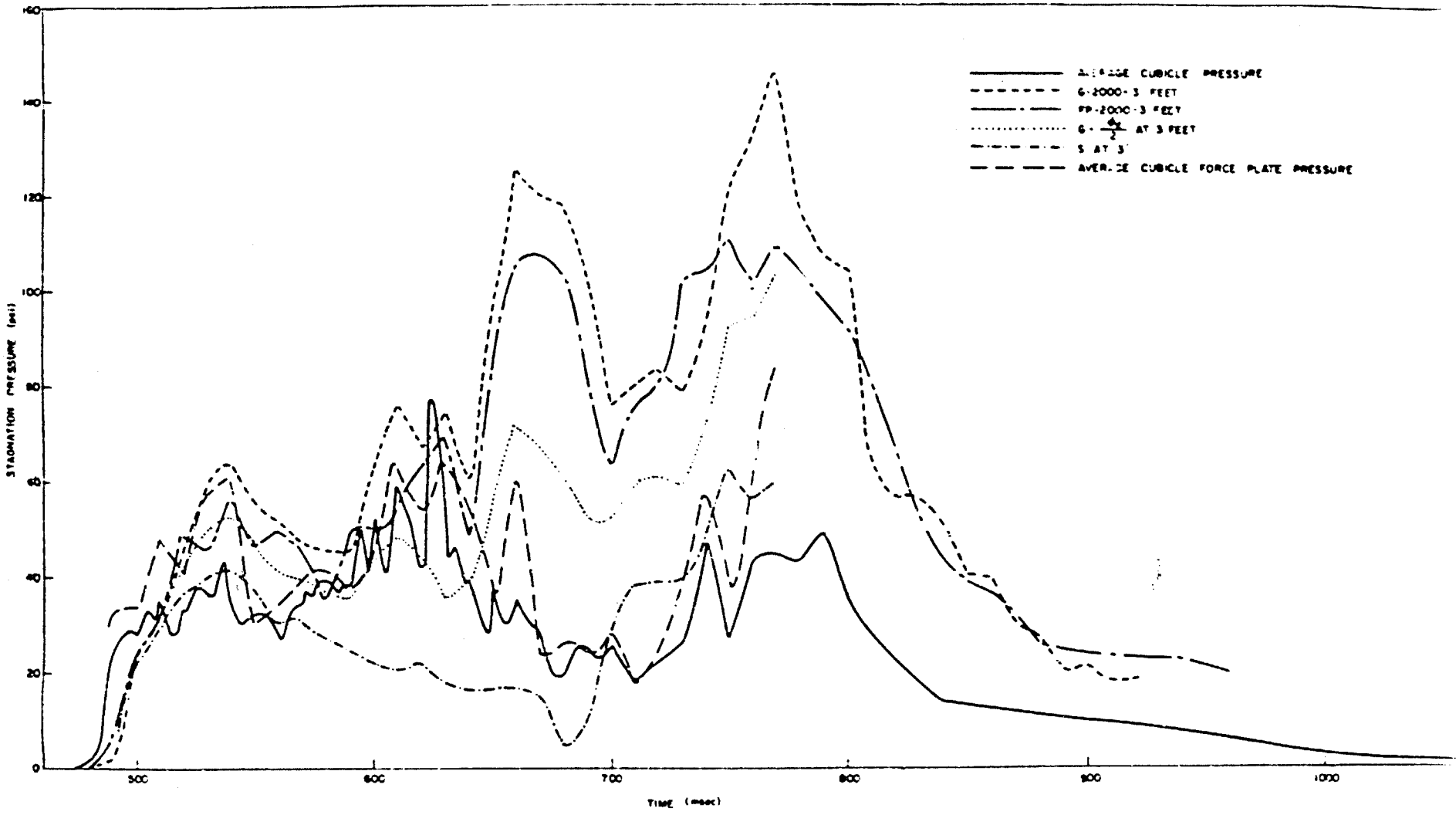

Fig. 3.16—Comparison of stagnation pressure on the cubicle front with the free-field stagnation measurements at the 3-ft level.

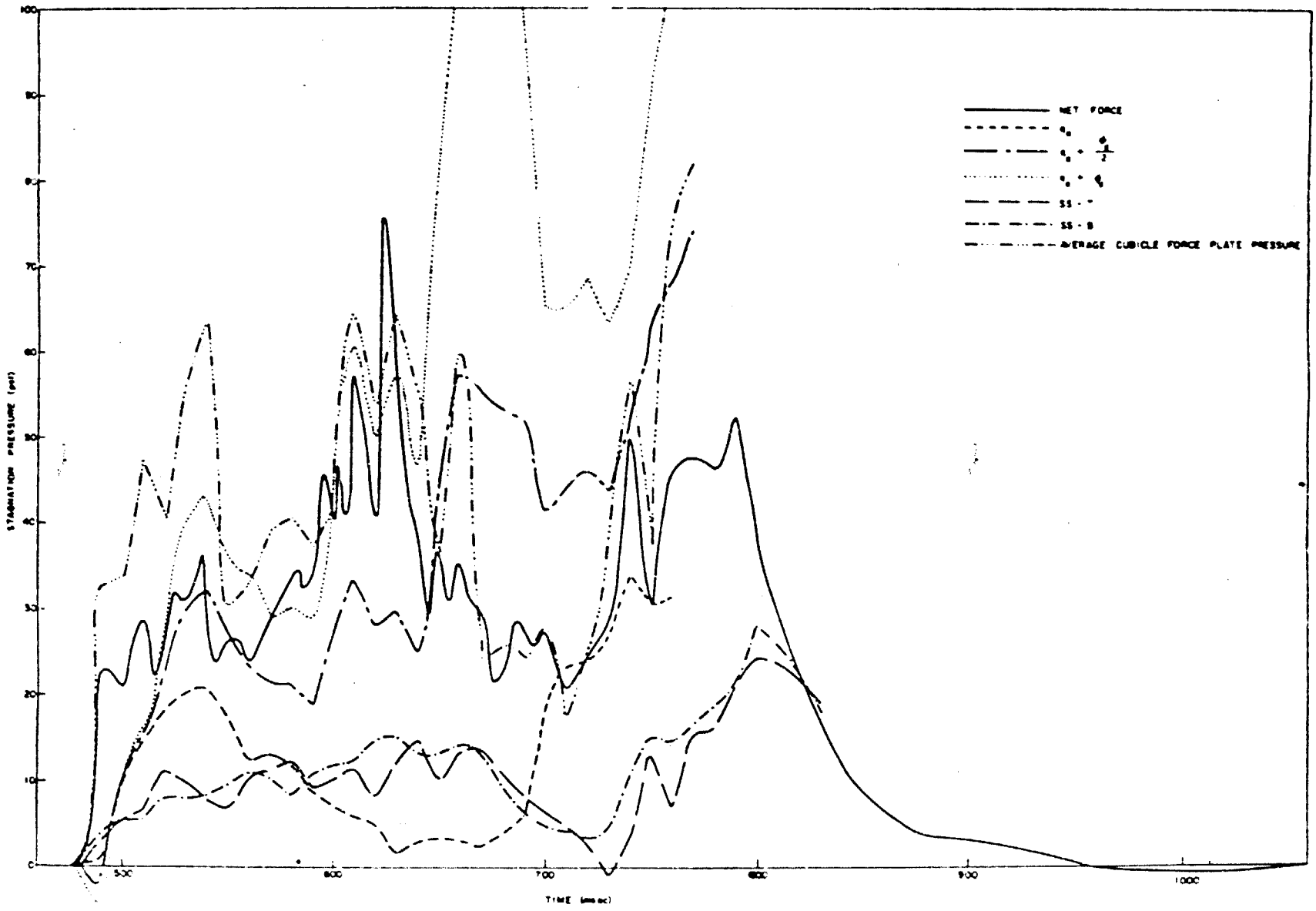

Fig. 3.17—Comparison of net translational force on the cubicle with the dynamic-pressure measurement at the 3-ft level. A comparison of the departures of the top and back of the cubicle from the overpressure is incorporated in the figure.

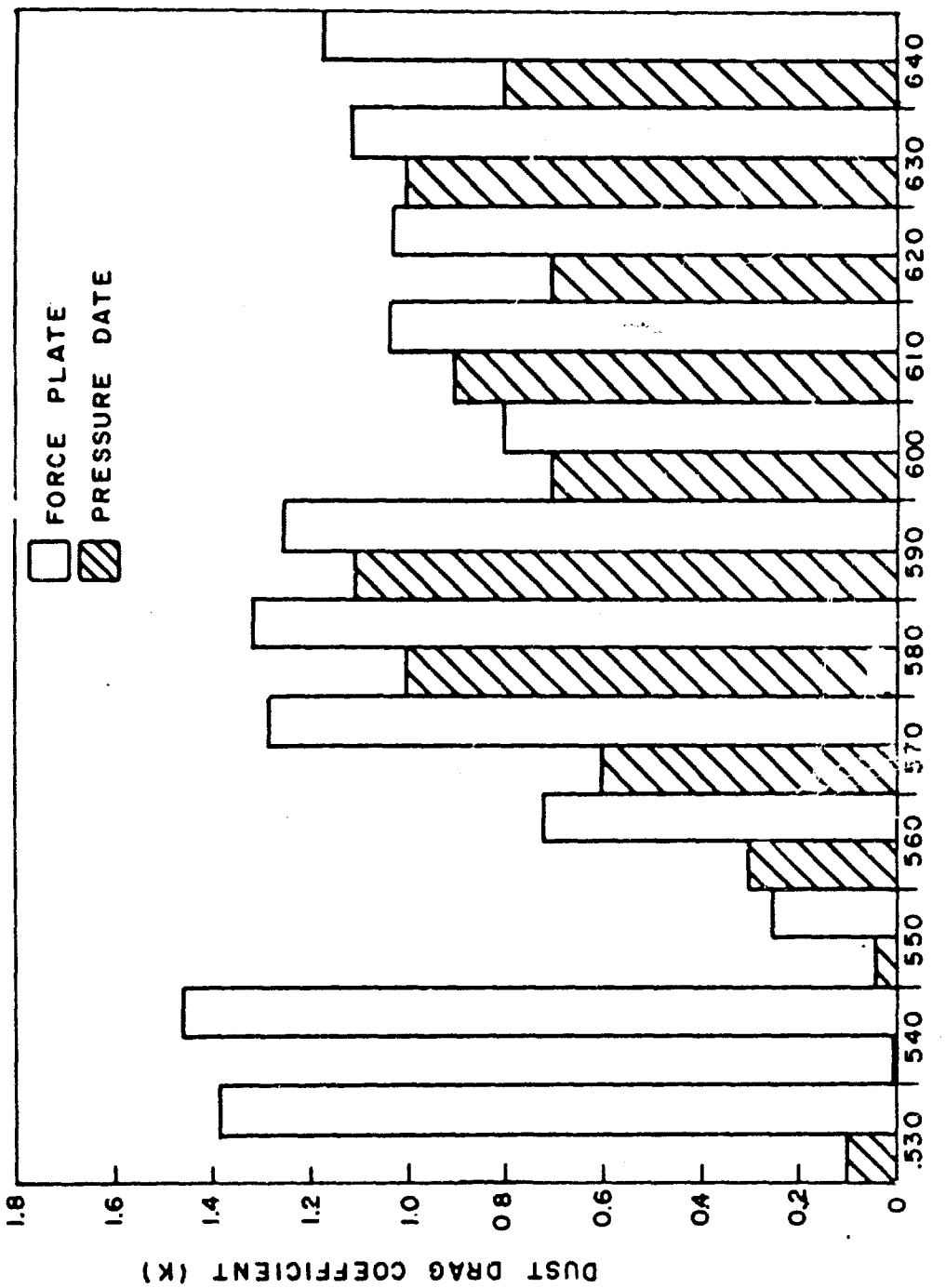

Fig. 3.18—Dust drag coefficients for the cubicle calculated from force-plate and pressure-gauge data.

Chapter 4

CONCLUSIONS

1. The dust filling of the pressure gauges detracted from the credibility of a few records. The fact that only a few gauges were involved, together with the estimated corrections to the records, led to only a small uncertainty in the over-all results. The force plates on the cubicle forward face indicated a somewhat greater pressure than the gauges. This was most noticeable at the 10-ft elevation and was probably the result of a difference in response of the instrument at this location to dust momentum flux; however, it should be admitted that the gauges affected by dust loading were quite critical.

2. The scouring on the front of the structure indicates either heavier dust concentrations near the ground, which reduced the velocity of penetrating particles, or higher velocity of particles near the top of the structure.

3. There was a pronounced asymmetry in the blast wave between the structure and the free-field measuring gauges only 35 ft away.

4. Dust concentrations encountered in this study were considerably higher at the 3-ft level than those measured in shot 12 of Operation Teapot. For a period at the 3-ft level, the contribution to stagnation pressure was almost entirely dust momentum flux. Nevertheless, the conclusions of the Operation Teapot results stand: dust is a symptom rather than a cause of high dynamic pressure per se which results from high mass velocity. This statement can be made because at the 10-ft level high dynamic pressures caused largely by air were observed. This high air velocity was transmitted later and incompletely to a heavily dust-laden layer below.

5. It would be necessary to study both loading and free-field conditions under a large number of conditions to develop a thorough understanding of how rapidly fluctuating dynamic pressures and accompanying high particulate concentrations affect the flow pattern and the blast loading. Until a prediction of more than the grossest features of the free-field overpressure-time and dynamic pressure-time can be made, it hardly seems advisable to pursue arduously their interrelations with loading. If, however, blast-loading experiments are planned, careful attention should be given to accompanying measurement of dynamic pressure and particulate concentrations as a function of time. The overemphasis on dust loading as a result of using the atypical conditions of Frenchman Flat may be misleading. If future loading experiments are planned, a location other than Frenchman Flat should be given careful consideration.

6. The oscillation of the overpressure measured on the structure is a characteristic of the precursor type wave and may be related to the spacial extent and distance apart of the turbulence vortices in the incident wave.

7. Future tests should consider a possible correlation between the frequency of the oscillation and the amplitude of the overpressure in the incident wave.

8. The spacial extent of the reflected pressure forward of the front of a structure is not adequately described by the dimensions of the front of the structure. The Mach number of the flow must also affect the distance to which reflected pressure will exert force on the footing.

9. For estimating cubicle loads in precursor zones with only information concerning overpressure, it sometimes would be adequate to use the following table for impulse considerations.

This table relates measured overpressure with the ratio of impulse on the structure to incident impulse. It should be kept in mind that structure dimensions are not being taken into account.

Incident overpressure	Impulse on structure / Incident impulse
13	3.60
20	2.94
75	3.54

10. A comparison of the free-field measurements with those obtained on the cubicle is confused by the striking asymmetry observed in the second half of the blast wave. In the first half of the blast wave, the average cubicle stagnation pressure according to the force plate agrees fairly well with the 3-ft Greg gauge measurement, suggesting that the total dust momentum flux is felt rather than one-half of it as would be expected from incompressible flow theory. The average stagnation pressures according to the pressure gauges first correspond to those obtained by the Snob gauge but gradually increase until they exceed the air stagnation pressure plus one-half the dust momentum flux.

11. A comparison of the net translational force per unit area on the cubicle according to force plates and pressure gauges with the dynamic pressure parameters derived from the 3-ft tower measurements shows the same trends: the net translational force according to the force plate corresponds to the sum of dynamic air pressure and dust momentum flux; whereas the net translational force according to pressure gauges at first corresponds to $q_a + (\phi_d/2)$ but finally approaches the full sum of air dynamic pressure, q_a, and dust momentum flux, ϕ_d.

12. Estimates of the dust drag coefficient in the arbitrary expression discussed in Sec. 3.6 give an average value of this parameter of 0.65 based on the cubicle pressure-gauge data or 1.07 based on the cubicle force-plate data.

13. Departure of overpressure measured on the top and the back of the cubicle from side-on pressure correlates with the sum of air dynamic pressure and dust momentum flux except during the first major peak observed at the tower but not observed at the cubicle.

14. The physics of the dust loading of structures is suggested to be complex from our measurements. This field attempt was frustrated to a considerable extent by the variation of the blast wave between the tower and the cubicle. Laboratory measurements should prove to be a more rapid and effective method of understanding dust loading of structures. Should future field studies of dust loading of obstacles be attempted, it would be prudent to place the free-field measurement in front of rather than beside the obstacle to avoid such asymmetries in the blast wave.